Biomarkers of Alzheimer-Associated Endosomal Dysfunction

Jessica Neufeld

Submitted in partial fulfillment of the
requirements for the degree of
Doctor of Philosophy
in the Graduate School of Arts and Sciences

COLUMBIA UNIVERSITY

2018

ABSTRACT

Biomarkers of Alzheimer-Associated Endosomal Dysfunction

Jessica Neufeld

Endosomal dysfunction has been mechanistically linked to Alzheimer's Disease (AD). To date, no in vivo biomarkers for this cellular deficit exist. Yet such biomarkers are required for determining its prevalence in AD and tracking its time course—both in disease progression and potential clinical trials. With this goal in mind, we made use of an assortment of mouse models bearing AD-related endosomal trafficking defects through selective deletion of retomer core proteins. We collected CSF and brain exosomes from these retromer-deficient models and performed a battery of molecular inquiries which included lipidomic and proteomic screens, as well as hypothesis-driven biochemistry. The results of this comprehensive investigation include the first characterization of the murine CSF lipidome and the deepest characterization to date of the murine CSF proteome.

Herein, we report that VPS26a haploinsufficiency in the brain imparts no detectable protein changes in the CSF as measured by labeled LC-MS/MS at three months of age. This deficit does, however, cause a reliable reduction of CSF sphingomyelin d18:1/18:1, which is exacerbated by age, extending to other sphingomyelins and other lipid classes including dihydrosphingomyelins and monohexosylceramides.

Complete knockout of its paralog VPS26b promotes an enrichment of BACE1-cleaved APP CTFs (β-CTFs) in brain-derived exosomes and may alter exosomal biogenic pathways. Similar trends were seen in a neuronal-specific knockout (via Camk2α-Cre recombinase) of retromer's linchpin, VPS35.

Most importantly, an unbiased proteomic screen of CSF collected from mice with a selective knock out of VPS35 in forebrain neurons (engineered using the Camk2α system) uncovered a total of 71 hits (52 parametric and 19 nonparametric) from the 1505 proteins detected. Pathway analysis and follow-up studies identified two distinct molecular categories with previously established relevance to AD: BACE1 substrates and MAPT (more commonly referred to as tau). We report that, both in vivo and in vitro, neuronal-selective knockout of VPS35 causes increased secretion of the N-terminal fragments (NTFs) of BACE1 substrates APLP1 and CHL1 as well as total tau, and importantly, that these events occur independent of cell death. Further, we find evidence of convergence of these pathways in both mouse and human CSF. However, as these BACE1 substrates likely accumulate in plaques, we propose CSF total tau as a biomarker of endosomal dysfunction with utility over the entire course of AD progression.

We have identified and validated a series of in vivo biomarkers that are reflective of AD-associated endosomal dysfunction. While clearly sensitive to this cellular pathology, future work is required to determine their specificity. Additionally, follow-up studies are required to show that interventions which rescue endosomal dysfunction affect this molecular profile. The identified biomarkers hold great promise for early detection of endosomal dysfunction in AD and

for tracking its course, during the disease progression and for clinical trials. Furthermore, the unexpected but validated finding, showing that increased CSF tau is reflective of AD-associated endosomal dysfunction, suggests that endosomal dysfunction is a universal deficit shared among AD patients in its earliest stages of disease.

Table of Contents

List of Figures

List of Tables

Acknowledgments

The scientific pursuit is a substantial undertaking, as the path from beginning to end is rarely straight or entirely prescribed. Accordingly, it requires passion, dedication, and often a sizeable support network to fulfill one's initial objective. I am blessed to lay claim to such an extensive and unwavering cast, without which, this journey would not have been possible.

I first wish to thank my fellow labmates who have shared their knowledge, expertise, and bench space with me over the past few years. In particular, I wish to acknowledge Sabrina Simoes, who assisted with the electron microscopy for this project and who has taught me more about science and life than I ever could have asked. I must also thank Andrea Urban, whose exceptional administrative support and holiday goodies kept all turbulence at bay. Finally, I would like to acknowledge Milankumar Kothiya for his outstanding technical assistance in the final phases of this project.

To our contributing collaborators Emily Chen, Estela Area Gomez, Robin Chan, Yimeng Xu, Larry Honig, David Kulick, Laurel Provencher, and Purvish Patel, I extend my utmost gratitude. I would also like to acknowledge Beverly Shelton and Xiaolan Shen, who provided expert training in murine CSF collection techniques, the cornerstone of this project.

I am indebted to the Pathology Department for granting me this exceptional training opportunity, and to Zaia Sivo for her unending advocacy. I also wish to acknowledge my thesis

committee members, Carol Troy, Clarissa Waites, Gil Di Paolo, for their exceptional advisement throughout the course of this project, and to Andrew Teich for his willingness to serve as additional counsel for the defense.

I wish to thank my family who has always encouraged me to shoot for the stars, and supported my dedication in getting there. And in particular, my brother Jason, whose weekly phone calls kept everything in perspective.

My work has been further blessed by the support of countless friends. I am particularly indebted to Noopur Khobrekar and Aidan Quinn for the gifts of their time and scientific wisdom, and to Lyuda Kovalchuke and Yelena Akhtiorskaya, to whom the word 'friendship' knows no bounds. I also wish to thank Fabrice Mercier, who learned more about retromer in the past three years than he ever intended, and whose love and ghee got me through all of life's greatest challenges.

Finally, I would like to thank my thesis advisor, Scott Small, for his invaluable mentorship over the course of this project. Scott has always provided both the tools and the counsel necessary to succeed. And importantly, his confidence in my ability to do so has never wavered. Scott has shown me what it means to be both a rigorous scientist and a diligent scholar, and his unending support along both trajectories has afforded me tremendous growth.

1 Chapter 1: Introduction

1.1 Alzheimer's Disease

1.1.1 Epidemiology

Alzheimer's disease (AD) is a devastating neurodegenerative disease, affecting more than 5.5 million Americans. it is currently the leading cause of dementia (Hebert, Weuve et al. 2013) and the sixth leading cause of death (Kochanek KD 2016). AD diagnosis hinges upon a convergence of pathological and cognitive symptoms; yet, heterogenic complexities pose challenge to diagnostic accuracy and therapeutic intervention. Nevertheless, AD is broadly categorized into two subgroups based on age of onset: early (EOAD) and late onset (LOAD). The former comprises those below the age of 65, while LOAD includes patients 65 and older.

Most AD cases appear sporadically without any clear inheritance pattern. However, dominantly inherited patterns have been reported, and are estimated to represent between 1% and 5% of all cases (Bird 1993). This dominantly inherited AD often presents at an earlier age and is therefore often termed early onset familial AD (eFAD or EOFAD).

Nearly two-thirds of those living with AD are women (Hebert, Weuve et al. 2013). The reason for this sex-based discrepancy remains unclear, although social (e.g. inequitable educational attainment for the current AD population) and biological distinctions (e.g. higher association with the APOE-4 genotype) have been proposed as contributing factors (Carter, Resnick et al. 2012, Altmann, Tian et al. 2014).

1.1.2 Risk factors

The majority of AD sufferers (96%) are 65 or older (Hebert, Weuve et al. 2013). In fact, one in ten adults over 65 has AD and the prevalence increases with age (up to 32% of adults over 85), rendering age the biggest risk factor for the disease (Hebert, Weuve et al. 2013).

A second risk factor is genetic predisposition, involving two types of associations: deterministic genes and risk genes. Deterministic genes are dominantly inherited and disease-causing. Mutations in APP, PSEN1, and PSEN1 comprise the large majority of these cases (Bird 1993); more recently, rare but causal mutations in SORL1 have also been reported (Pottier, Hannequin et al. 2012, Vardarajan, Zhang et al. 2015, Verheijen, Van den Bossche et al. 2016).

Risk genes, on the other hand, increase one's likelihood to develop the disease, as determined by genome wide association studies (GWAS). Such genes include APOE, which is currently the largest genetic risk factor for sporadic AD. Heterozygosity for the APOE4 allele increases one's risk for developing AD roughly 3-fold, while homozygosity increases the risk 12- to 15-fold (Michaelson 2014, Wu and Zhao 2016). Interestingly, the rare APOE2 allele appears to lower this risk (Wu and Zhao 2016). A growing number of other genes linked to AD have been identified through genetics studies in recent years (Figure 1.1) (Guerreiro, Bras et al. 2013, Karch and Goate 2015), though none confer as high a risk for disease development as APOE4.

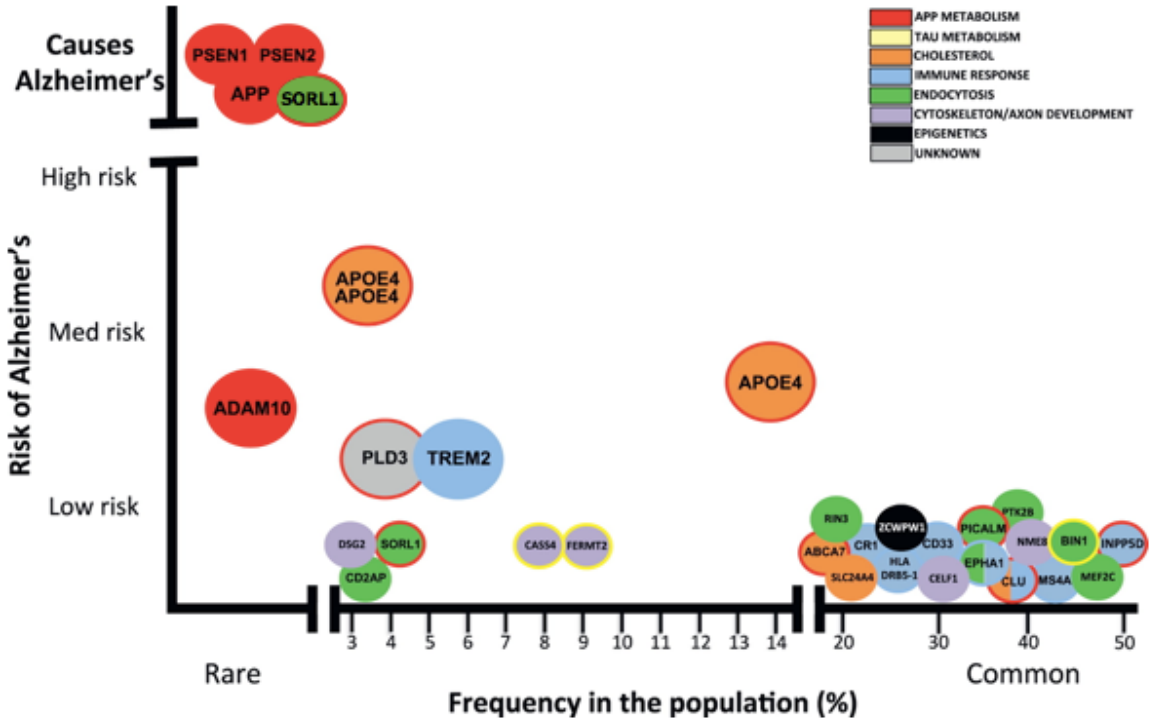

Figure 1.1 The genetics of AD.

A growing number of genes have been linked to AD, including both deterministic and risk genes (adapted from: (Guerreiro, Bras et al. 2013, Karch and Goate 2015)).

Numerous environmental risk factors including diet, exercise, education, and life activities have been proposed in the last two decades as the result of epidemiological investigations (Luchsinger, Tang et al. 2001, Scarmeas, Zarahn et al. 2003, Scarmeas, Stern et al. 2006, Luchsinger 2008, Scarmeas, Luchsinger et al. 2009, Duncan, Nikelski et al. 2017). Though the mechanistic impact of such factors remains unclear, there is growing consensus that they might impact one's

'cognitive reserve' which is thought to protect the brain against AD-related pathology (Scarmeas, Zarahn et al. 2003, Scarmeas, Zarahn et al. 2004, Stern 2006).

1.1.3 Pathological hallmarks

AD was first described over 100 years ago by German physician Alois Alzheimer. While examining the post-mortem brain of a patient with severe memory defects, he noticed abnormal accumulations which he termed plaques and tangles (Figure 1.2). These hallmarks have since comprised the general histopathological criteria for AD diagnosis. In 1911, the amyloid nature of these extracellular plaques was described by the German neuropathologist Max Bielschowsky, but it wasn't until the 1980s that scientists identified beta amyloid (Aβ), the peptide at the core of amyloid plaques (Kirschner, Inouye et al. 1987). In 1986, biochemical studies uncovered tau (Mapt) as the pathological building block of neurofibrillary tangles (Grundke-Iqbal, Iqbal et al. 1986, Kosik, Joachim et al. 1986). Debate lingers regarding which post-translationally modified forms contribute most to these aberrant intracellular accumulations (Grundke-Iqbal, Iqbal et al. 1986, Askanas, Engel et al. 1994, Novak 1994); however, it is largely accepted that hyperphosyphorylation of tau is a pathologic event which promotes tangle formation (Alonso, Zaidi et al. 2001, Gong and Iqbal 2008, Wang, Xia et al. 2013, Hu, Zhang et al. 2016).

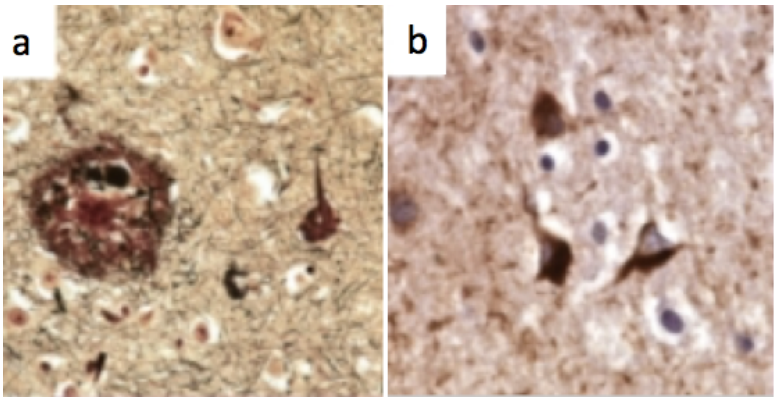

Figure 1.2 The pathological hallmarks of AD.

Silver staining of an AD brain reveals extracellular amyloid plaques (a) and intracellular neurofibrillary tangles (b) (Serrano-Pozo, Frosch et al. 2011).

1.1.4 Diagnostic challenges

A major hurdle in the treatment and research of AD over the past several decades has been the absence of reliable clinical biomarkers. Common presenting symptoms include memory deficits, personality changes, and disorientation (APA 2017). Yet, not all patients present with the same constellation of symptoms and many of these symptoms are shared among other types of transient or progressive neuropathies, rendering behavioral criteria alone insufficient. In the early 1990s, nearly 90 years after its recognition as a disease, a cerebrospinal fluid (CSF)-based biomarker profile (centering on Aβ and tau levels) for AD provided a major step forward in antemortem diagnostics and disease management. To note, it was initially hypothesized that CSF from AD patients would contain higher levels of Aβ, reflecting its increased accumulation in the brain; surprisingly, however, studies revealed that AD CSF contained strikingly less Aβ (Fagan, Mintun et al. 2006), which was retrospectively attributed to its preferential sequestration in plaques.

Recent technological advancements have paved the way for the development of diagnostic biomarkers using additional modalities. Imaging biomarkers, for example, rely upon radiolabeled compounds which can be targeted towards specific biological components such as extracellular amyloid and neurofibrillary tau. A compound named 11C-PIB has demonstrated early promise in the labeling of amyloid plaques (Archer, Edison et al. 2006). Additional plaque-targeting tracers bearing the more stable F18 radioisotope have also been developed. These include florbetapir, florbetaben, flutemetamol, and the more recent fluselenamyl. Radioligands targeting neurofibrillary tangles include AV-1451 (T807/flortaucipir), MK-6240, PI-2620, THK5317, PBB3, and JNJ-067. The growing arsenal of neuroimaging tools targeting these two histopathological hallmarks renders imminent their in vivo visualization, which could improve diagnostic acuity and histopathological monitoring.

1.1.5 The amyloid hypothesis

The predominant theory of AD pathogenesis, termed the amyloid hypothesis (or amyloid cascade hypothesis), was proposed in 1991 (Hardy and Allsop 1991) following the discovery of disease-causing mutations in APP in early-onset AD (Chartier-Harlin, Crawford et al. 1991). This theory posits that increased accumulation of extracellular Aβ peptide aggregates is the initial pathogenic event which gives rise to all disease-related neuropathology (Hardy and Allsop 1991). Despite looming speculation, this hypothesis has remained the dominant theory for nearly two decades, motivating extensive study of the underlying biochemistry and providing the field a long-awaited molecular drug target.

APP, the holoprotein of Aβ, is a type-I membrane protein highly expressed in the brain, where it is thought to contribute to the structural and functional integrity of neuronal synapses (Priller, Bauer et al. 2006, Tyan, Shih et al. 2012). It can be cleaved by various enzymes along two general pathways, yielding fragments with distinct functional properties. These two pathways are (1) amyloidogenic and (2) nonamyloidogenic, named for their capacity to generate the Aβ peptide (Figure 1.3).

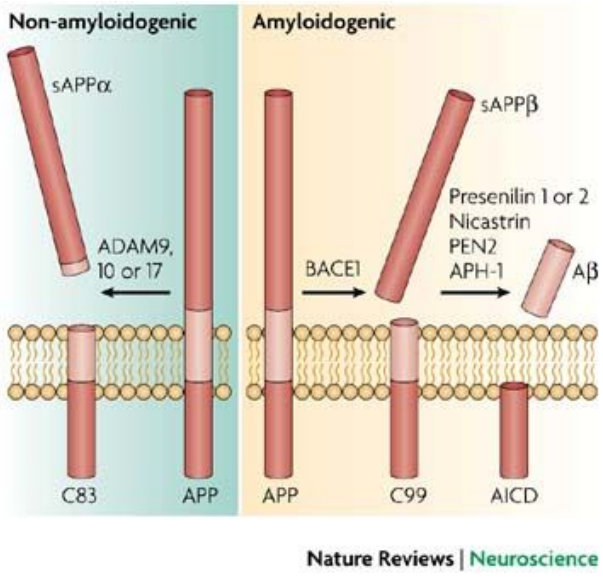

Figure 1.3 The processing pathways of amyloid precursor protein (APP).

Two pathways define the processing fate of APP. The non-amyloidogenic pathway is initiated by enzymatic cleavage of ADAM9, ADAM10, or ADAM17 to yield sAPPα and the 83-amino acid C-terminal fragment (C83 or α-CTF). Amyloidogenic cleavage begins with cleavage by BACE1 to yield sAPPβ and the 99-amino acid C-terminal fragment (C99 or β-CTF). This C99 fragment

undergoes subsequent cleavage by a γ-secretase complex (composed of presinilin 1 or 2, nicastrin, PEN2, and APH-1) to yield Aβ and the APP intracellular domain (AICD) (LaFerla, Green et al. 2007).

The amyloidogenic pathway gives rise to Aβ via sequential cleavage of APP by a beta-secretase (BACE1) and a γ-secretase complex, yielding a peptide of either 40 amino acids (Aβ40) or 42 amino acids (Aβ42) depending on the site of gamma cleavage. Studies have shown that Aβ42 is more prone to aggregation (i.e. more pathogenic) than Aβ40 and accordingly serves as the central molecular culprit of the amyloid hypothesis (Bitan, Kirkitadze et al. 2003).

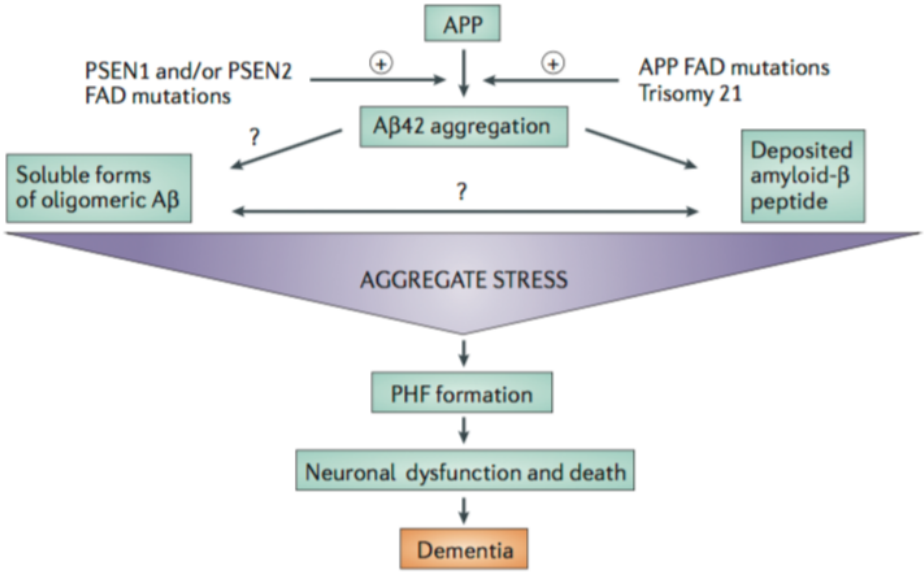

Figure 1.4 The amyloid cascade hypothesis.

This leading theory of AD pathogenesis asserts that the accumulation of Aβ42 is the central, initiating event which gives rise to all subsequent pathology. Though various aggregate forms of Aβ42 may have differential pathologic effects, their accumulation is presumed causal of

downstream events including paired helical formation (PHF) of tau, neuronal loss, and cognitive decline (Karran, Mercken et al. 2011) .

This leading theory, informed by a growing body of research, asserts that the aggregation of Aβ42 promotes a cascade of cytotoxic effects (Figure 1.4) which include tau dysregulation, neurofibrillary tangle formation, and ultimately neuronal death. Several details, however, remain unclear. For example, debate has ensued regarding which aggregate form of Aβ42 (monomeric, oligomeric, or deposited plaque) contribute most to disease pathology (Walsh, Klyubin et al. 2002, Glabe 2006), and in general, the mechanism through which these events promote tau dysregulation (Zheng, Bastianetto et al. 2002, Manczak and Reddy 2013, Bloom 2014).

The amyloid hypothesis is strengthened by several key findings. First, autosomal dominant, disease-causing mutations in APP and gamma-secretase presenilins PSEN1 and PSEN2 have been identified (Levy-Lahad, Wasco et al. 1995, Sherrington, Rogaev et al. 1995). The pathogenic impact of these mutations is attributed to increased Aβ42 generation through either an increased production of Aβ (both Aβ40 and Aβ42) altogether or an increase in the ratio of Aβ42/Aβ40. Second, Down's Syndrome patients are at substantially higher risk for AD, with more than half ultimately developing the disease. This has been attributed to the extra copy of APP (on chromosome 21), and therefore substantially elevated levels of its metabolic products which include Aβ (Teller, Russo et al. 1996). Third, genome wide association studies (GWAS) have identified associations in several genes which have purported roles in Aβ clearance (such as APOE and clusterin) to AD (Zlokovic, Martel et al. 1996, Tanzi, Moir et al. 2004). In fact, APOE status is

currently the strongest genetic risk factor for sporadic AD, with the APOE4 allele accounting for roughly half of all AD cases (Ashford 2004). Though the precise pathological contribution of APOE4 is debated, studies have demonstrated its decreased clearance capacity for extracellular Aβ as compared with APOE2 and APOE3 (Strittmatter, Weisgraber et al. 1993, Bales, Verina et al. 1999, Holtzman, Bales et al. 2000, Shibata, Yamada et al. 2000, Holtzman 2001, Ashford 2004).

Yet, despite its rise as the predominant theory of AD pathogenesis in the past two decades, several challenges to the amyloid hypothesis remain. First, there is an anatomical mismatch between extracellular plaques and neurotoxicity in AD brains. Specifically, the medial temporal lobe, which undergoes the primary and most extreme neurotoxicity (Khan, Liu et al. 2014, Altmann, Ng et al. 2015) bears the least plaque burden in the cortex (Braak and Braak 1991, Altmann, Ng et al. 2015). Second, the overall deposition of Aβ in the AD brain does not correlate with cognitive decline; in fact, extensive amyloid plaques have been documented in non-demented, cognitively 'normal' individuals (Rentz, Locascio et al. 2010). Third, other histopathological events such as endocytic abnormalities appear to precede local amyloid deposition in AD brains (Cataldo, Peterhoff et al. 2000), raising question as to the positioning of amyloid accumulation along the pathological timeline of AD. And fourth, to date, a growing list of therapies targeting extracellular amyloid have largely failed to show efficacy in treating the disease. One must consider that the failure of Aβ-targeting therapies could derive from neurodegeneration occurring prior to intervention. However, taken together, these observations pose challenge to the predominant theory of AD pathogenesis and motivate the quest for additional drug targets.

1.1.6 The endosome as an emerging therapeutic target

Though not considered a canonical biomarker of AD, endosomal dysfunction has increasingly been recognized as a salient feature of its cytopathology. Cataldo, et al. described an abnormal enlargement (2.5-fold) of neuronal endosomes as an early event in AD pathology (Cataldo, Barnett et al. 1997) and later reported that this cellular event precedes localized Aβ deposition in both sporadic AD and Down Syndrome patients (Cataldo, Peterhoff et al. 2000). Other groups have also described endosomal enlargement as a feature of IPSC-derived neurons from patients with both sporadic (Israel, Yuan et al. 2012) and autosomal-dominant forms of AD (Raja, Mungenast et al. 2016).

Furthermore, genetic studies have linked a growing number of genes involved in endosomal trafficking to AD. These include SORL1, BIN1, PICALM, ABCA7, CD2AP, SNX1, SNX3, RAB7A, and KIAA1033 (Rogaeva, Meng et al. 2007, Vardarajan, Bruesegem et al. 2012, Guerreiro, Bras et al. 2013, Lambert, Ibrahim-Verbaas et al. 2013, Karch and Goate 2015, Steinberg, Stefansson et al. 2015). As such, endosomal trafficking has risen as one of the major categories of AD-related genes (Small, Simoes-Spassov et al. 2017) (Figure 1.5). And, as mentioned previously, causal mutations in the endosomal trafficking receptor SORL1 have been identified (Pottier, Hannequin et al. 2012, Vardarajan, Zhang et al. 2015, Verheijen, Van den Bossche et al. 2016), underscoring a pathogenic role for endosomal dysfunction in AD.

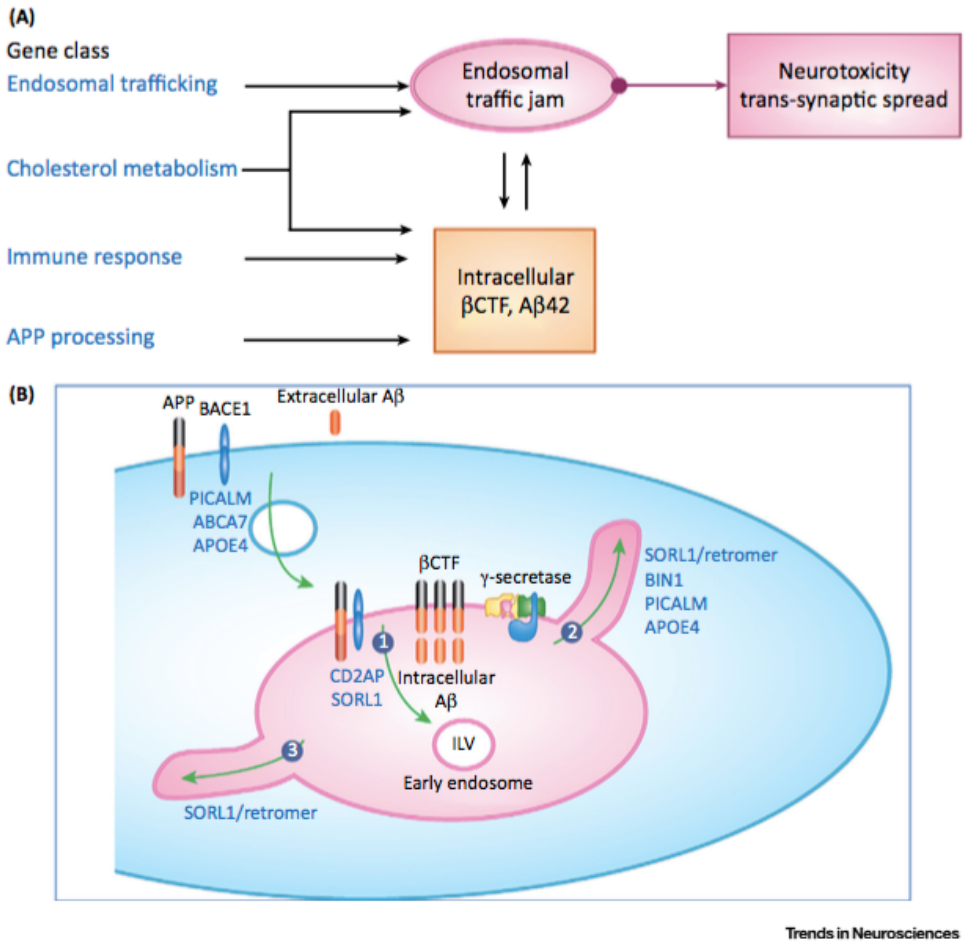

Figure 1.5 Endosomal trafficking in AD.

(a) Genetic studies have identified variants in a growing number of genes which confer increased risk of AD. These genes broadly coalesce into four functional categories including endosomal trafficking. As studies have shown defects in the other three gene categories can lead to endosomal trafficking defects, this category represents a common final pathway for downstream neurotoxic events. (b) Endosomal trafficking genes linked to AD perform distinct functions which can affect sorting dynamics at the endosomal hub. Endosomal traffic jams, now thought to play a role in AD pathogenesis, result from defects to the degradation pathway (1), the recycling pathway (2), and/or the retrograde pathway (3) (Small, Simoes-Spassov et al. 2017).

Finally, expression profiling studies of post-mortem brain tissue have identified a significant reduction of endosomal trafficking proteins (VPS35, VPS26a, and Beclin-1) and lipids (PI3P) in the areas of the brain most affected in AD (Small, Kent et al. 2005, Pickford, Masliah et al. 2008, Morel, Chamoun et al. 2013). Though expression profiling of post-mortem brains is often limited to late stage AD, Beclin-1 reduction was described in a post-mortem study of patients in the initial symptomatic stage of mild cognitive impairment (MCI), positioning its decline as an early event in AD pathology (Pickford, Masliah et al. 2008).

The genetic and biochemical studies linking endosomal trafficking deficits to AD have motivated mechanistic exploration of the resulting molecular pathology. As a result of this research, there is growing consensus that endosomal dysfunction can promote Aβ accumulation through a variety of mechanisms (Wen, Tang et al. 2011, Morel, Chamoun et al. 2013, Nixon 2017, Small, Simoes-Spassov et al. 2017); these include trafficking defects which increase the retention time of APP and/or its amyloidogenic cleavage enzymes in the endosome, thereby promoting their interaction (Wen, Tang et al. 2011, Bhalla, Vetanovetz et al. 2012). Interestingly, the reverse has also been demonstrated: that amyloidogenic APP processing can promote endosomal dysfunction due to cytotoxic effects of amyloidogenic APP products (Jiang, Mullaney et al. 2010, Xu, Weissmiller et al. 2016, Small, Simoes-Spassov et al. 2017). Accordingly, endosomal dysfunction has been proposed as a common cellular pathway capable of mediating subsequent AD-related pathology (Small, Simoes-Spassov et al. 2017) (Figure 1.5) and a novel drug target for discovery (Berman, Ringe et al. 2015, Small, Simoes-Spassov et al. 2017).

1.2 The retromer assembly

1.2.1 Retromer as a master conductor of endosomal trafficking

Retromer has been termed a master conductor of endosomal trafficking, as it coordinates the transport of protein cargo out of the endosome along two pathways: the retrograde pathway toward the trans-golgi network (TGN) or the recycling pathway toward the plasma membrane (Figure 1.6a). Retromer was first described in yeast in in the late 1990s (Seaman, Marcusson et al. 1997, Seaman, McCaffery et al. 1998); its mammalian orthologs were identified shortly thereafter (Edgar and Polak 2000, Haft, de la Luz Sierra et al. 2000) and have been studied extensively in the years since.

Early studies in yeast revealed a critical role for retromer in endolysosomal health. Specifically, Seaman et al. demonstrated that retromer traffics receptor VPS10p along the retrograde pathway, ensuring continuous delivery of its ligand carboxypeptidase Y (CPY) from the TGN to the prevacuolar endosome (Seaman, Marcusson et al. 1997, Seaman, McCaffery et al. 1998). They further showed that mutations in retromer caused an increased vacuolar retention of VPS10p and an abnormal secretion of vacuolar protease CPY into the extracellular space. Follow-up studies confirmed a similar role for retromer in the mammalian system: lysosomal delivery of protease cathepsin D via retrograde trafficking of its receptor, the cation-independent mannose-6-phosphate receptor (CIM6PR) (Arighi, Hartnell et al. 2004). Numerous studies in the years since have unveiled a multitude of other retromer cargo including mammalian VPS10 domain-

containing receptors (e.g. SORL1) and glutamate receptors (e.g. GluR1) (Small and Gandy 2006, Zhao, Nothwehr et al. 2007, Lane, Raines et al. 2010).

The term 'retromer' refers not simply to one protein, but instead a multi-modular assembly of proteins which must organize biochemically to traffic endosomal cargo to the appropriate destination (Small and Petsko 2015). These modules of retromer assembly have been grouped into five categories (Figure 1.6b) which coalesce around their functional contribution: cargo recognition, membrane recruiting, tubulation, actin-remodeling, and the cargo to be trafficked to its destination (Small and Petsko 2015).

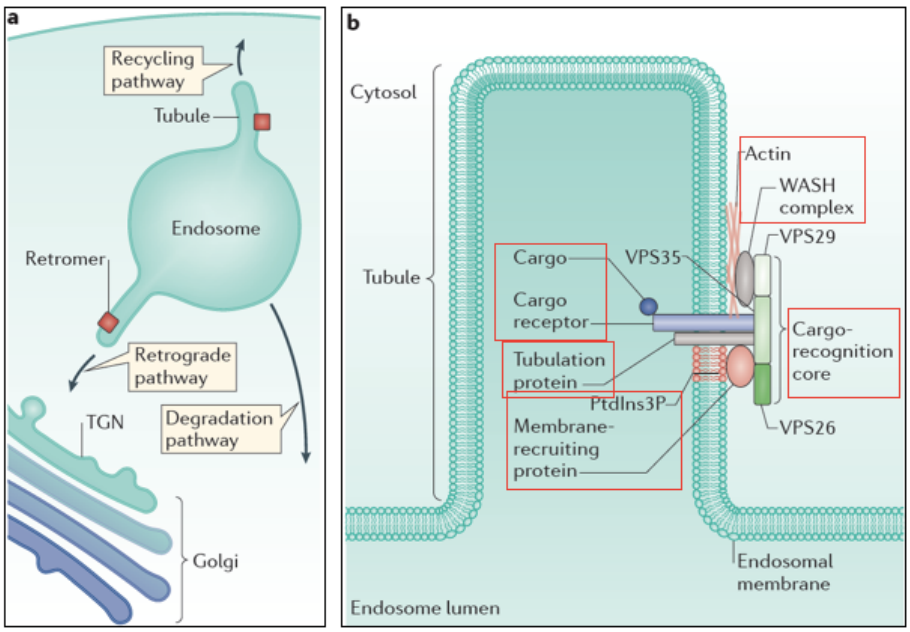

Figure 1.6 The retromer assembly.

(a) Retromer traffics cargo in two of the three routes out of the endosome: the recycling pathway and the retrograde pathway. (b) The five modules of retromer assembly include the cargo

recognition core (which includes VPS35, VPS29, and either VPS26a or VPS26b), the membrane recruiting module (which includes both proteins and lipids such as PI3P), the tubulation module, actin-remodeling components, and the cargo and receptors to be trafficked out of the endosome (adapted from (Small and Petsko 2015)).

Though individual components of this assembly may vary in a context-dependent manner, the cargo recognition core, which consists of 3 vacuolar protein sorting proteins (VPS35, VPS29, and either VPS26a or VPS26b), is an essential and unifying component of the retromer assembly (Figure 1.6b). In fact, expression of these core proteins is often tightly regulated within the cell, and a deficiency in any one of these proteins results in concomitant reduction of its trimeric binding partners (unpublished data). Recent studies suggest that core protein paralogs VPS26a and VPS26b form distinct trimers with VPS35 and VPS29 and that these assemblies may perform different functions in the brain (Kerr, Bennetts et al. 2005, Kim, Lee et al. 2010, Bugarcic, Vetter et al. 2015).

This core trimer is recruited to the endosomal membrane via components of the membrane recruiting module, which can include proteins such as sorting nexin-3 (SNX3) (Harterink, Port et al. 2011) and RAB7A (Rojas, van Vlijmen et al. 2008, Seaman, Harbour et al. 2009, Harrison, Hung et al. 2014). The endosomal-enriched lipid phosphatidylinositol-3-phosphate (PI3P) also contributes to membrane recruitment of the retromer assembly through binding of SNXs via their phox homology domain (Cozier, Carlton et al. 2002) and is therefore included in this functional category.

Essential also for this trafficking process is the generation of a nascent tubule toward the direction of cargo transport. This function is performed by the membrane tubulation module, comprised of sorting nexins SNX1, SNX2, SNX5, and SNX6 (Rojas, Kametaka et al. 2007, Wassmer, Attar et al. 2007). Heterodimers of these sorting nexins directly bind the cargo recognition core while stabilizing membrane curvature via carboxy- terminal BIN–amphiphysin–RVS (BAR) domains (Attar and Cullen 2010, Mim and Unger 2012).

An actin-remodeling module binds to the retromer assembly via VPS35 where it gives support to the budding tubule via the generation of actin patches (Harbour, Breusegem et al. 2010). The proteins involved in this process include members of the WASH complex: WAS protein family homologue 1 (WASH1), FAM21, strumpellin, coiled-coil domain-containing protein 53 (CCDC53) and KIAA1033 (Gomez and Billadeau 2009, Derivery and Gautreau 2010, Harbour, Breusegem et al. 2010).

The fifth module of retromer assembly consists of the cargo and/or cargo receptors to be transported out of the endosome. While various cargo of retromer continue to be unearthed, several bearing neurological relevance have been identified to date. These include VPS10-domain containing receptors (SORL1, SORCS1, SORCS2, SORCS3, and sortilin), several of which have been recognized for their role in the transport of APP out of the endosome (Small, Kent et al. 2005, Rogaeva, Meng et al. 2007, Bhalla, Vetanovetz et al. 2012, Fjorback, Seaman et al. 2012, Lane, St George-Hyslop et al. 2012). As mentioned above, CIM6PR, which delivers cathepsin D to the

endolysosomal system, has also been verified as a retromer cargo (Arighi, Hartnell et al. 2004, Seaman 2004). Finally, several neuronal signaling (GluR1 (Temkin, Morishita et al. 2017)) and microglia phagocytic (CD36 and TREM2 (Lucin, O'Brien et al. 2013)) receptors have also been shown to rely on retromer for transport along the recycling pathway (Lucin, O'Brien et al. 2013, Choy, Park et al. 2014).

1.2.2 Retromer in AD

Retromer was first linked to AD by our lab in 2005 through a microarray experiment which revealed that the entorhinal cortex of AD brains are deficient in retromer core components VPS35 and VPS26 (Small, Kent et al. 2005). Though the reason for declining retromer levels in AD was unclear at the time, recent work suggests that both genetics and environment can play a role (Rogaeva, Meng et al. 2007, Morabito, Berman et al. 2014).

Follow-up studies also revealed that silencing VPS35 in vitro increases Aβ production, suggesting that this defect might be upstream of AD pathology (Small, Kent et al. 2005). A cellular mechanism was later uncovered upon the identification of APP receptor SORL1 as a retromer cargo, highlighting the amyloidogenic effects of extended endosomal retention of APP (i.e. that trafficking matters) (Small and Gandy 2006, Muhammad, Flores et al. 2008, Small and Duff 2008, Lane, Raines et al. 2010, Lane, St George-Hyslop et al. 2012). Follow-up studies have confirmed that retromer deficiency (via knockdown of VPS35 or VPS26a) can lead to increased amyloidogenic processing through trafficking defects in APP (Muhammad, Flores et al. 2008, Bhalla, Vetanovetz et al. 2012, Choy, Cheng et al. 2012). Interestingly, retromer has also been

shown to traffic BACE1 out of the endosome (Wen, Tang et al. 2011) (where it is thought to impart the majority of its amyloidogenic effects on APP (Small and Gandy 2006)). This suggests an additional mechanism through which retromer dysfunction enhances Aβ accumulation, increasing retention of the initiating amyloidogenic enzyme as well as its substrate APP in the neuronal endosome.

Genetics studies have further supported a pathological role of retromer in AD. To date, variants have been identified in genetic components of all 5 retromer modules which confer an increased risk for AD (Rogaeva, Meng et al. 2007, Vardarajan, Bruesegem et al. 2012, Lambert, Ibrahim-Verbaas et al. 2013) . As mentioned previously, causal mutations in retromer receptor SORL1 has also been discovered (Pottier, Hannequin et al. 2012, Vardarajan, Zhang et al. 2015), positioning retromer dysfunction upstream of the resulting pathology in at least a subset of cases.

1.2.3 Retromer deficiency as a model of AD-related endosomal dysfunction

Retromer deficiency in vitro recapitulates several aspects of AD-related endosomal dysfunction. First, knockdown of retromer core proteins promotes Aβ accumulation through increased retention of APP and BACE1 in the endosome (Wen, Tang et al. 2011, Bhalla, Vetanovetz et al. 2012). Second, it results in an enlargement of endosomes (Offe, Dodson et al. 2006, Bhalla, Vetanovetz et al. 2012), purportedly through an accumulation of cargo at the limiting membrane. Third, retromer deficiency disrupts delivery of protease cathepsin D to the endolysosomal system, resulting in its increased extracellular secretion (and increased cathepsin D secretion into the CSF has been reported in AD brains) (Schwagerl, Mohan et al. 1995). Fourth, it causes an

increase in free cholesterol (also reported in AD (Cutler, Kelly et al. 2004, Xiong, Callaghan et al. 2008)), and its redistribution to late endocytic compartments (Marquer, Tian et al. 2016). Finally, recent work in human iPSC-derived neurons demonstrates that retromer deficiency promotes hyperphosphorylation of tau, and that this effect is independent of its effects on Aβ (Young, Fong et al. 2018).

Mouse models of retromer deficiency, generated by selective deletion of the cargo recognition core, also exhibit enhanced accumulation of Aβ in the brain (Muhammad, Flores et al. 2008, Wen, Tang et al. 2011). Furthermore, they demonstrate defects in long-term potentiation (which may be reversed using gamma-secretase inhibitors (Muhammad, Flores et al. 2008)) and hippocampal-dependent memory tasks (Muhammad, Flores et al. 2008, Wen, Tang et al. 2011).

1.3 The search for biomarkers of endosomal dysfunction

1.3.1 Rationale

Endosomal dysfunction is clearly linked to AD pathology, and represents a novel therapeutic target for discovery (Berman, Ringe et al. 2015, Small, Simoes-Spassov et al. 2017). Critical to this pursuit, however, is the identification of a biomarker of endosomal dysfunction, serving three primary purposes: 1) addressing the epidemiology of endosomal dysfunction in AD; 2) tracking the disease course; and 3) properly stratifying and monitoring patients in upcoming clinical trials. The project described herein was designed to address this unmet need through identification of a clinically relevant biomarker of AD-related endosomal dysfunction.

1.3.2 Hypothesis

The general hypothesis motivating this investigation is that AD-related endosomal dysfunction in the murine brain will impart molecular changes in the extracellular milieu which can be detected via clinically useful biofluids. Prior in vitro studies have demonstrated that endosomal defects can promote both protein and lipid alterations in the cellular secretome (Rojas, van Vlijmen et al. 2008, Yuyama, Yamamoto et al. 2008, Sullivan, Jay et al. 2011). To our knowledge, this study is the first to fully translate such logic into a discovery-driven investigation of AD-related endosomal dysfunction in the murine brain.

1.3.3 Strategy

Our study design broadly involves the generation of mouse models of endosomal dysfunction, the collection and analysis of biological reservoirs molecular biomarkers using unbiased screens, and ultimately their translation to human subjects (Figure 1.7). This strategy is outlined in more detail in the sections that follow.

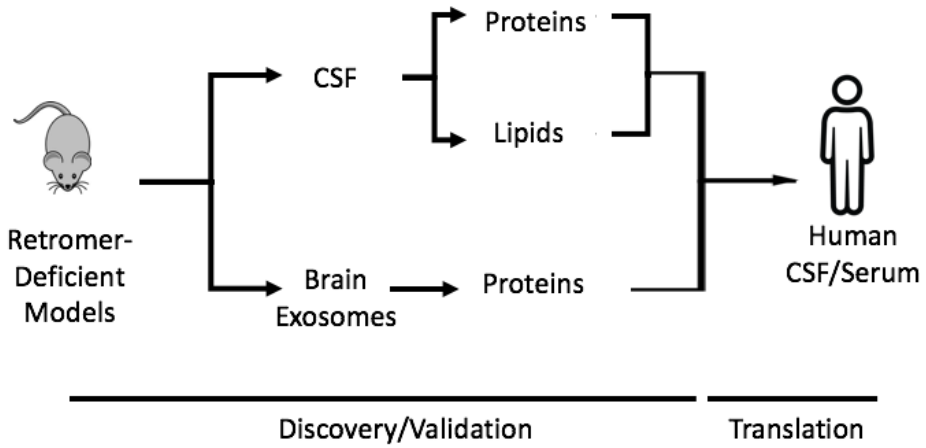

Figure 1.7 The search for biomarkers of AD-related endosomal dysfunction.

This project involves the collection of CSF and brain exosomes from retromer-deficient mouse models for investigation of proteomic and lipidomic changes which can be translated to human subjects. Utility of such a biomarker includes uncovering the epidemiology of endosomal dysfunction in AD, as well as proper patient stratification and monitoring for upcoming clinical trials of endosome-targeting agents.

1.3.3.1 Techniques

We have opted to investigate molecular changes that arise in both the CSF and in purified brain exosomes from our mouse models of endosomal dysfunction. CSF is an intuitive reservoir as retromer dysfunction has been shown to impact the cellular secretome (e.g. enhanced secretion of cathepsin D and Aβ, proteins which are readily detected in CSF) (Muhammad, Flores et al. 2008, Rojas, van Vlijmen et al. 2008, Bhalla, Vetanovetz et al. 2012). It is also now a technically feasible haven for discovery as protocols for murine CSF collection have been developed and successfully reported in a growing number of studies (Barten, Cadelina et al. 2011, Schelle, Hasler et al. 2017). Biomarkers identified in this fluid could therefore directly translate to human subjects as CSF collection in humans is a well-established clinical procedure.

Brain-derived exosomes represent the second reservoir for discovery in this project. As exosomes derive from the limiting endosomal membrane (which is altered in retromer dysfunction) (Bhalla, Vetanovetz et al. 2012), it follows that these changes might be reflected in the secreted exosomes. In fact, in vitro studies have confirmed elevation of C-terminal fragments of retromer cargo APP in exosomes following knockdown of core protein VPS35 (Sullivan, Jay et al. 2011). The

recent development of two critical techniques position brain-derived exosomes as a feasible haven for biomarker discovery. The first is a protocol for isolating exosomes from the murine brain (Perez-Gonzalez, Gauthier et al. 2012). The second is a protocol for isolating brain-derived exosomes from human serum (Goetzl, Boxer et al. 2015, Goetzl, Mustapic et al. 2016). Together these make possible the indirect translation from findings in murine brain exosomes to human brain-derived serum exosomes, which can be obtained clinically through venipuncture.

We have chosen to investigate both protein and lipid changes as both can be altered in the cellular secretome as a result of endosomal dysfunction (Rojas, van Vlijmen et al. 2008, Yuyama, Yamamoto et al. 2008, Strauss, Goebel et al. 2010, Sullivan, Jay et al. 2011, Bhalla, Vetanovetz et al. 2012). These molecular approaches will be described further in the ensuing chapters.

1.3.3.2 Mouse Models

We have amassed an assortment of retromer-deficient mouse models, distinct in either the deleted cargo recognition core protein or in the region of genetic defect (Figure 1.8). The Camk2α knockout models (VPS35 and VPS26a), restrict retromer deficiency to forebrain neurons. And the use of VPS26a in particular restricts the molecular defect to the VPS26a-containing assembly (while VPS35 depletion affects both VPS26a- and VPS26b-containing assemblies). Knockout of VPS26b—the brain-enriched VPS26 paralog (Kerr, Bennetts et al. 2005)—provides another model of regional retromer deficiency (in this case, of only the VPS26b-containing assembly). Finally, use of the VPS26a-haploinsufficient (knockout is embryonic lethal) model allows exploration of retromer deficiency in all brain cells, as studies have suggested that deficiency of the VPS26a-

containing retromer assembly in AD may not be entirely limited to neurons (Lucin, O'Brien et al. 2013).

a.

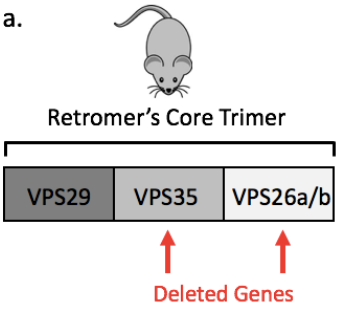

b.

Mouse Model	Deficiency Type	Deficient Cell Type
VPS35$^{fl/fl}$ Camk2α-Cre KO	Complete knockout	Forebrain neurons
VPS26b$^{-/-}$	Complete knockout	All cells
VPS26a$^{fl/fl}$ Camk2α-Cre KO	Complete knockout	Forebrain neurons
VPS26a$^{+/-}$	Haploinsufficiency	All cells

Figure 1.8 Mouse models of retromer-dependent endosomal dysfunction.

(a) Retromer-deficient models have been generated by deletion of cargo recognition core proteins VPS35, VPS26a, or VPS26b. (b) These models differ not only in the choice of core protein, but also the level and selectivity of deletion.

Finally, our design includes the translation of the most compelling CSF or exosomal findings to human subjects, either directly in the case of CSF or via extraction of brain-derived exosomes from human serum (Goetzl, Boxer et al. 2015).

We acknowledge that the analysis of two classes of molecules (lipids and proteins) in two biological reservoirs (CSF and exosomes) for the four retromer-deficient models listed above is an ambitious undertaking, requiring substantial time, materials, and animals. As such, we have chosen a self-refining approach, limiting our effort to those studies deemed the most fruitful and eliminating the continued use of techniques or animal models which carry limited promise of

biomarker discovery. Thus, not all techniques were performed for all rodent models, and not all findings were fully translated to human subjects.

2 Chapter 2: CSF Lipidomics

2.1 Introduction

2.1.1 Lipids and the endosome

Lipids comprise a diverse class of molecules which are critical for many aspects of cellular function including membrane formation, energy metabolism, signaling, and intracellular trafficking. Furthermore, lipids form the enclosing structure for not only cellular entities but an entire host of microvesicles (e.g. ectosomes, exosomes) they release into the extracellular space. In fact, studies have demonstrated that genetic defects which impede endolysosomal dynamics can affect not only internal lipid metabolism (Chen, Gordon et al. 2005), but also the population of secreted lipids (Strauss, Goebel et al. 2010), thus providing an extracellular signal of intracellular endosomal dysregulation. It follows, therefore, that retromer dysfunction may lead to alterations in intracellular lipid localization, and ultimately extracellular secretion.

2.1.2 Lipid dysregulation in AD

Lipid dysregulation has been observed in various pathologies including AD (Foley 2010, Di Paolo and Kim 2011, Morel, Chamoun et al. 2013). These observations include altered cholesterol metabolism and deficiencies of endosomal trafficking substituents such as PI3P (Foley 2010, Di Paolo and Kim 2011, Morel, Chamoun et al. 2013), an essential component for retromer assembly

(Rojas, van Vlijmen et al. 2008). As such dysregulation can result from endosomal dysfunction (Marquer, Tian et al. 2016), it is reasonable to postulate that these two observations may be linked in the AD brain.

2.1.3 Mass spectrometry of lipids

The advent of mass spectrometry in recent decades has paved the way for lipidomic investigation of cells, tissues, and biofluids, and has furthered our understanding of their biological relevance. LC-MS allows both qualitative and quantitative analyses and has shown great promise in biomarker discovery of various biological fluids (Capodivento, Visigalli et al. 2017, Zarrouk, Debbabi et al. 2017).

2.1.4 CSF lipidomics strategy

CSF collection in mice is not trivial. Roughly 5uL of fluid can be extracted from each mouse through the cisterna magna via a post-mortem technique, though the amount can vary based on a multitude of factors such as age, gender, and diet. Special care is required to minimize blood contamination as an intricate network of blood vessels overlay this tiny pocket of fluid, and substantial practice is warranted to attain the requisite precision and consistency for molecular profiling. Accordingly, the first step of this project involved mastery of high quality murine CSF collection, which is reported in the results that follow.

Upon commencement of this project, only a handful of murine CSF studies had been published, and none included lipidomics. Therefore, considering the relatively low concentration of lipids in

human CSF (roughly 10-13ug/mL) (Seyer, Boudah et al. 2016), we opted for a pooling approach, intended to maximize the amount of fluid for discovery while still operating within the limits of our mouse husbandry capacity. CSF collection from this retromer model yielded roughly 5-10uL per mouse (versus several milliliters from humans). Here, we chose to pool samples to a final volume of 30uL per biological replicate in order to boost the signal/noise ratio for the less abundant lipid species and ultimately expand the array of detectable lipids available for biomarker discovery.

2.1.5 Choice of the retromer-deficient model

We began our studies with the VPS26a-haploinsufficient mice for several reasons. First, haploinsufficiency is likely more reflective of the extent of retromer deficiency in AD patients than a complete knockout of retromer core proteins. Second, as retromer deficiency in AD may not be limited to neurons (Lucin, O'Brien et al. 2013), we chose to begin with a model in which the genetic deficit is shared among all cell types in the brain.

2.2 Results

2.2.1 Collection of high quality CSF

Murine CSF collection is a highly-skilled procedure which requires much practice to yield consistent results. In order to perform lipidomic investigations of murine CSF, we first needed to ensure that we could collect high quality samples from our rodent models. As blood contamination could have tremendous impact on the results of our analyses (due to the distinct

molecular profiles of these two biofluids), we implemented a sensitive hemoglobin ELISA for quality assessment of individual samples.

CSF was collected from 40 agouti mice using a post-mortem procedure (Figure 2.1) and assessed for quality. Previously published blood contamination thresholds for murine CSF studies include 0.003% (Barten, Cadelina et al. 2011) and roughly 0.01% (Dislich, Wohlrab et al. 2015) (reported threshold for visible contamination). Using these two criteria we are able to isolate contamination-free CSF in these mice in 87% of samples (at a threshold of 0.003% blood contamination) or 95% (at a threshold of 0.01% blood contamination). Samples passing the most stringent of thresholds was used for downstream analyses.

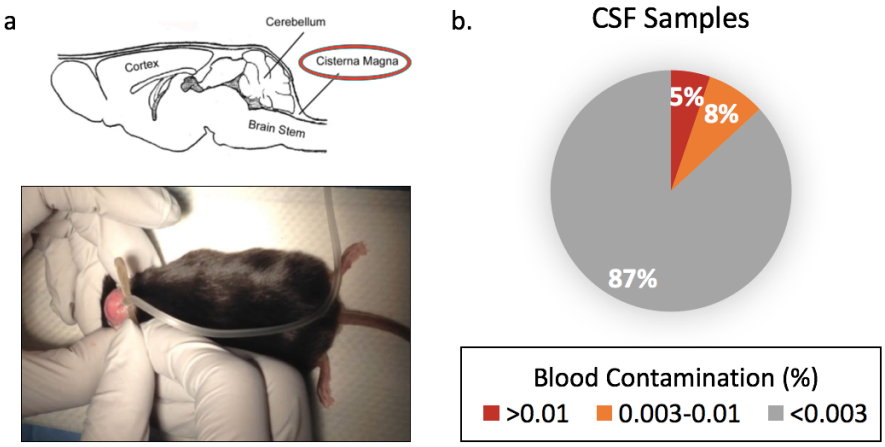

Figure 2.1 Collection of high quality CSF.

(a) Murine CSF was collected through the cisterna magna in a post-mortem procedure. (b) Forty samples were obtained from agouti mice and assessed for quality using two blood contamination thresholds which have been previously reported: 0.003% and 0.01% (Levy-Lahad, Wasco et al. 1995, Scarmeas, Stern et al. 2006, Barten, Cadelina et al. 2011, Dislich, Wohlrab et al. 2015).

2.2.2 The murine CSF lipidome closely resembles that of humans

Utility of this strategy for purposes of biomarker discovery hinged greatly upon both our ability to detect lipids in a small volume of CSF and on substantial similarity in the composition of the mouse and human CSF lipidome. As murine lipidomic studies had not yet been reported at the time of this study, we felt it imperative to first characterize the murine CSF lipidome and compare its composition to that of human CSF.

To this end, we performed a pilot of LC-MS on lipids extracted from biological replicates of 30uL of pooled wildtype agouti CSF. First, it is worth noting that we were able to detect signal for nearly all lipid classes that are present in human CSF and that their overall contribution to the CSF lipidome is remarkably similar to that of humans (Figure 2.2a; results from independent runs). The limited volume (30uL for mice versus 300uL for humans), however, largely restricts discovery to the most highly abundant lipid species (cholesteryl esters, free cholesterol, phosphatidylcholine, sphingomyelins, diacylglycerol, triacylglycerol, and lysophosphatidylcholine). And often, within each lipid class, not all individual lipid species detectable in human CSF are detectable in such a small volume of wildtype mouse CSF (Figure 2.2b).

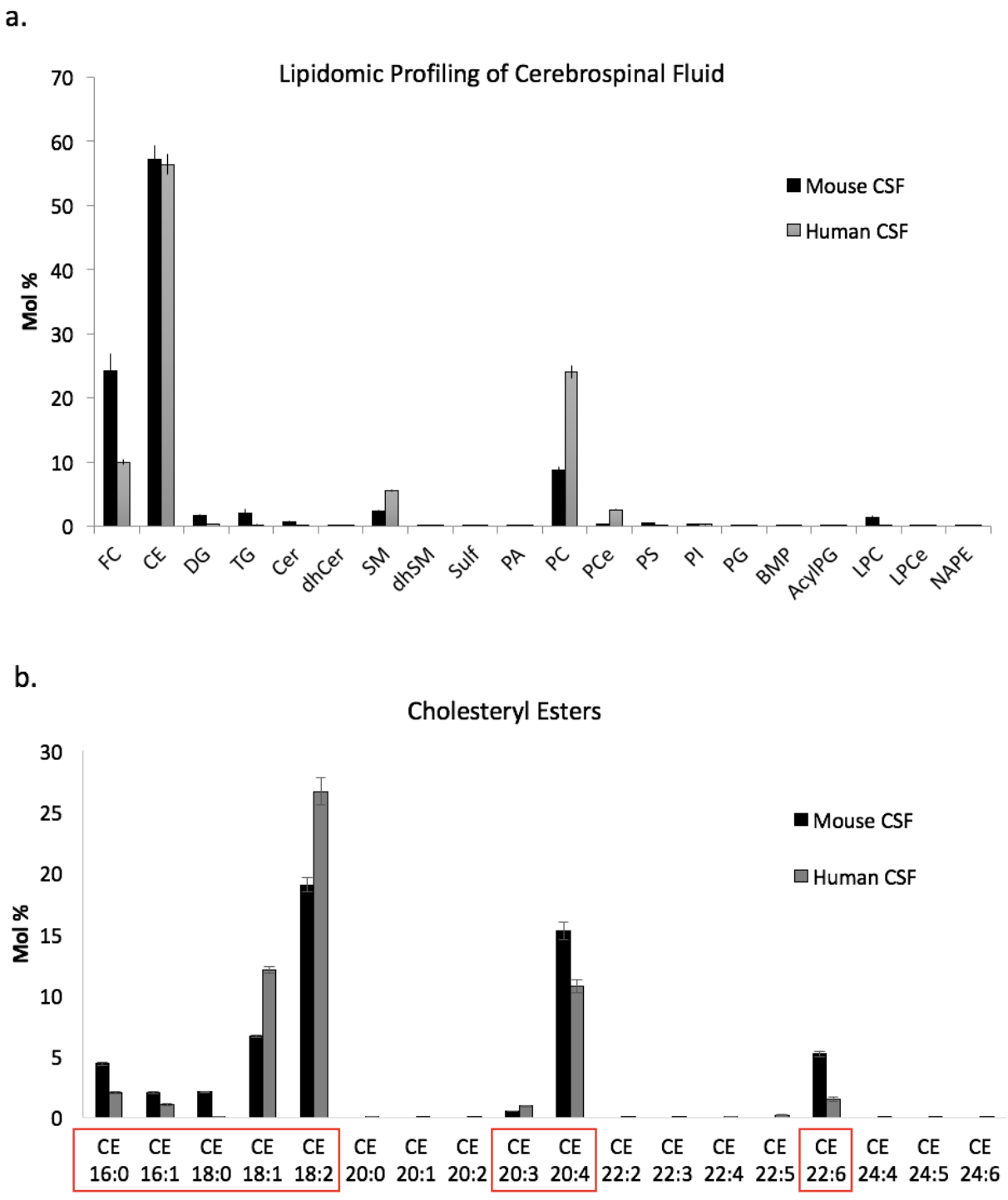

Figure 2.2 Comparison of the mouse and human CSF lipidome.

(a) High quality CSF from agouti wildtype mice underwent lipid extraction and was run via LC-MS in parallel (using six pooled biological replicates of 30uL each); internal standards provided

absolute quantitation. Separately, human (non-demented control) CSF samples were run via LC-MS in parallel using 300uL per sample. Lipid classes are reported as a percentage of total detected lipid species (mol %); FC=free cholesterol; CE=cholesteryl ester; AC= acyl carnitine ; MG=monoacylglycerol; DG=diacylglycerol; TG=triacylglycerol; Cer=ceramide; dhCer= dihidroceramide; SM=sphingomyelin; dhSM=dihidrosphingomyelin; GalCer=galactosylceramide; Sulf=sulfatide; PA= phosphatidic acid; PC=phosphatidylcholine; PCEe=phosphatidylcholine ether; PS=phosphatidylserine; PI=phosphatidylinositol; PG=phosphatidylglycerol; BMP=bismonoacylglycerophosphate; AcylPG=acyl-phosphatidylglycerol; LPC=lysophosphatidylcholine; LPCe=lysophosphatidylcholine ether; NAPE=N-acyl phosphatidylethanolamine; NSer= N-acyl serine. (b) Lipid classes are further broken down into the individual molecules which comprise that class. Of the eighteen cholesteryl esters identified in human CSF, the eight most highly abundant were also detected in 30uL of murine CSF (red boxes), suggesting a high level of similarity in the murine and human CSF lipidome.

2.2.3 Lipidomic screen reveals sphingomyelin changes in the CSF of VPS26a-haploinsufficient mice

We therefore applied this pooling approach to our investigation of CSF lipid changes in the VPS26a$^{+/-}$ mice (Figure 2.3). High quality CSF from 3-month-old VPS26a$^{+/-}$ males and littermate controls were pooled into six biological replicates. Following lipid extraction and addition of internal standards, LC-MS was performed for all twelve replicates in parallel.

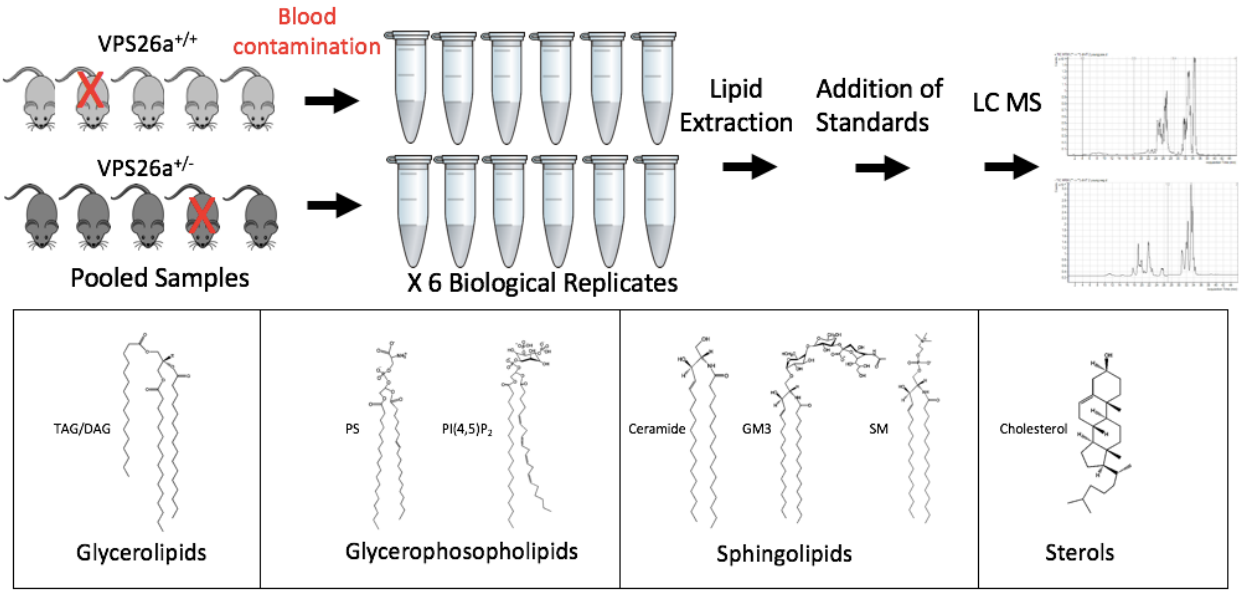

Figure 2.3 VPS26a$^{+/-}$ CSF lipidomics study overview.

CSF was collected from VPS26a$^{+/-}$ mice and control littermates. Contamination-free samples were pooled into biological replicates and run via LC-MS following lipid extraction and the addition of internal standards for absolute quantitation.

A global comparison of the general lipid classes revealed no significant changes in the CSF from 3-month-old VPS26a$^{+/-}$ mice as compared with their littermate controls (Figure 2.4a). However, a closer look at the individual lipid species suggested altered sphingomyelin secretion into the CSF by the VPS26a-haploinsufficient brain (Figure 2.4b). In particular, four sphingomyelin species (d18:1/18:1, d18:1/22:1, d18:1/24:1, and d18:1/26:0) were decreased in CSF from the VPS26a knockdown mice. Interestingly, SM d18:1/18:1 was able to distinguish the two genotypes with a 92% diagnostic accuracy ($p<0.01$) in a regression model.

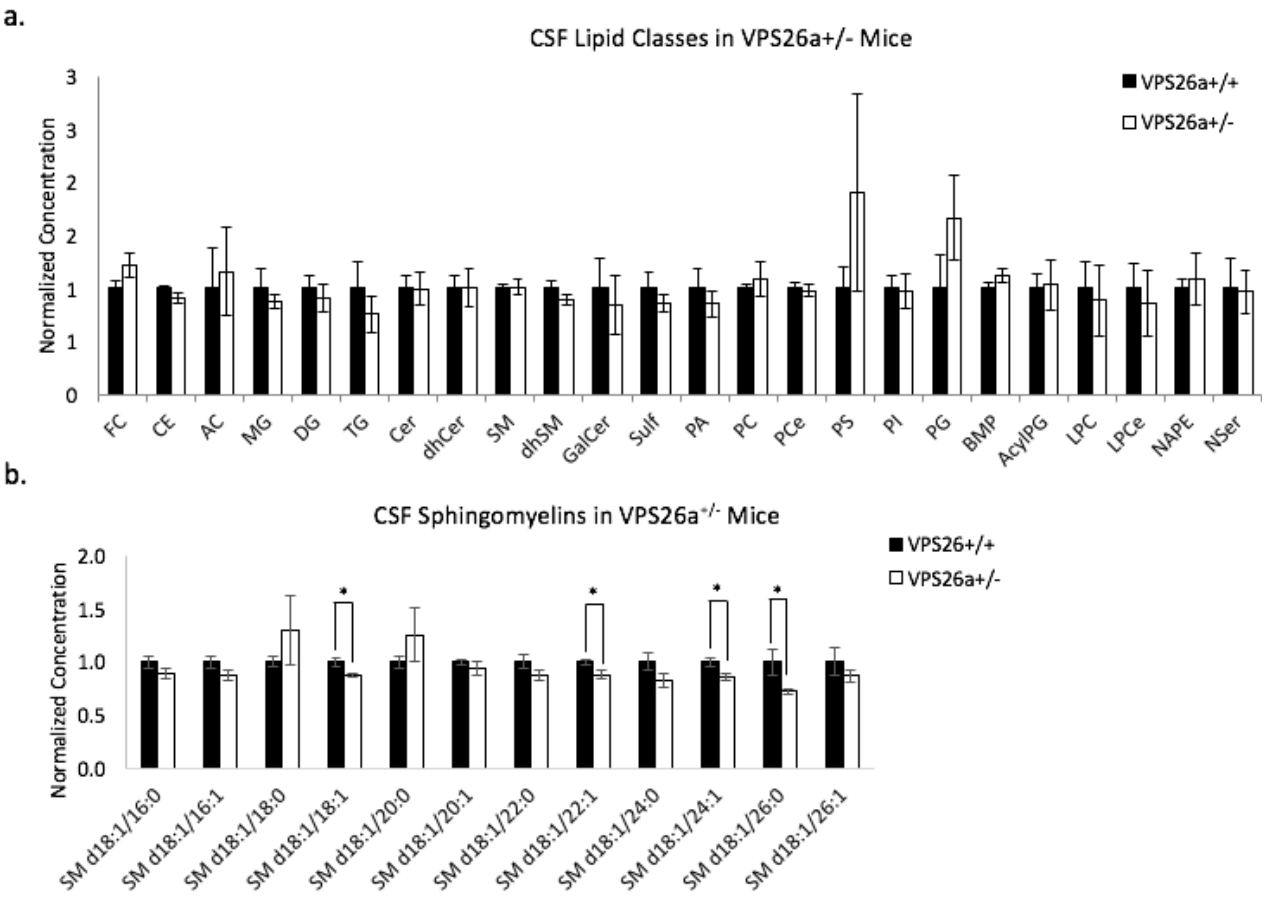

Figure 2.4 Lipidomic screen reveals altered sphingomyelin profile in VPS26a$^{+/-}$ CSF.

(a) VPS26a haploinsufficiency imparts no significant changes to the classes of CSF lipids. Values are normalized to total lipid content and then to the wildtype and represent the mean +/- SEM (n=6); FC=free cholesterol; CE=cholesteryl ester; AC= acyl carnitine ; MG=monoacylglycerol; DG=diacylglycerol; TG=triacylglycerol; Cer=ceramide; dhCer= dihidroceramide; SM=sphingomyelin; dhSM=dihidrosphingomyelin; GalCer=galactosylceramide; Sulf=sulfatide; PA= phosphatidic acid; PC=phosphatidylcholine; PCEe=phosphatidylcholine ether; PS=phosphatidylserine; PI=phosphatidylinositol; PG=phosphatidylglycerol; BMP=bismonoacylglycerophosphate; AcylPG=acyl-phosphatidylglycerol; LPC=lysophosphatidylcholine; LPCe=lysophosphatidylcholine ether; NAPE=N-acyl

*phosphatidylethanolamine; NSer= N-acyl serine. (b) A breakdown of individual sphingomyelin species reveals decreases in SM d18:1/18:1, d18:1/22:1, d18:1/24:1, and d18:1/26:0. Values are normalized to total lipid content and then to the wildtype and represent the mean +/- SEM (n=6; *P-values<0.5)*

We sought to validate these findings from our initial screen in a new cohort of mice using CSF from individual samples. Here, we selected a more targeted approach, assessing only positive-mode lipids which includes the sphingomyelin class. This allowed us to concentrate signal in the lipid category of interest instead of splitting into three modes. We were hopeful that this approach would compensate for the smaller volume available for this follow-up validation. Despite our efforts, however, we were unable to detect two of the sphingomyelin species (d18:1/26:0 and d18:1/26:1) from the first cohort of pooled CSF. Among the remaining ten, d18:1/18:1 was once again markedly reduced in the retromer-deficient CSF, confirming its decrease in the VPS26a-deficient brain, while most remaining sphingomyelin species showed a trend toward decrease (Figure 2.5).

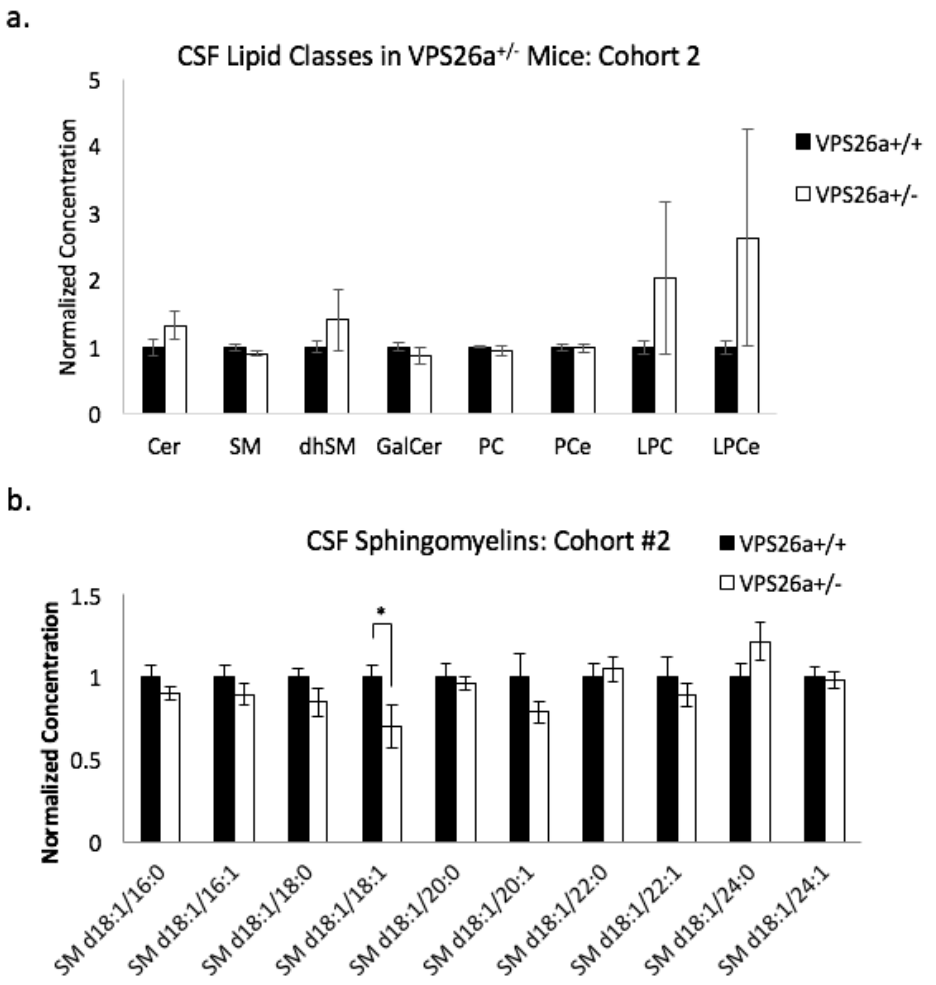

Figure 2.5 Follow-up study in new cohort confirms decrease of SM d18:1/18:1 in VPS26a$^{+/-}$ CSF. *A follow-up analysis of CSF from individual 3-month-old VPS26a$^{+/-}$ mice and littermate controls was conducted. (a) No changes in the positive mode lipid classes were observed. Values are normalized to total lipid content and then to the wildtype and represent the mean +/- SEM (n=6); Cer=ceramide; SM=sphingomyelin; dhSM=dihidrosphingomyelin; GalCer=galactosylceramide; PC=phosphatidylcholine; PCEe=phosphatidylcholine ether; LPC=lysophosphatidylcholine; LPCe=lysophosphatidylcholine ether. (b) A breakdown of individual sphingomyelin species reveals decreases in SM d18:1/18:1, d18:1/22:1, d18:1/24:1, and d18:1/26:0. Values are normalized to total lipid content and then to the wildtype and represent the mean +/- SEM (n=6; *P-values<0.5)*

*(b) Among the ten sphingomyelins detected in these samples, SM d18:1/18:1 was again significantly reduced in VPS26a$^{+/-}$ CSF. Values are normalized to the wildtype and represent the mean +/- SEM (n=8; *P-value<0.05).*

2.2.4 Reductions in VPS26a$^{+/-}$ CSF sphingomyelins are more pronounced with age and extend to other lipid groups

Curious as to what effect age might have on the CSF sphingomyelin profile in these mice, we repeated this experiment using individual samples in 6-month-old mice. Again, sphingomyelin d18:1/18:1 was reduced in the CSF, as well as d18:1/20:1, and d18:1/20:0, d18:1/22:0, and d18:1/24:0 (Figure 2.6b). Generally, all sphingomyelin species showed a downward trend in the VPS26a$^{+/-}$ mice, and in fact the entire class of sphingomyelins was reduced (Figure 2.6a), a trend which did not reach significance in younger cohorts.

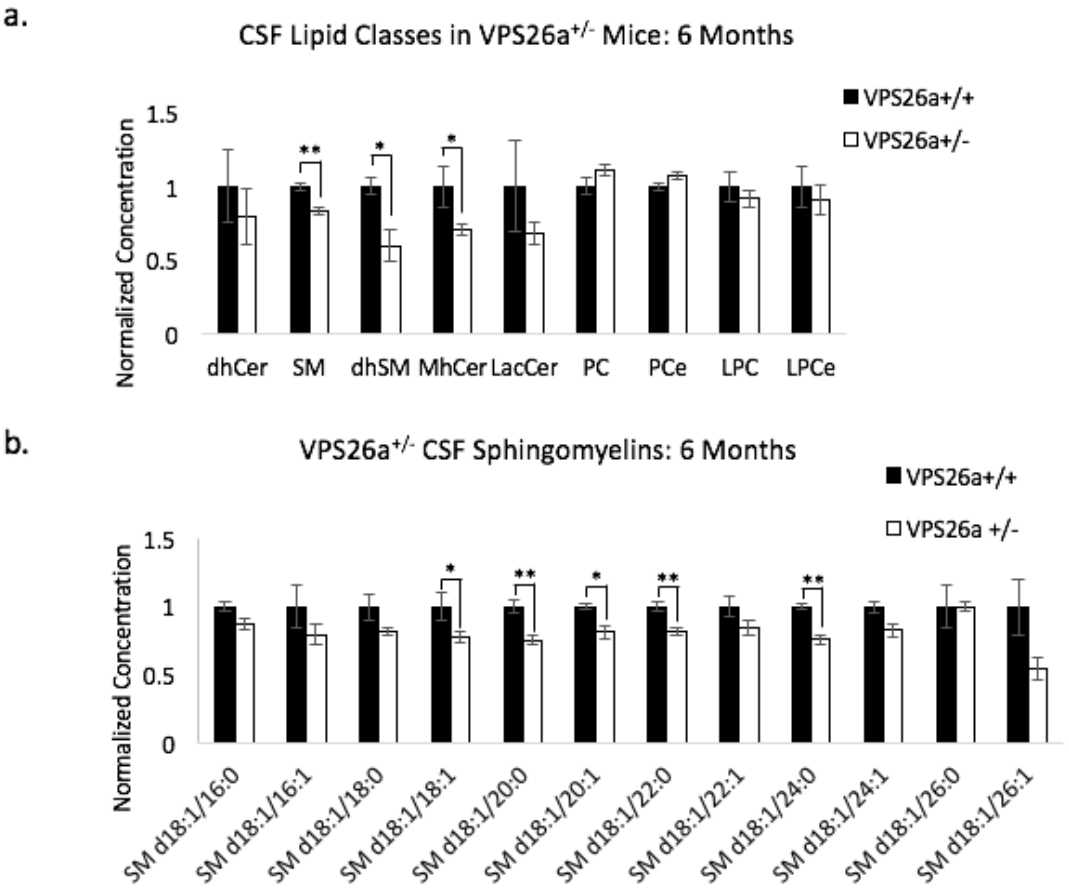

Figure 2.6 Age exacerbates sphingomyelin profile in VPS26a$^{+/-}$ CSF and extends effects to other lipid classes.

*In a targeted investigation of positive-mode CSF lipids, three entire lipid classes are significantly reduced: sphingomyelins (SM), dihydrosphingomyelins (dhSM), and monohexosylceramides (MhCer). Values are normalized to the wildtype and represent the mean +/- SEM (n=3-5; *P-value<0.05, **P-value<0.01); dhCer= dihidroceramide; Cer=ceramide; LacCer= lactosylceramide; GalCer=galactosylceramide; PC=phosphatidylcholine; PCEe=phosphatidylcholine ether; LPC=lysophosphatidylcholine; LPCe=lysophosphatidylcholine ether. (b) A breakdown of individual sphingomyelin species reveals reduction of five lipids in the VPS26a$^{+/-}$ CSF: SM d18:1/18:1, SM*

*d18:1/20:0, SM d18:1/20:1, SM d18:1/22:0, SM d18:1/24:0. Values are normalized to the wildtype and represent the mean +/- SEM (n=3-5; *P-value<0.05, **P-value<0.01).*

Unexpectedly, alterations in other lipid classes appeared in the 6-month-old VPS26a$^{+/-}$ CSF; these included reductions in both dihydrosphingomyelins and monohexosylceramides (Figure 2.6a). Taken together, these studies indicate progressive sphingolipid dysregulation in the VPS26a-haploinsufficient brain, which can be detected via CSF reporters such as sphingomyelin d18:1/18:1 at three months (and likely other species at later time points).

2.2.5 Sphingomyelin dysregulation in the VPS26a$^{+/-}$ brain is non-neuronal

VPS26 haploinsufficiency results in a knockdown of this core retromer protein in all cells of the brain. As VPS26a is expressed in all brain cell types (Figure 2.7a) (Zhang, Chen et al. 2014), it is difficult to speculate which cell type might be responsible for imparting these sphingoliid changes. In order to explore this in vivo, we made use of our VPS26a neuron-specific knockout (via Camk2α-Cre recombinase). Since VPS26a deficiency in this mouse model is restricted to neurons, a comparison of CSF lipidomics from the two VPS26a models can indicate whether the sphingomyelin dysregulation is driven by neuronal retromer deficiency or instead by other cell types. (We acknowledge this isn't a perfect comparison since the VPS26a$^{+/-}$ model is haploinsufficient for VPS26a while the VPS26a Camk2α knockout model is fully depleted of the gene in neurons. However, if the sphingomyelin changes were coming from neurons, we would expect an even more pronounced phenotype in the Camk2α knockouts.)

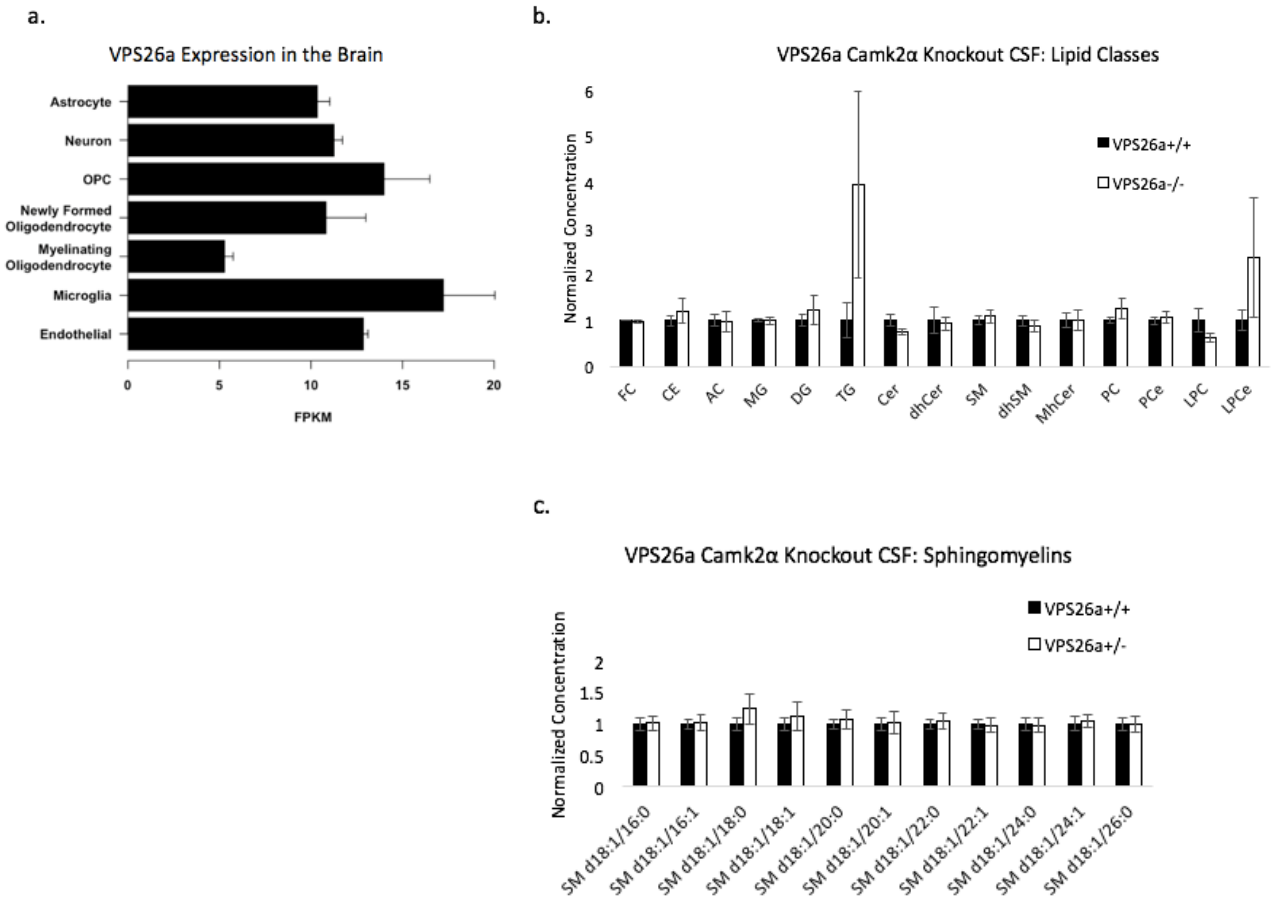

Figure 2.7 Sphingomyelin alterations in VPS26a-haploinsufficient mice derive from non-neuronal origins.

*(a) VPS26a is expressed in many cell types in the brain (Zhang, Chen et al. 2014). A global assessment of lipidomic changes reveals no changes in sphingomyelins (SM), dihydrosphingomyelins (dhSMs), or monohexosylceramides (MhCer) in the VPS26a Camk2α mice, as noted at this age in the VPS26a-haploinsufficient mice. (b) Additionally, no changes in any sphingomyelins are observed in the VPS26a Camk2α CSF. Values are normalized to the wildtype and represent the mean +/- SEM (n=4-6; *P<0.05).*

To this end, we collected CSF from 6-month-old VPS26a Camk2α knockout mice and littermate controls and repeated the lipidomics experiment. A comparison of lipid classes reveals a distinct global profile in the CSF of these retromer-deficient mice as compared with the VPS26a$^{+/-}$ model. Changes in sphingomyelins, dihydrosphingomyelins, and monohexosylceramides observed in CSF from 6-month-old VPS26a$^{+/-}$ mice are not shared in the 6-month-old VPS26a Camk2α knockouts (Figure 2.7b). Furthermore, a breakdown of the sphingomyelin class reveals no changes in any individual lipid species (Figure 2.7c). We therefore conclude that the sphingomyelin changes observed in VPS26a$^{+/-}$ CSF are the result of retromer deficiency in a non-neuronal cell type.

An additional conclusion from this comparison is that retromer deficiency in different cell types of the brain can lead to distinct CSF lipid profiles, and that complete knockdown of VPS26a in neurons imparts no detectable changes to the CSF lipidome.

2.3 Discussion

The study of lipids in the context of pathology has gained increasing momentum over the past few decades, propelled by advancements in mass spectrometry technology. To our knowledge, this study represents the first attempt in utilizing this technology to characterize the mouse CSF lipidome, and to gauge its feasibility in reporting on endosomal dysfunction in the brain. The overwhelming similarity in the lipid profile of mouse and human CSF suggests this technique as a fruitful means of biomarker discovery.

Despite the small volume of mouse CSF available for mass spectrometry, 172 lipid species were detected and quantified in our initial screen using pooled replicates of 30uL each. This is over 50% of the number detected in 300uL of human CSF (318 species) using the same technology. It is worth mentioning that pooling CSF from mice of the same genotype (30uL volume) was favorable over analyzing individual samples (7uL volume) in maximizing the number of quantifiable lipids (by 20% in the case of sphingomyelins). In the end, we deem murine CSF lipidomics a feasible means of biomarker detection in at least half of the human CSF lipidome.

In this study, we conclude that VPS26a haploinsufficiency alters the sphingomyelin profile in murine CSF and that the profile intensifies with age, extending into other lipid classes (dihydrosphingomyelins and monohexosylceramides). The most consistent of these changes is sphingomyelin is SM d18:1/18:1, which was depicted in all cohorts from each age group.

It is interesting to note, however, that all of these changes seem to derive entirely from non-neuronal cells. In fact, complete deletion of VPS26a in neurons (via Camk2α-Cre) resulted in no significant alterations in the CSF. We wonder whether this might indicate a more prominent role for the VPS26a-containing assembly in a glial cell type, at least in its effects on the extracellular lipidome.

Determining the source of these sphingomyelin changes in the brain would require the generation of alternative cell type-specific knockdown models, or alternatively, in vitro knockdown of individual cell types for lipidomic assessment of their secretome. Furthermore,

studies of CSF sphingomyelins in AD patients have provided conflicting results (though a majority suggest elevation of this lipid class in AD) (Kosicek, Zetterberg et al. 2012, Fonteh, Ormseth et al. 2015), rendering the development of a sphingomyelin biomarker a potentially complicated task. As this project progressed simultaneously along multiple fronts, we opted to instead focus our efforts on our parallel proteomic studies which yielded more compelling results.

3 Chapter 3: Brain Exosomes

3.1 Introduction

3.1.1 Exosome biology

Exosomes are small (30-150nm), secreted, membrane-bound products of the endosomal system. They can travel via bodily fluids within and between organs, carrying with them preserved material from their originating cells (Costa-Silva, Aiello et al. 2015, Hoshino, Costa-Silva et al. 2015, Zhang, Zhang et al. 2015), and are thought to be fairly resistant to circulating proteases in biological fluids. As such, they have been increasingly studied in the past decade for their ability to report on disease states (Goetzl, Boxer et al. 2015, Abner, Jicha et al. 2016, Goetzl, Mustapic et al. 2016). More recently, they have even been implicated in various pathologies, as primers for metastasis of primary tumors and vehicles for the spread of protein aggregates in AD (Perez-Gonzalez, Gauthier et al. 2012, Asai, Ikezu et al. 2015, Xiao, Zhang et al. 2017).

3.1.2 Exosomes as reporters of endosomal dysfunction

Four key observations support the hypothesis that retromer-mediated endosomal dysfunction in the murine brain might alter the content of secreted exosomes. First, it has been demonstrated by several independent studies that endolysosomal dysfunction can alter the protein and/or lipid profile of exosomes (Yuyama, Yamamoto et al. 2008, Strauss, Goebel et al. 2010, Alvarez-Erviti, Seow et al. 2011). Second, retromer dysfunction specifically has been shown to alter the protein content of exosomes in vitro (Sullivan, Jay et al. 2011). Third, proteins which comprise the cargo recognition core of retromer have been detected in exosomes of bodily fluids (Reinhardt, Sacco et al. 2013). And fourth, a recent study of neuronally-derived exosomes from AD patients revealed changes in a group of endolysosomal proteins (Goetzl, Boxer et al. 2015).

3.1.3 Brain exosome biomarker strategy

Importantly, two recent advancements in exosome isolation make feasible the study of murine brain exosomes for biomarker discovery. First, a technique for isolating brain-derived exosomes in human serum was described (Goetzl, Boxer et al. 2015, Goetzl, Boxer et al. 2015, Abner, Jicha et al. 2016), providing the first ever acquisition of brain-specific exosomes in vivo. And second, the development of a protocol for isolating adult mouse brain exosomes (Perez-Gonzalez, Gauthier et al. 2012, Asai, Ikezu et al. 2015) allows the interrogation of rodent models of disease, reducing the translational hurdles and boosting the exosome yield over conventional cell culture studies. Thus, at least in theory, biomarkers identified in murine brain exosomes can now be developed for evaluation in human serum-circulating exosomes of brain origin.

As a result, we endeavored to characterize the brain exosomes from several of our retromer-deficient models. Informed by our lipidomic study in the VPS26a-haploinsufficient mice (where we noted a mild CSF lipidomic phenotype of non-neuronal origin), we opted to perform our work in complete retromer knockout models: the VPS35$^{fl/fl}$ Camk2α-Cre KO and the VPS26b knockout.

3.2 Results

3.2.1 Isolation of brain-derived exosomes from wildtype mice: validation of technique

Exosome isolation from rodent brains is not a trivial task (Perez-Gonzalez, Gauthier et al. 2012). It includes multiple rounds of ultracentrifugations, and an 18-hour iodixanol (optiprep) gradient separation (Figure 3.1a). We initially sought to validate this protocol using previously established biochemical and physical properties of exosomes (Figure 3.1b-d). In a pilot of wildtype mice, we determined that gradient fractions 4-7 are enriched in exosomal markers alix and flotillin-1, contain 30-150nm vesicles of exosomal morphology, and float between 1.07 and 1.11g/mL, similar to those reported previously for iodixanol gradient isolations (Collino, Pomatto et al. 2017, Klingeborn, Dismuke et al. 2017). As such, we utilized these exosome-enriched fractions for all downstream analyses described herein.

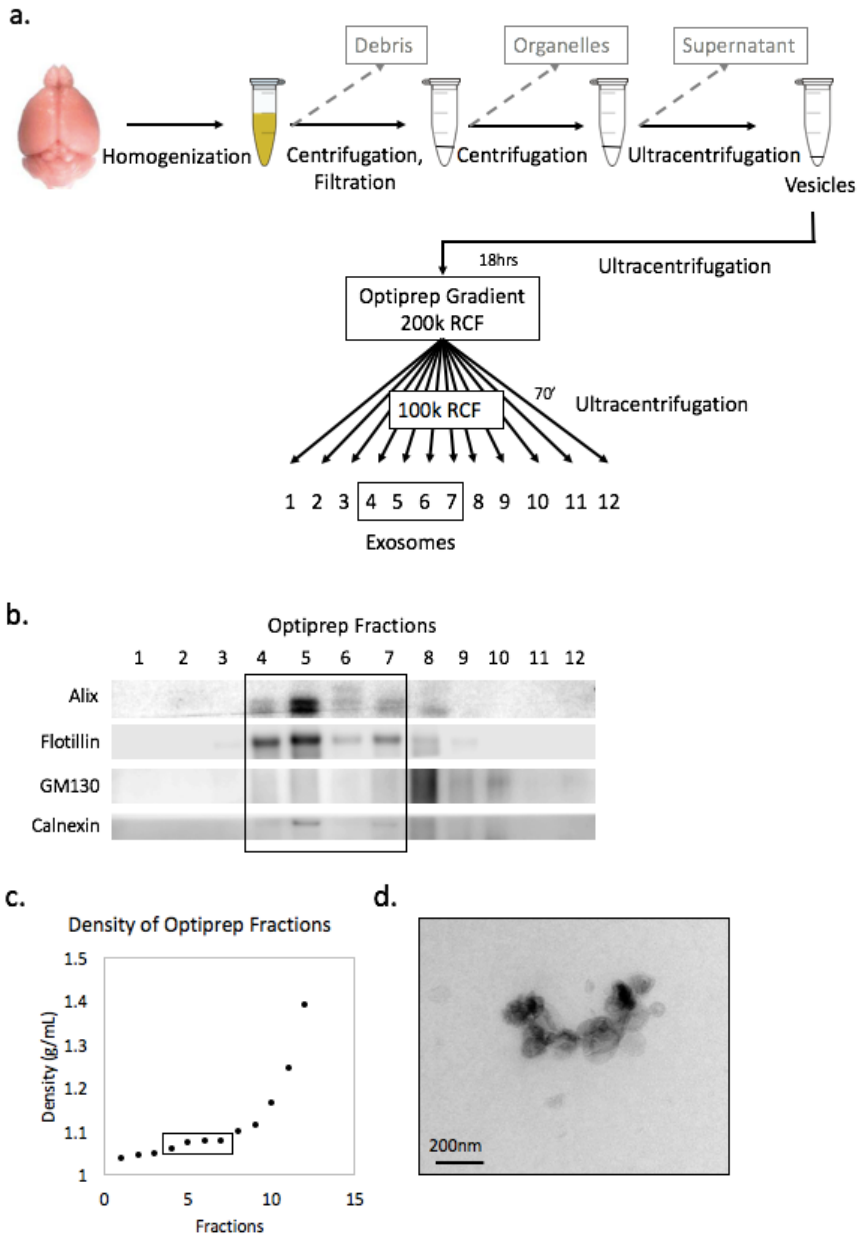

Figure 3.1 Isolation of high quality exosomes from adult murine brain.

(a) Exosome isolation from brain tissue requires multiple steps. (b) Exosome-enriched fractions are positive for markers alix and flotillin-1 with limited contamination from other cellular compartments (golgi as measured by GM130 and ER as measured by calnexin). (c) These fractions float at a density of 1.07-1.11g/mL, similar to that previously reported for iodixanol gradients

(Collino, Pomatto et al. 2017, Klingeborn, Dismuke et al. 2017). (d) Electron microscopy reveals vesicles 30-150nm in diameter displaying the conventional exosome morphology.

3.2.2 Retromer core proteins are present in brain exosome fractions

Several groups have reported the presence of retromer cargo recognition core proteins in exosomes of various tissues or fluids (Gonzales, Pisitkun et al. 2009, Demory Beckler, Higginbotham et al. 2013, Skogberg, Gudmundsdottir et al. 2013). Therefore, we wondered whether we could detect these retromer proteins in brain-derived exosomes of adult mice. Using the technique described above, we isolated exosomes from the brains of wildtype mice and probed for retromer core proteins VPS35 and VPS26a (Figure 3.2a). In fact, both of these proteins were present preferentially in the exosome-enriched fractions. In a separate study, we also detected retromer core protein VPS26a on intraluminal vesicles (ILVs) of multi-vesicular bodies (MVBs) in neuronal cultures (Figure 3.2b); as MVBs can ultimately give rise to exosomes via fusion with the plasma membrane, we present this observation in support of the notion that retromer cargo proteins can associate with exosomes in the brain.

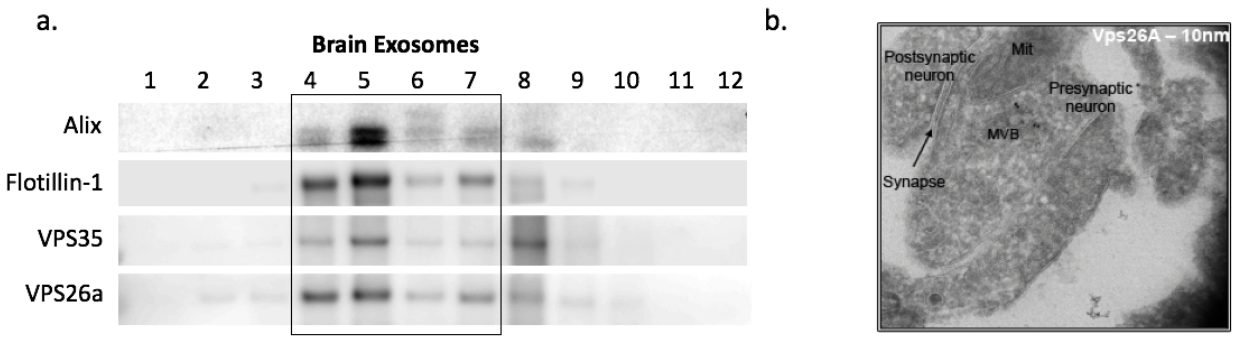

Figure 3.2 Retromer cargo recognition core proteins are present in brain exosome fractions.

(a) Cargo recognition core proteins VPS35 and VPS26a are detected in exosome fractions isolated from wildtype mouse brain. (b) Retromer core protein VPS26a is found on intraluminal vesicles (ILVs) of a multivesicular body (MVB) in wildtype mouse neurons.

3.2.3 Brain exosomes derived from retromer-deficient mice have reduced retromer protein levels

We next asked whether the levels of retromer proteins in brain-derived exosomes would reflect those in the brain tissue, and as such, provide a means of reporting on retromer deficiency in the brain. To investigate, we isolated brain exosomes from two retromer knockout models (VPS26b knockout and VPS35 Camk2α knockout) and compared the levels of retromer cargo proteins with those in exosomes of the controls (Figure 3.3).

Mice lacking neuronal-enriched core protein VPS26b exhibit a deficiency of core proteins VPS35 and VPS29 in the brain, while levels of its paralog VPS26a are largely unchanged, attributed to their nonreduntant inclusion in distinct retromer assemblies (Figure 3.3a). Brain exosomes from these mice reveal a noticeably similar pattern among retromer protein levels (Figure 3.3a).

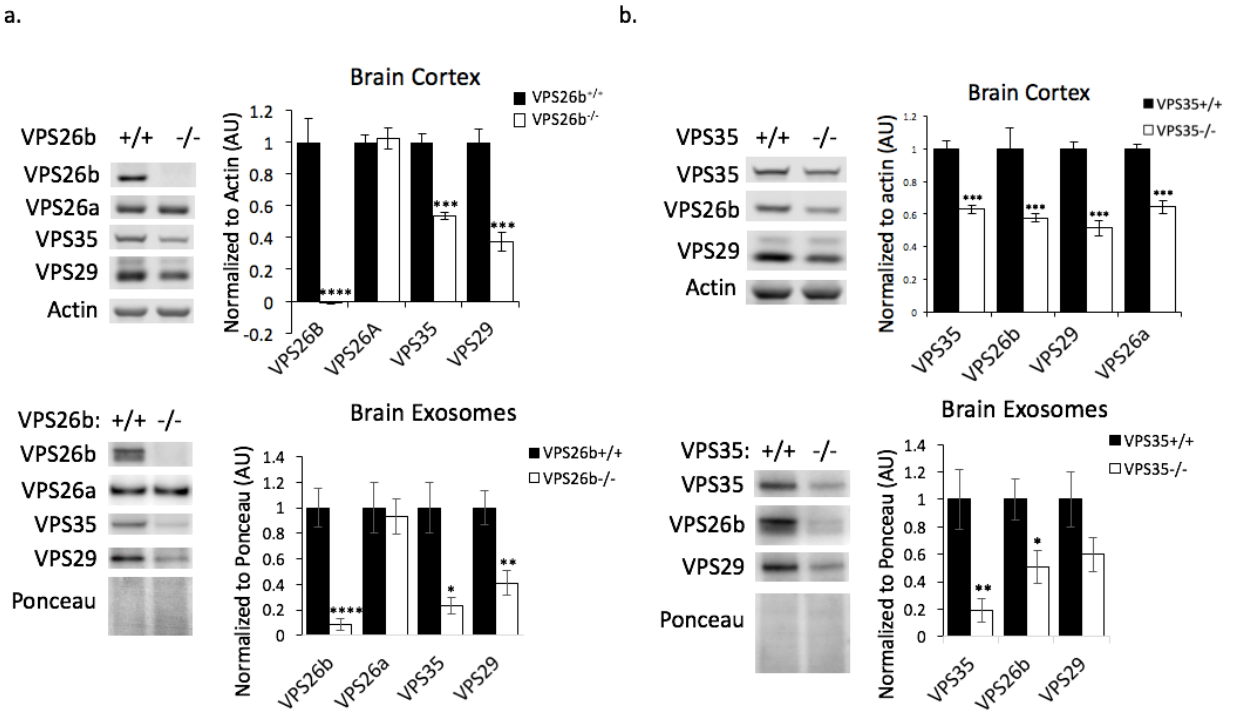

Figure 3.3 Murine brain exosomes reflect retromer deficiency in the brain.

*(a) Mice bearing homozygous deletion of core protein VPS26b have reduced levels of core proteins VPS35, VPS26a, and VPS29 but no changes in VPS26a in both brain tissue and in brain-derived exosomes. (b) Mice with neuron-specific deletion of VPS35 (via Camk2α-Cre) show decreased levels of other core proteins in both the brain and in brain-derived exosomes. Values are normalized to the wildtype and represent the mean +/- SEM (n=3-9; *P-value<0.05, **P-value<0.01, ***P-value<0.001, ****P-value<0.0001; with brain lysate contribution from Sabrina Simoes).*

Knockout of the VPS35 via Camk2a-Cre recombinase causes a loss of all retromer core proteins in the brain (Figure 3.3b). Of the core proteins measured in exosomes from these mice (VPS35, VPS26b, and VPS29), we found a similar pattern of deficiency (Figure 3.3b). Collectively, these

data suggest that brain-derived exosome fractions, which contain retromer core proteins, may offer utility as a reporter of retromer levels in the brain.

3.2.4 Brain exosomes derived from retromer knockout mice are enriched in β-CTFs

While a biomarker of retromer deficiency may prove useful for a subset of patients, it is possible that AD-related retromer dysfunction can result from genetic mutations which have no effect on overall retromer levels. Therefore, we sought to investigate other functional readouts of retromer deficiency which might be released in association with exosomes.

APP, as described above, is a transmembrane protein which can be cleaved by several membrane-associated proteases in various cellular compartments. The resulting C-terminal fragments (CTFs) have been found in exosomes from cultured cells (Sullivan, Jay et al. 2011), as well as brain-derived exosomes (Perez-Gonzalez, Gauthier et al. 2012). Retromer deficiency increases retention of APP in the endosome (Bhalla, Vetanovetz et al. 2012), where it is most likely to be cleaved by BACE1 (Small and Gandy 2006), and endosomal membrane (bearing the BACE1-cleaved CTF) serves as starting material for exosomal biogenesis. Therefore, we hypothesized that exosomes from retromer-deficient brains would be enriched in these BACE1-cleaved CTFs (β-CTFs). In fact, the elevation of CTFs in exosomes has previously been described as a result of retromer deficiency in HEK-293 cells (Sullivan, Jay et al. 2011).

To this end, we isolated exosomes from the two models described above and their wildtype littermates and probed the samples with an antibody directed toward an epitope within the β-

CTF region of APP (M3.2). Interestingly, brain exosomes from both the neuron-enriched and neuron-selective knockouts (VPS26b knockout and VPS35 Camk2α knockout) revealed a striking elevation in the levels of β-CTFs (Figure 3.4a). We were unable to detect full-length APP in the brain exosomes of either the wildtype or knockout mice, which corroborates prior reports that full-length APP is scarcely found in exosomes as compared with its cleaved C-terminal fragments (Perez-Gonzalez, Gauthier et al. 2012). A comparison with hippocampal lysate from the VPS26b knockouts (Figure 3.4b) indicates that this effect is concentrated in the endosomal compartments which give rise to these exosomes. Taken together, these findings demonstrate that increased amyloidogenic processing of APP in the endosome of neuronal retromer knockouts can be detected in brain-derived exosomes via enrichment of β-CTFs.

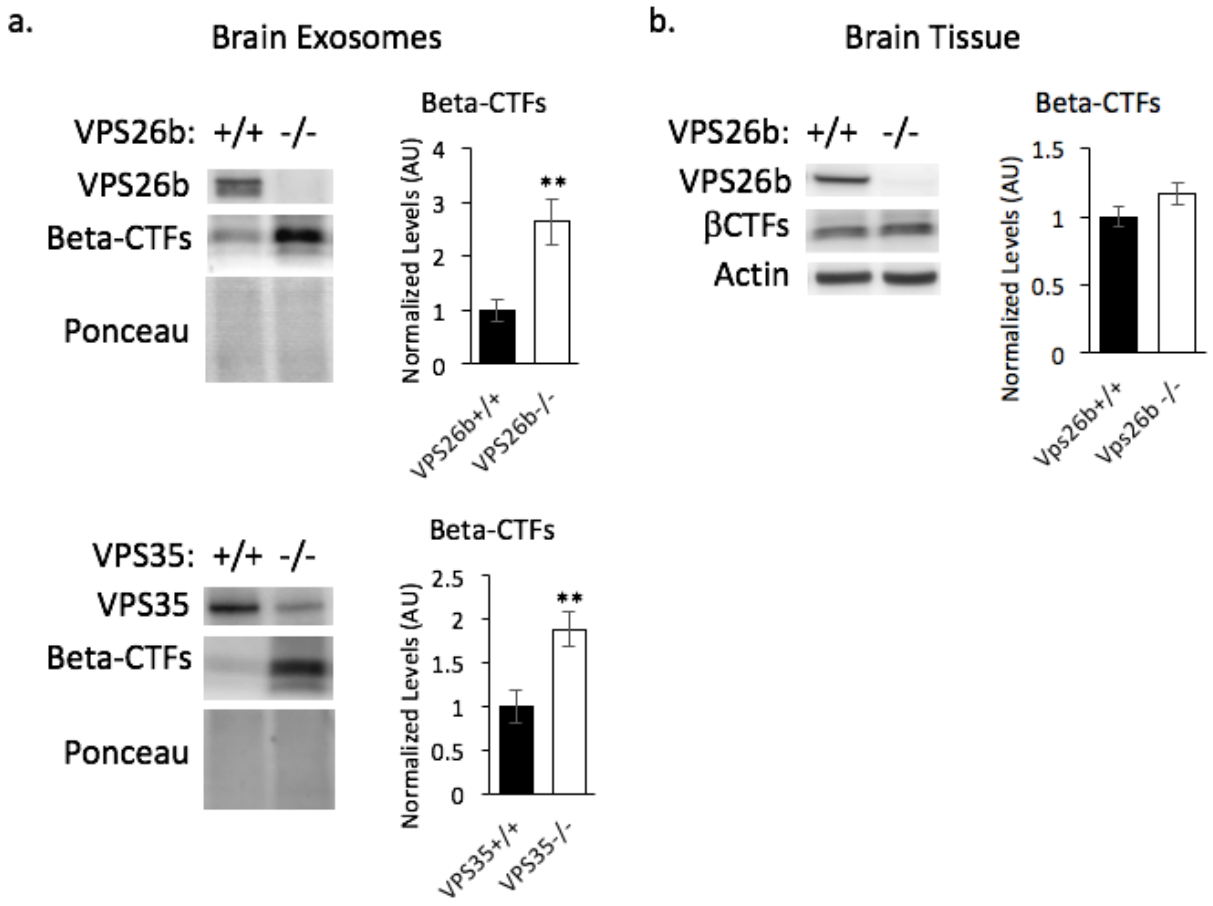

Figure 3.4 Retromer deficiency in vivo promotes β-CTF accumulation in exosomes.

*(a) Full knockout of VPS26b and neuronal-selective knockout of VPS35 (via Camk2α Cre) increase the accumulation of β-CTFs detected in purified brain exosomes. Values are first normalized to ponceau and then the wildtype average and represent the mean +/- SEM (n=8-9; *P-value<0.05, **P-value<0.01). (b) Hippocampal tissue lysates from VPS26b knockout mice show only a modest trend toward increase in β-CTFs (n=4; tissue lysate contributed by Sabrina Simoes).*

3.2.5 Brain exosomes from retromer knockout mice have decreased levels of exosomal markers alix and flotillin-1

In the course of our brain exosome studies, we happened upon an entirely unexpected finding: that brain exosomes from retromer knockout mice contain lower levels of two conventional exosome markers alix and flotillin-1 (Figure 3.5). Though this trend did not reach significance in the VPS35 Camk2α knockout mice (perhaps due to high variability between samples), it was clear in the VPS26b knockout model, with a roughly 50% reduction as measured by immunoblot.

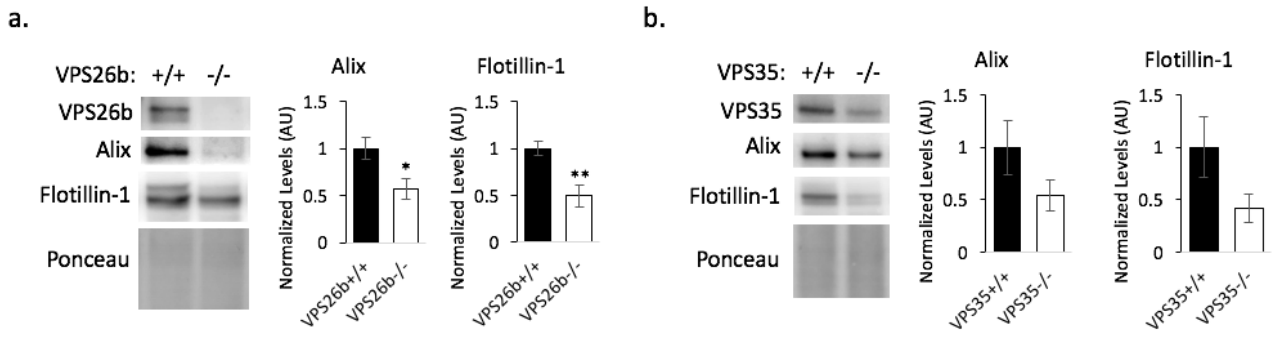

Figure 3.5 Brain exosomes from VPS26b knockout mice contain reduced levels of canonical exosome markers

*(a) Brain exosomes isolated from VPS26b knockout mice have markedly reduced levels of exosome markers alix and flotillin-1 as measured by western blot. (b) A trend toward decrease of alix and flotillin-1, though not significant, is also observed in the VPS35 Camk2α model. Values are first normalized to ponceau and then the wildtype average and represent the mean +/- SEM (n=8; *P-value<0.05, **P-value<0.01).*

As alix and flotillin are often used to confirm exosomal identity, we wondered whether the decrease in these proteins in the exosomal fractions suggest changes in exosomal biogenesis, and possibly their morphology. Accordingly, we examined the brain exosomes from retromer

knockout (VPS26b$^{-/-}$) and control (VPS26b$^{+/+}$) mice using electron microscopy. Though overall exosomal morphology seemed to be fairly consistent between the two groups, we noted what seemed to be a shift toward smaller (<50nM in diameter) exosomes in the retromer knockout fractions as compared with the control (Figure 3.6). This descriptive observation was not tested statistically using biological replicates. However, if true, this finding would further suggest that retromer-dependent endosomal dysfunction can alter the biogenic pathways of exosomes, in addition to regulating their content.

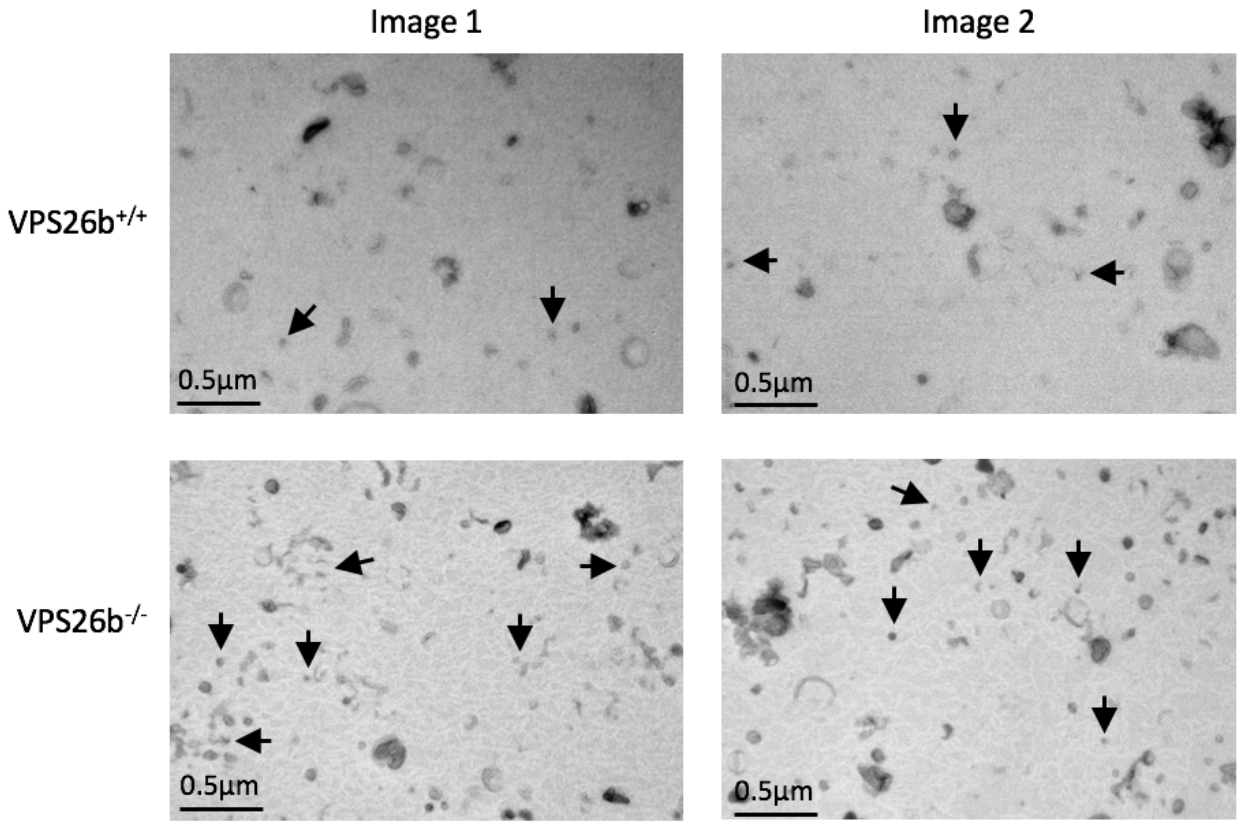

Figure 3.6 Descriptive electron microscopy reveals enrichment of smaller vesicles in VPS26b$^{-/-}$ brain exosomes.

A descriptive analysis (n=1) of exosome-containing fractions from VPS26$^{-/-}$ vs control brains reveals a perceived enrichment of smaller (<50nm vesicles, examples indicated with black arrows) in the knockout condition. Statistics were not performed.

3.3 Discussion

Our studies confirm the presence of cargo recognition core proteins in the exosome-containing fractions from murine brain and reveal that their levels reflect that of the cells from which they originate. Thus, at least in specific cases of retromer deficiency, they may be suited to report on overall retromer levels in the brain. We opted not to immediately pursue this finding for biomarker development, however, given that AD-related endosomal dysfunction may not be limited to a reduction of retromer levels.

Prior studies have demonstrated that endolysosomal dysfunction can alter the composition of secreted exosomes (Yuyama, Yamamoto et al. 2008, Strauss, Goebel et al. 2010, Sullivan, Jay et al. 2011). Our work is among the first to show confirmation of this phenomenon in vivo and that brain-derived exosomes might report on brain-specific endosomal dysfunction. Given retromer's role in diverting APP from amyloidogenic processing by BACE1 in the endosome (Small, Kent et al. 2005, Small and Gandy 2006, Wen, Tang et al. 2011, Bhalla, Vetanovetz et al. 2012), it isn't surprising that retromer deficiency promotes accumulation of β-CTFs, which can be loaded onto ILVs and secreted as exosomes into the extracellular space (Perez-Gonzalez, Gauthier et al. 2012). It is reasonable to postulate, however, that any cellular defect resulting in increased APP (or its

cleavage enzyme BACE1) in the neuronal endosome might promote the increased accumulation of these amyloidogenic fragments in brain-derived exosomes.

Unfortunately, we were unable to translate this finding to human patients, as we failed to detect β-CTFs in serum exosomes of brain origin via immunoblot. This result could arise from at least three different possibilities. First, this lack of detection could simply be due to inadequate sensitivity of the available technologies; in this case, the development of a more sensitive assay (such as a simoa (Childs-Disney, Wu et al. 2007, Wu, Milutinovic et al. 2015)) for the detection of β-CTFs could be useful. The second possibility is that exosome-associated β-CTFs are not fully retained in exosomes that cross the blood-brain barrier. As cleavage enzymes such as α-secretase (ADAM10), BACE1, and γ-secretase (nicastrin) have been detected in brain-derived exosome fractions (Perez-Gonzalez, Gauthier et al. 2012), one must consider that CTFs from the brain might be progressively processed throughout their transport into the bloodstream. And third, it remains entirely possible that exosomes which house β-CTFs simply do not cross the blood-brain barrier. While a growing number of studies have shown delivery of exosomes from the bloodstream into the brain (Yang, Martin et al. 2015, Khalyfa, Gozal et al. 2017), few have described the reverse transport (Goetzl, Boxer et al. 2015, Goetzl, Mustapic et al. 2016), and the mechanisms for exosomal traverse of the blood-brain remain largely unclear. (Whether exosomes are delivered across this barrier in a content-specific manner is currently unknown but should be considered as one potential explanation for the lack of β-CTFs in circulating serum exosomes.) If either of the latter two possibilities are true, then continued work for the development of an exosome-based biomarker should be strategized to overcome the challenge

of transport into the bloodstream. Accordingly, collection and interrogation (e.g. via mass spectrometry) of neuronally-derived exosomes already circulating in the bloodstream of mice with neuron-specific retromer deficiency could provide an optimal haven for discovery.

Finally, we report an unexpected finding: that retromer deficiency in vivo may alter exosome biogenic pathways. This conclusion is supported by a decrease in exosome markers alix and flotillin-1 in the exosome fractions from retromer-deficient mice and a potential (as yet descriptive) shift in exosome size. Recent studies by other labs have demonstrated that Alix may be functionally regulated by Arf6 (Ghossoub, Lembo et al. 2014), which can also regulate retromer (Marquer, Tian et al. 2016). Though the directionality of these relationships doesn't clarify the observed transcriptional effects of retromer deficiency on alix in our studies, it supports the notion that these processes of retromer-dependent endosomal trafficking and exosome biogenesis are tightly linked in the mammalian brain. Interestingly, work by one of our collaborators revealed that neuronally-derived exosomes from AD patients are smaller and are deficient in canonical exosome markers (in this case TSG101 and CD81) than those from controls (Tran 2017).

4 Chapter 4: CSF Proteomics

4.1 Introduction

4.1.1 Endosomal dysfunction and the secreted proteome

It is well documented that defects in endolysosomal function can alter the secreted proteome (Rojas, van Vlijmen et al. 2008, Tholen, Biniossek et al. 2011, Tholen, Biniossek et al. 2014). Moreover, recent work has demonstrated that retromer-dependent endosomal dysfunction results in an increased secretion of Aβ (Bhalla, Vetanovetz et al. 2012) and cathepsin D (Rojas, van Vlijmen et al. 2008). Both of these molecules migrate into the CSF, and in fact accumulate in AD patients along with other key components of the endolysosomal system (Schwagerl, Mohan et al. 1995, Armstrong, Mattsson et al. 2014). Taken together, these observations lead us to hypothesize that retromer deficiency in the rodent brain will induce measurable proteomic alterations in the CSF.

4.1.2 CSF Proteomics biomarker strategy

As mentioned previously, CSF collection in rodents is a highly technical procedure which yields minimal fluid (roughly 5uL). Nonetheless, several groups have successfully performed proteomics on murine CSF, detecting over 700 proteins in as little as 2uL of fluid per replicate (Smith, Angel et al. 2014, Dislich, Wohlrab et al. 2015). We therefore opted to use such an unbiased approach to maximize our biomarker discovery efforts in favor of hypothesis-driven immunoblotting (which is empirically biased, relies on availability of reactive antibodies, and can require even more CSF per replicate to detect signal).

CSF is relatively low in protein content (0.2-0.8mg/mL in humans (Rozek, Ricardo-Dukelow et al. 2007, Shores and Knapp 2007)) as compared with other biofluids such as serum (60-80mg/mL). Furthermore, CSF proteins span a wide dynamic range, up to 12 orders of magnitude in humans

(Huhmer, Biringer et al. 2006, Schutzer, Liu et al. 2010), with albumin and immunoglobulins occupying a large majority of the total (Yuan and Desiderio 2005). Therefore, as in the lipidomics study, we selected a strategy that involved the pooling of individual samples in the hopes of increasing the number of detectable proteins available for biomarker discovery.

Our study design involved the collection of high quality (blood contamination-free) CSF samples to be pooled into biological replicates of 30uL each. These were run via LC MS/MS using either a labeled or unlabeled approach, and any resulting hits from the screen were followed up in biochemical analyses of new cohorts.

We elected to begin with the VPS26a-haploinsufficient model as we felt the levels of retromer knockdown would be more reflective of that seen in AD patients and as this model does not limit retromer dysfunction to neurons. We later performed a similar study on the VPS35 knockout model, which exhibits full neuronal deletion (via Camk2α-Cre) of this linchpin to retromer's core. Results from each study are included in this section.

4.2 Results

4.2.1 CSF from VPS26a$^{+/-}$ mice reveals no apparent protein alterations as measured via LC/MS-MS

High quality CSF was collected from 3-month-old VPS26a$^{+/-}$ mice and wildtype littermates and pooled into 4 biological replicates per genotype. These samples were each labeled with distinct isobaric TMT tags and run via LC/MS-MS along with a composite reference sample, which was

used for normalization (Figure 4.1). This strategy interprets signal from each isobaric tag as relative sample contribution (i.e. relative quantitation) for the proteins identified.

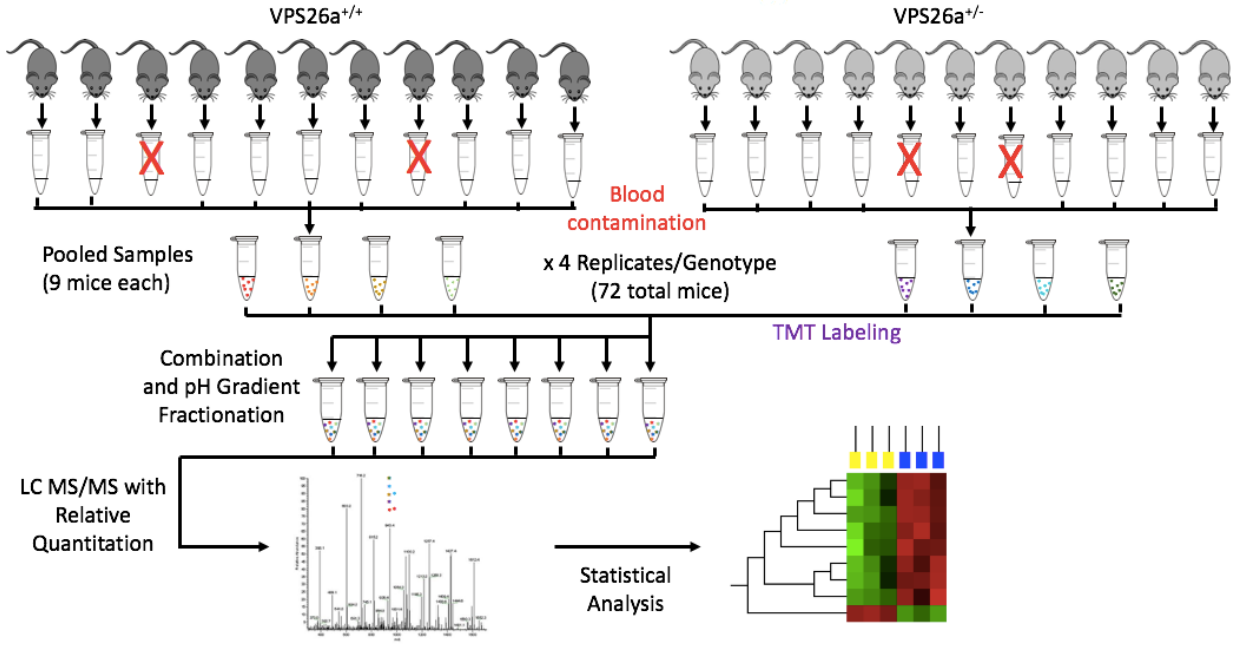

Figure 4.1 Overview of labeled LC-MS/MS approach for proteomic analysis of VPS26a$^{+/-}$ CSF. *CSF was collected from 3-month-old VPS26$^{+/-}$ males and littermate controls and assessed for blood contamination via hemoglobin ELISA. Contamination-free samples were subsequently pooled into biological replicates of 30uL each (n=4 per genotype). Proteins were digested and labeled with a distinct isobaric TMT tag, combined, and fractionated by pH to reduce sample complexity. LC-MS/MS was subsequently performed on the fractionated samples followed by statistical analyses.*

Using this labeled approach, 1215 quantifiable proteins were positively identified in the combined CSF. Histograms of the log ratios (sample/reference) for all identified proteins reveal fairly normal distributions among the biological replicates (Figure 4.2).

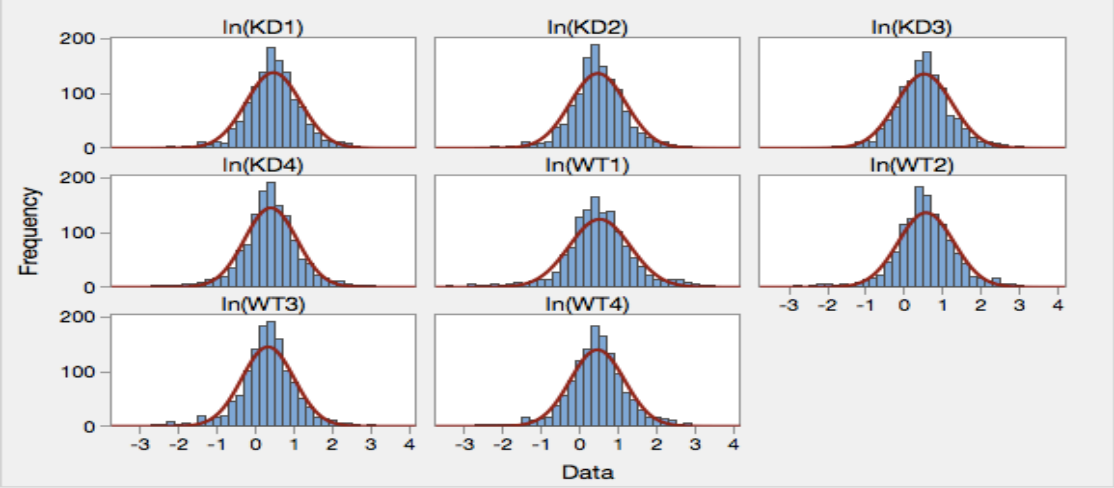

Figure 4.2 Quality assessment reveals normally distributed protein quantitation for all samples. *For each sample, relative quantitation for each protein (measured as sample/reference signal) was performed and reported logarithmically (log ratio). A histogram of these 1215 log ratios is normally distributed for each of the four VPS26a$^{+/-}$ (KD1-4) and VPS26a$^{+/+}$ (WT1-4) samples.*

Surprisingly, however, of all 1215 proteins detected, none were significantly altered in the VPS26a$^{+/-}$ CSF after controlling for multiple testing. In fact, a correlation plot of the log ratios for the retromer-deficient (KD) CSF versus control (WT) reveals an R-squared of 0.95 (Figure 4.3) indicating a very high level of correlation of CSF proteins between the two genotypes.

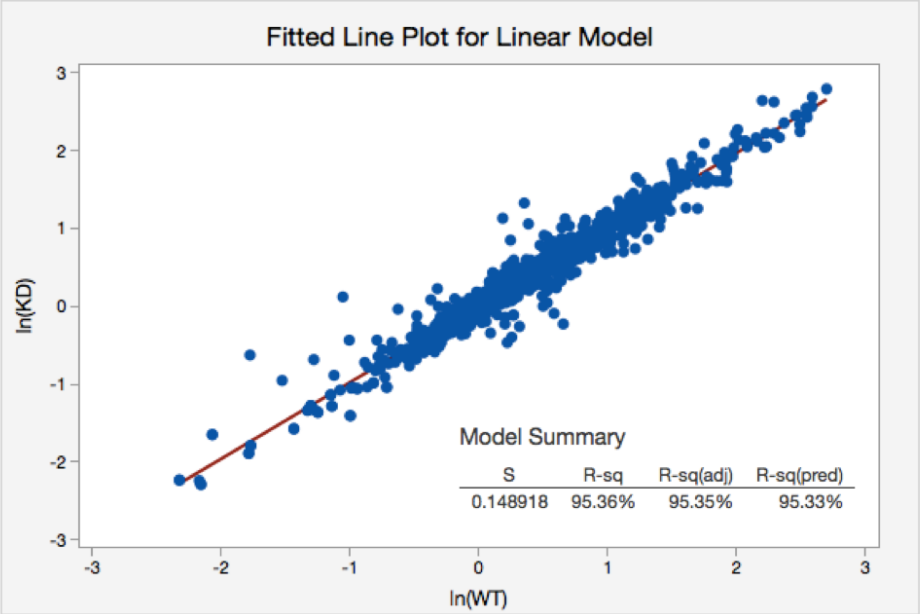

Figure 4.3 Global CSF profile in VPS26a$^{+/-}$ mice largely resembles that of littermate controls.

A comparison of mean log ratios between the VPS26a$^{+/-}$ (KD) and littermate controls (WT) reveals a high level of correlation between the two samples.

We wondered whether perhaps the statistical 'penalty' for multiple comparison was masking real but modest protein changes within our dataset. Therefore, we loosened discovery restrictions and performed a regression analysis to reveal the top statistical candidates (though none met the multiple testing-corrected significance threshold). Among the handful of statistical candidates were several which have been previously linked to the endosomal system. These included folate receptor 1 (FOLR1), GDNF family receptor alpha 1 (GFRA1), profilin (PFN1), and platelet-activating factor acetylhydrolase 1b3 (PAFAH1B3). GFRA1 is known to be trafficked by SORL1, a retromer cargo, out of the endosome (Glerup, Lume et al. 2013). FOLR1 undergoes endosomal recycling back to the cell surface, though the precise mechanism remains unclear (Wibowo, Singh et al. 2013). PFN1 is involved in actin remodeling, one of the five functions of the

retromer assembly, and influences CD36 recycling which has been shown to depend on retromer (Romeo, Moulton et al. 2007, Harbour, Breusegem et al. 2010, Lucin, O'Brien et al. 2013). And PAFAH1B3 plays a critical role in endosomal tubule formation, another function of the retromer assembly (Bechler, Doody et al. 2011). All of these proteins were elevated in the VPS26a knockdown CSF except for PAFAH1B3. As these 'hits' were only identified through a loosening of the statistical parameters, it was imperative that we assess their CSF levels in a new cohort of VPS26a$^{+/-}$ mice. We thus turned to immunoblot in pursuit of antibodies with reactivity in murine CSF.

Of these proteins, only PAFAH1B3 had a commercially available antibody which showed reliable reactivity in murine CSF. Initial optimization studies in mouse CSF indicated that large volumes of CSF (20uL per replicate) were required to detect signal. We therefore performed a western blot using pooled CSF from VPS26a$^{+/-}$ mice and littermate controls to assess PAFAH1B3 levels in the CSF. Due to the large volume required per lane, only two biological replicates were used per condition. While we realize this small sample size is insufficient for most biochemical assays, our goal was the identification of a distinctive biomarker of endosomal dysfunction. Thus, we reasoned that this follow-up validation (of pooled samples which should minimize variance among samples within each genotype) should properly inform on the purported decrease of PAFAH1B3 in the CSF of these mice. Results of the immunoblot revealed, however, that the levels of this protein are unchanged in the CSF of VPS26a$^{+/-}$ mice (Figure 4.4), rendering the initial statistical assessment of this protein (as unchanged) correct.

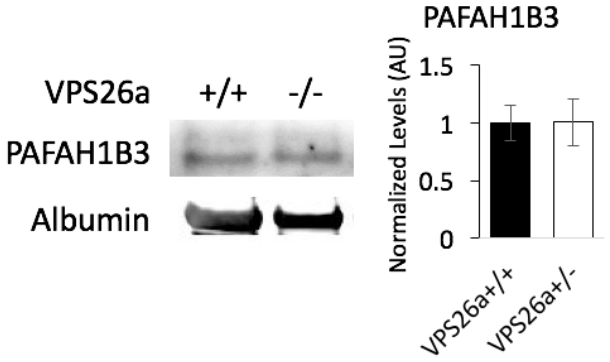

Figure 4.4 PAFAH1B3 is unchanged in VPS26a$^{+/-}$ CSF.

Immunoblot of pooled CSF reveals no change in PAFAH1B3 levels in retromer knockdown mice (n=2 due to limited availability of CSF). Values are first normalized to ponceau and then the wildtype average and represent the mean +/- SEM.

We ultimately conclude that VPS26a haploinsufficiency results in a mild CSF proteomic phenotype, with no detectable changes vis LC-MS/MS at the age of three months. Perhaps, as is the case for the CSF lipidome, age might exacerbate proteomic changes, allowing detection at a later time point (e.g. six months), or perhaps a complete knockout is better suited for such high-throughput biomarker discovery.

4.2.2 Mass spectrometry reveals enrichment of BACE1 substrate N-terminal fragments and total tau in CSF of VPS35 Camk2α knockout mice

4.2.2.1 Mass spectrometry of VPS35 Camk2α mice provides deepest characterization of murine CSF proteome to date

Informed by the above-mentioned work in our VPS26a$^{+/-}$ model, we opted to repeat the CSF proteomic screen using a neuron-specific retromer knockout model at six months of age hoping that these two adjustments would help exacerbate a proteomic phenotype we might be able to detect.

In this instance, we employed a similar pooling strategy, but owing to the low levels of protein in CSF collected from this model (0.10-0.16μg/mL as compared with 0.68-0.8μg/mL in the prior model), we opted for an unlabeled approach (Figure 4.5), which requires sequential runs of each biological replicate.

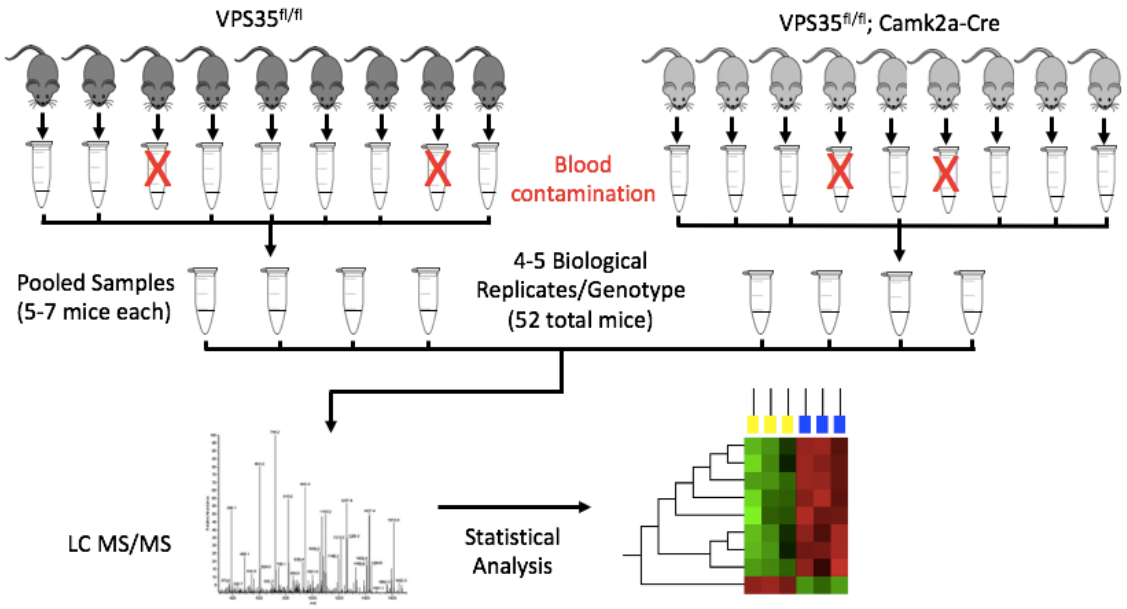

Figure 4.5 Overview of labeled LC-MS/MS approach for proteomic analysis of VPS35 Camk2α knockout CSF.

CSF was collected from 6-month-old VPS35 knockout males and littermate controls and assessed for blood contamination via hemoglobin ELISA. Contamination-free samples were subsequently

pooled into biological replicates of 30uL each (n=4-5 per genotype). Proteins were digested and labeled with a distinct isobaric TMT tag, combined, and fractionated by pH to reduce sample complexity. LC-MS/MS was subsequently performed on the fractionated samples followed by statistical analyses.

Using this strategy, 1505 proteins were positively identified in the CSF by 1 unique peptide (1048 proteins by 2 unique peptides). To date, prior proteomics studies of murine CSF (using a similar unlabeled approach on smaller volumes) have detected as many as 817 proteins by one unique peptide and 715 with at least two unique peptide sequences (Smith, Angel et al. 2014, Dislich, Wohlrab et al. 2015) (Figure 4.6), rendering this yet the deepest characterization to date of the murine CSF proteome.

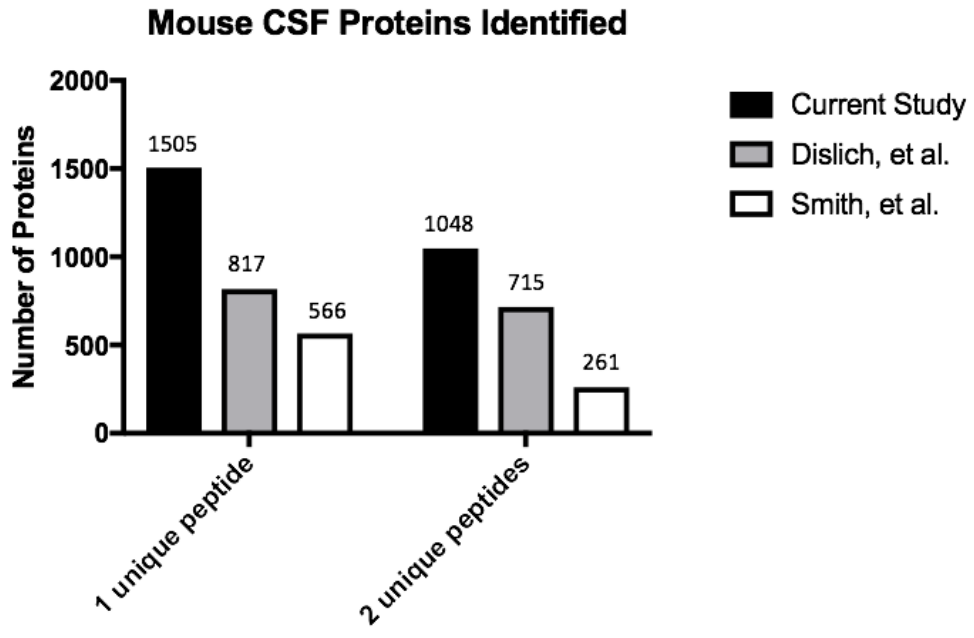

Figure 4.6 Comparison with prior murine CSF proteomic studies.

Using a pooled, unlabeled approach in the VPS35 Camk2α knockout model, we identified nearly double the proteins reported previously with one unique peptide, and roughly one third more than previously reported with two unique peptides (Smith, Angel et al. 2014, Dislich, Wohlrab et al. 2015).

Technical replicates were highly correlated (Figure 4.7a) as were the mean scores for biological replicates of the same genotype (Figure 4.7b), indicating robustness of technique. Quality assessments performed by our Proteomic Core identified one outlier from each genotype which was removed prior to downstream analyses.

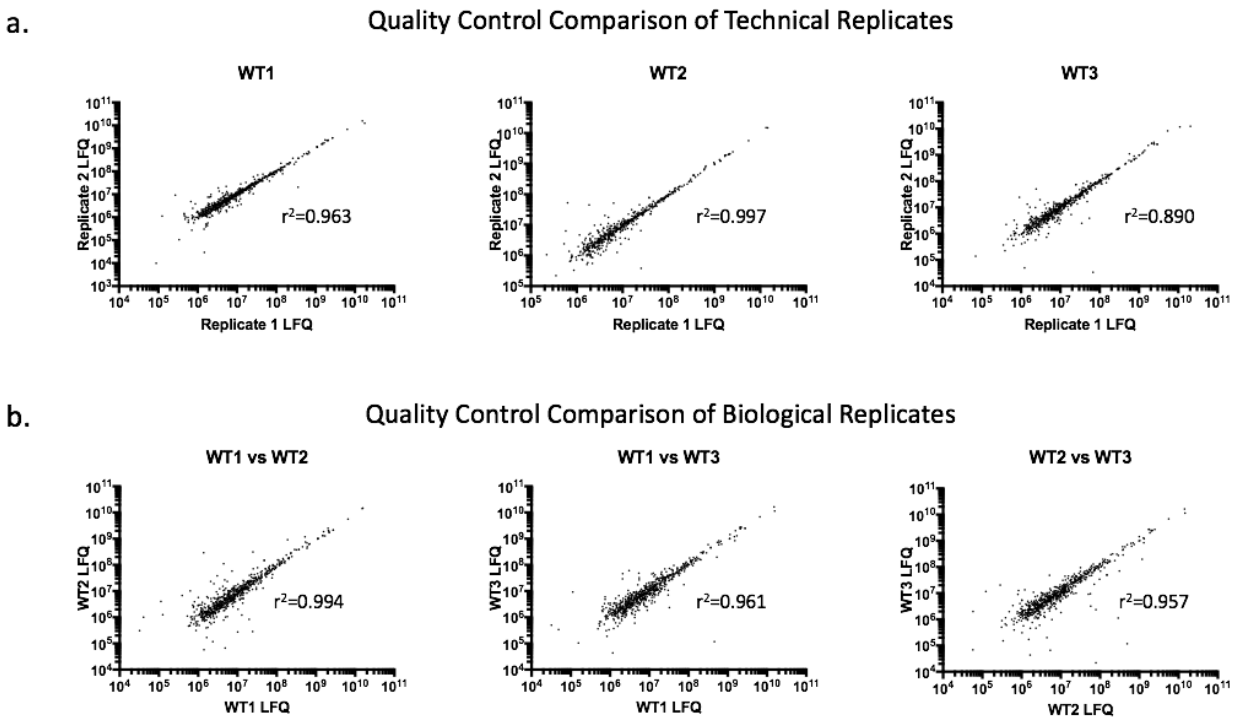

Figure 4.7 Quality assessment reveals high levels of correlation between replicates.

(a) A comparison of label-free quantification (LFQ) intensities for each protein reveal a high correlation between technical replicates. (b) A comparison of LFQ intensities for each protein in biological replicates (represented as the mean of technical duplicates) demonstrates high correlation between biological replicates.

In our quest for a CSF biomarker of retromer dysfunction, we decided to employ two analytical strategies: 1) a standard parametric analysis of proteins detected in samples from both genotypes, and 2) a nonparametric analysis in which we asked which proteins are present in one condition but not the other (as such a categorical distinction might provide even greater biomarker potential).

4.2.2.2 Parametric analysis reveals changes in BACE1 substrate N-terminal fragments and apolipoproteins

Of the 1505 proteins identified in this study, 52 were significantly altered in the VPS35 knockout CSF as determined by standard ANOVA (Table 4.1). Within this list, a class of elevated proteins were of particular interest: BACE1 substrates (CHL1, APLP1, and APLP2, and APP) (Figure 4.8a). Peptides from these BACE1 substrates mapped onto the N-terminal fragments (NTFs), suggesting mechanistic convergence upon BACE1 cleavage (Figure 4.8b), which liberates the NTF into the endosomal lumen (and ultimately the extracellular space).

Table 4.1 Parametric Hits of VPS35 Camk2a CSF Proteomics.

Accession	Symbol	p-value	q-value	Direction
P40142	Tkt	6.26E-08	0.0001	↓
Q06335	Aplp2	2.83E-07	0.0002	↑
P17182	Eno1	9.96E-07	0.0003	↓
P17563	Selenbp1	1.12E-06	0.0003	↓
P70296	Pebp1	1.14E-06	0.0003	↓
Q06890	Clu	1.11E-06	0.0003	↑
G3UYU6	Ptprd	2.47E-06	0.0005	↑
O70362	Gpld1	3.30E-06	0.0005	↑
P01029	C4b	2.79E-06	0.0005	↑
P06909	Cfh	4.44E-06	0.0005	↑
P08905	Lyz2	4.10E-06	0.0005	↑
P09411	Pgk1	3.31E-06	0.0005	↓
P70232	Chl1	2.69E-06	0.0005	↑
P45376	Akr1b1	5.86E-06	0.0006	↓
P63054	Pcp4	7.80E-06	0.0008	↑
Q8VCM7	Fgg	7.99E-06	0.0008	↓
A0A0R4J0X7	Gapdhs	1.05E-05	0.0009	↓
H7BX99	F2	1.16E-05	0.0009	↑
P08226	Apoe	1.31E-05	0.0009	↑
P32848	Pvalb	1.00E-05	0.0009	↓
Q9D0F9	Pgm1	1.32E-05	0.0009	↓
P55065	Pltp	1.48E-05	0.001	↑
A0A087WR50	Fn1	1.84E-05	0.0011	↑
P08249	Mdh2	1.78E-05	0.0011	↓
P97290	Serping1	1.63E-05	0.0011	↑
Q61361	Bcan	1.74E-05	0.0011	↑
P01887	B2m	2.25E-05	0.0012	↑
P13020	Gsn	2.10E-05	0.0012	↑
Q9CPU0	Glo1	2.35E-05	0.0012	↓
P15626	Gstm2	3.20E-05	0.0016	↓
P17183	Eno2	3.34E-05	0.0016	↓
Q62000	Ogn	3.19E-05	0.0016	↑
Q640N1	Aebp1	4.04E-05	0.0018	↑
A0A075B664	Iglv2	4.42E-05	0.0019	↓
Q03157	Aplp1	4.36E-05	0.0019	↑
Q8R480	Nup85	5.36E-05	0.0022	↓
P50247	Ahcy	6.07E-05	0.0025	↓
E9QPX1	Col18a1	6.45E-05	0.0026	↑
P21550	Eno3	7.23E-05	0.0028	↓
A0A0R4J107	Apeh	7.85E-05	0.003	↓
P51910	Apod	8.21E-05	0.003	↑
P00920	Ca2	8.89E-05	0.0032	↓
P02802	Mt1	9.13E-05	0.0032	↓
P29699	Ahsg	9.68E-05	0.0033	↑
Q9DCD0	Pgd	9.75E-05	0.0033	↓
P12023	App	1.09E-04	0.0036	↑
Q04447	Ckb	1.16E-04	0.0037	↓
Q5NC80	Nme1	1.24E-04	0.0039	↓
P02089	Hbb-b2	1.31E-04	0.004	↓
P12960	Cntn1	1.32E-04	0.004	↑
P14152	Mdh1	1.35E-04	0.004	↓
Q62165	Dag1	1.39E-04	0.004	↑

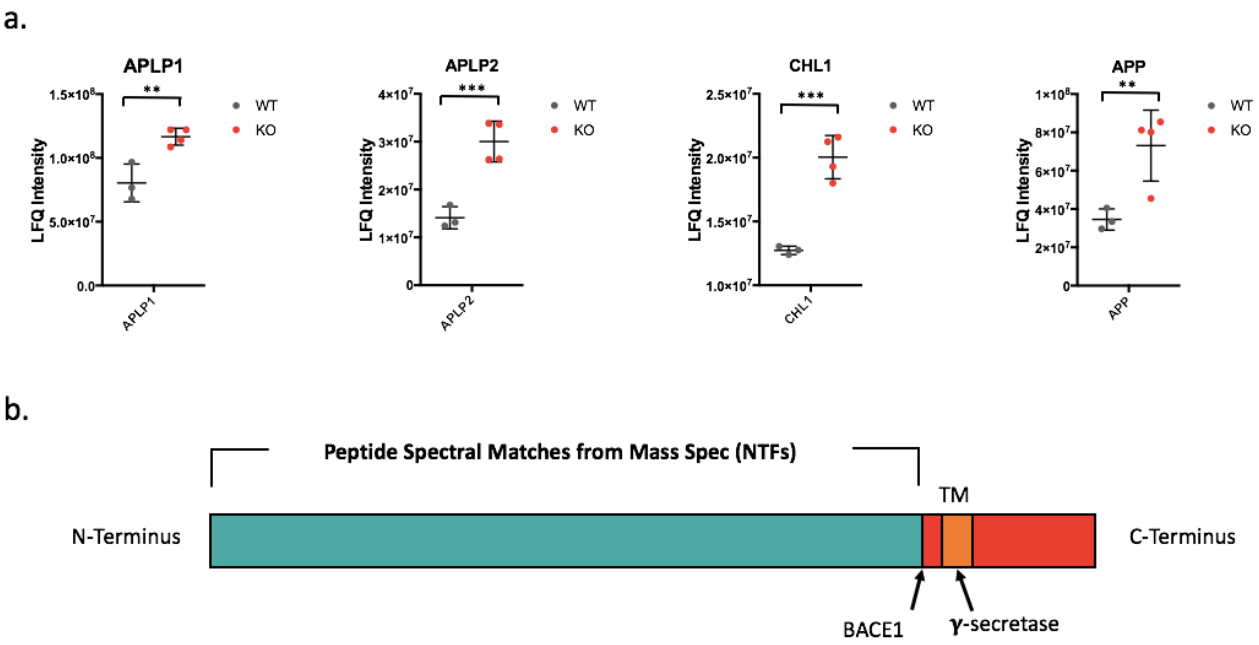

Figure 4.8 BACE1 substrate NTFs are elevated in CSF from VPS35 Camk2α knockout mice.

(a) *Mass spectrometry of VPS35 Camk2α knockout CSF reveals significant increases in BACE1 substrates APLP1, APLP2, CHL1, and APP. (b) Peptides map to the N-terminal fragment (NTF) for each BACE1 substrate detected. Values are reported as LFQ intensity and represent the mean of technical duplicates. Bars represent mean +/- SD (n=3-4; *P-value<0.05 **P<0.01, ***P<0.001).*

4.2.2.3 Nonparametric Analysis Uncovers Changes in CSF Total Tau

We then performed a nonparametric analysis, looking for proteins which present in one condition but not the other, as such proteins (which would be overlooked using standard ANOVA analyses) could carry high biomarker potential. We first employed this strategy looking for proteins present in at least four technical replicates (of eight total) only the VPS35 Camk2α knockout CSF but completely absent in controls. This query resulted in a list of 11 proteins (Figure 4.9) spanning various functional categories. Interestingly, among these categorical hits was Mapt

(tau), a protein which has clear pathologic ties to AD (Grundke-Iqbal, Iqbal et al. 1986, Bejanin, Schonhaut et al. 2017) and is reliably elevated in the CSF of AD patients (Andreasen, Minthon et al. 2001). We then used a similar strategy to identify proteins present in at least four technical replicates of the control CSF but absent from all knockout samples. This yielded a list of 8 additional nonparametric hits (Figure 4.9).

Nonparametric Hits	
VPS35$^{+/+}$ Only	**VPS35$^{-/-}$ Only**
Abhd14b	Adgrg6
Dsg1a	Cep70
Gsto1	Adamts4
Dnpep	Gm5591
Glud1	Syn1
Me1	Basp1
P01878	Cdh15
Aldh1l1	Mapt *
	Cdh1
	Fbln2
	Fgfr1

Figure 4.9 Nonparametric analysis reveals presence of Mapt (tau) in only retromer knockout CSF.

In a nonparametric analysis of the VPS35 Camk2α CSF mass spectrometry data, eight proteins were detected in at least four technical replicates of the wildtype CSF and absent from all knockout replicates and 11 proteins in at least four technical replicates of controls but absent from all wildtype replicates. Notably, mapt (tau) is present in only the retromer knockout CSF.

4.2.2.4 Ingenuity Pathway Analysis (IPA) indicates APP, MAPT, and PSEN1 among the top upstream regulators of CSF changes in VPS35 neuronal knockout mice

To further clarify the wealth of information gained from this CSF study (which includes 52 parametric hits and 19 nonparametric hits), we turned to ingenuity pathway analysis (IPA) (Kramer, Green et al. 2014) to determine which genes might be 'regulating' the global CSF changes in our VPS35 knockout model. This software relies upon established transcriptional interactions to predict upstream molecular convergence of global changes in large datasets (Kramer, Green et al. 2014). Of the top six potential regulators, three of them (APP, MAPT, and PSEN1) are pathologically linked to AD, and the top two (APP and MAPT) are aberrantly processed proteins which comprise the current CSF diagnostic profile (Figure 4.10).

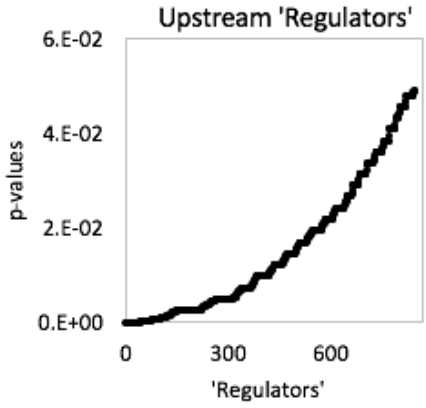

Top Upstream 'Regulators'

Rank	'Regulator'	p-value
1	APP	7.52E-14
2	MAPT	1.05E-12
3	HTT	8.30E-11
4	DHT	3.76E-10
5	VCAN	1.03E-09
6	PSEN1	1.81E-09

Figure 4.10 Ingenuity Pathway Analysis (IPA) implicates AD-related proteins as upstream regulators in VPS35 knockout CSF.

IPA reveals APP, Mapt, and PSEN1 among the top six upstream 'regulators' of the potential 843 identified in this set.

4.2.3 BACE1 Substrate NTFs and Total Tau are confirmed as hits in a new cohort of VPS35 Camk2α knockout mice

4.2.3.1 BACE1 substrate NTFs are confirmed via immunoblot in vivo and in vitro

Intrigued by the BACE1 substrate hits, we sought to confirm their elevation in vivo in a new cohort of mice using immunoblot technique. Of this list (CHL1, APLP1, APLP2, and APP), we identified available antibodies for both CHL1 and APLP1 (directed at the N-terminal region) that that were reactive in mouse CSF. Both of these proteins were again elevated in the CSF of the new cohort, confirming the initial mass spectrometry results (Figure 4.11a). Molecular weight comparison with cortical lysates (via immunoblot migration) suggests that these are indeed the NTFs, not the full-length protein (data not shown). In vitro work supported these findings, as levels of CHL1 and APLP1 NTFs were increased in the media from VPS35$^{fl/fl}$ neurons infected with Cre.GFP virus versus that of the control (Figure 4.11b).

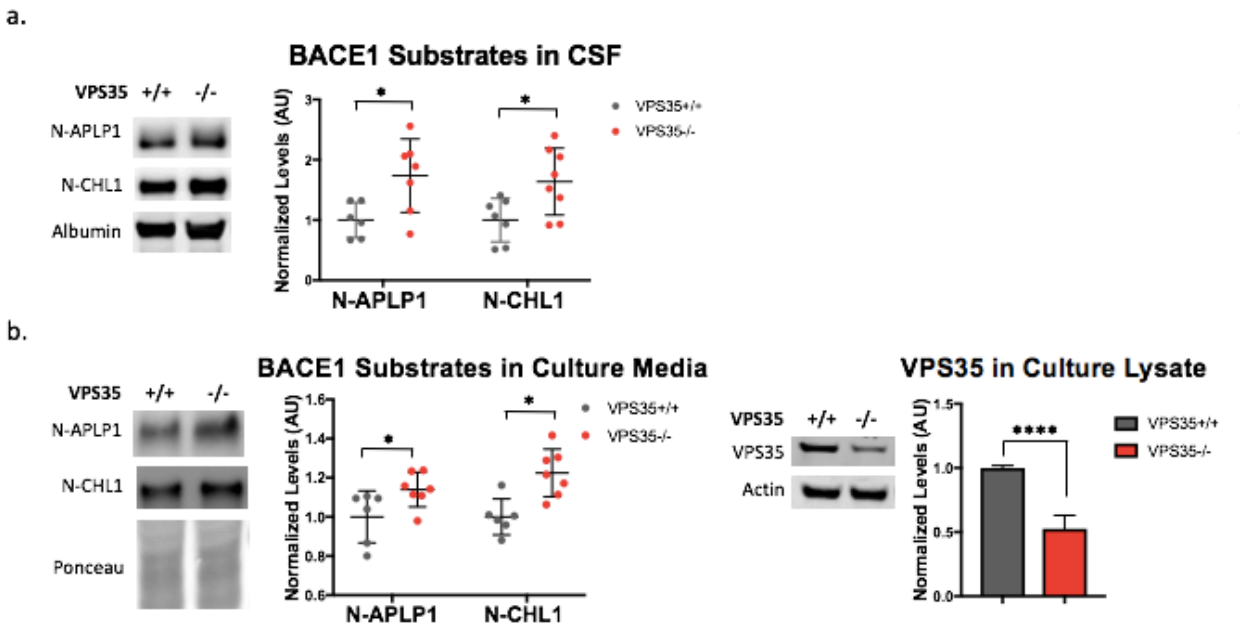

Figure 4.11 Elevation of BACE1 substrate NTFs in VPS35 knockouts is confirmed in vivo and in vitro.

*(a) CSF from a new cohort of VPS35 Camk2α knockout mice and littermate controls reveals a significant increase in the NTFs of BACE1 substrates APLP1 and CHL1, confirming these hits from the initial proteomic screen. Bars represent mean +/- SD (n=6-8; *P<0.05). (b) Media from cultured primary VPS35$^{fl/fl}$ neurons infected with Cre.GFP (VPS35+/+) or Δ-Cre.GFP (VPS35-/-) is enriched in NTFs from BACE1 substrates APLP1 and CHL1. Bars represent mean +/- SD (n=6-7 from 2 independent experiments; *P<0.05).*

4.2.3.2 Single molecule array (simoa) confirms elevation of total tau in VPS35 Camk2α knockout CSF

Detection of tau in mouse CSF has been a challenging task, as levels in CSF are roughly 50,000-fold lower than that of brain tissue (Barten, Cadelina et al. 2011). As a result, to our knowledge, no one has managed to detect this protein in murine CSF using conventional immunoblot or ELISA in wildtype mice. In fact, efforts on our part to detect tau in murine using both immunoblot and MSD ELISA were unsuccessful. Therefore, we turned to single molecule array (simoa), a recently developed technology which boasts detection down to the level of a single molecule. Using this approach, we were able to reliably detect total tau in as little as 5uL of murine CSF. Furthermore, a comparison of VPS35 Camk2α-Cre knockout mice and their littermate controls revealed a striking increase in the knockout CSF (Figure 4.12), confirming this nonparametric hit from our initial screen.

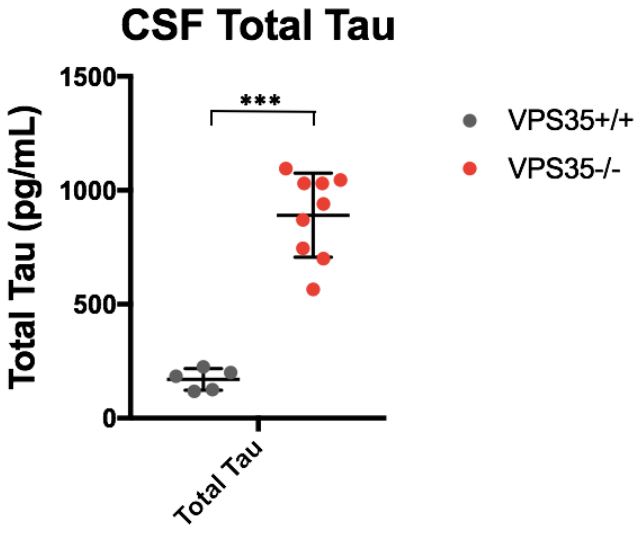

Figure 4.12 Total tau is significantly elevated in VPS35 Camk2α knockout CSF.

*In a new cohort of VPS35 Camk2α knockout mice, CSF total tau is markedly increased in the knockout as compared with control. Dots represent raw values. Bars represent mean +/- SD (n=5-9; *P<0.05, **P<0.01, ***P<0.001).*

We further validated this finding in vitro through knockout of VPS35 (via lentiviral delivery of Cre-recombinase in VPS35$^{fl/fl}$ primary neurons). Here, a comparison with controls revealed an elevation in secreted total tau from the VPS35 knockouts while levels of secreted lactate dehydrogenase (LDH) was unchanged (Figure 4.13), indicating that the increase in extracellular tau results from an active mechanism independent of cell death.

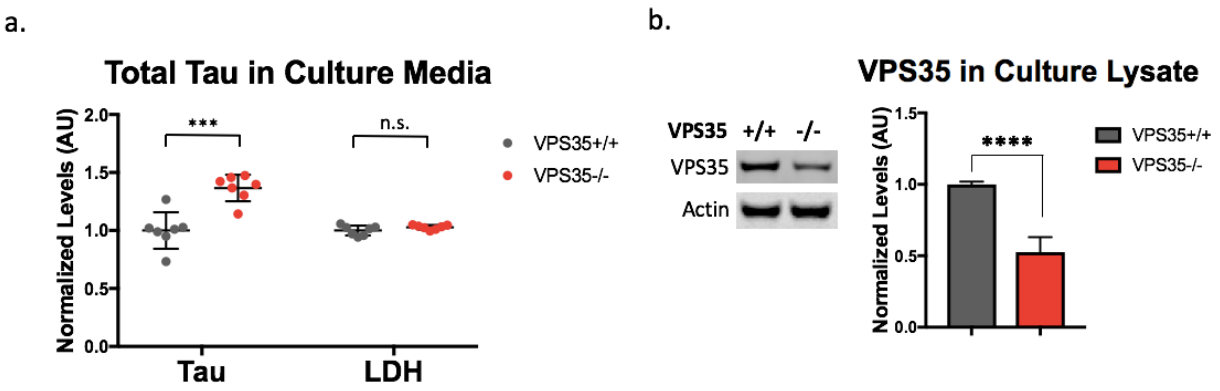

Figure 4.13 Total tau is enriched in media from VPS35-/- neuron cultures.

*VPS35$^{fl/fl}$ primary neurons were treated with Cre.GFP (VPS35$^{-/-}$) or Δ-Cre.GFP (VPS35$^{+/+}$). (a) Total tau and LDH were measured in the media using MSD technology and promega Cyto-tox assay, respectively. Values were normalized to total protein and then to the control. Bar graphs represent mean +/- SEM (n=7, *P<0.05; **P<0.01; ***P<0.001). (b) Immunoblot of neuronal culture lysate demonstrates lentiviral knockdown of VPS35. Values are normalized to the loading control and to the wildtype mean. Bar graphs represent mean +/- SEM (n=5-6, *P<0.05; **P<0.01; ***P<0.001; ****P<0.0001).*

4.2.4 Translation to humans positions CSF total tau as a biomarker of endosomal dysfunction in AD

4.2.4.1 BACE1 Substrate NTFs are highly correlated in mouse and human CSF

During the course of our murine CSF validation studies, we stumbled upon an intriguing and unanticipated finding: that BACE1 substrate NTFs APLP1 and CHL1 are highly correlated in mouse CSF (Figure 4.14a). We therefore turned to human CSF (non-demented controls) to see whether this relationship held (Figure 4.14b). Using a similar immunoblot approach, we discovered that

APLP1 and CHL1 NTFs are also highly correlated in the CSF of human subjects. As these NTFs are liberated by the same cleavage enzyme (BACE1), we reason this suggests that the levels of APLP1 and CHL1 NTFs in the CSF depend primarily on the activity and/or localization of BACE1.

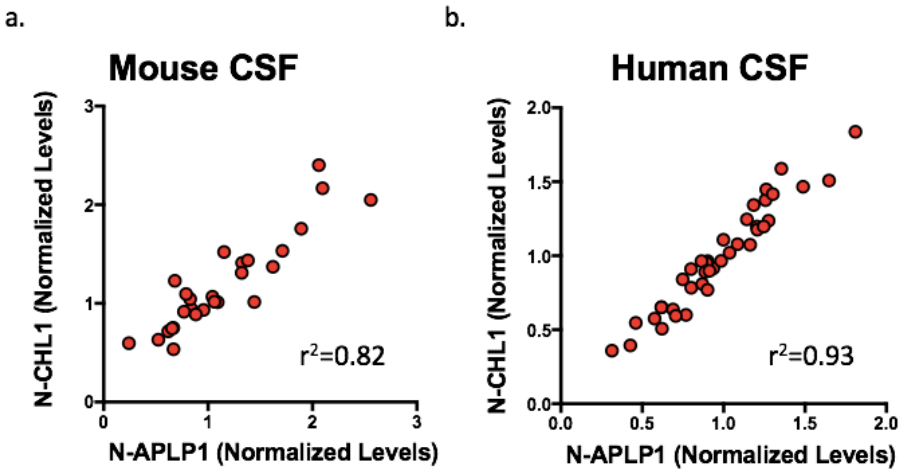

Figure 4.14 NTFs of BACE1 substrates are correlated in mouse and human CSF.

CSF from mice (n=27) (a) and healthy control (n=39) CSF (b) reveals a striking correlation (p<0.0001 for mouse and human) between the NTFs of APLP1 and CHL1 as measured by immunoblot. Values are normalized to albumin and the group average before combining cohorts from different blots.

4.2.4.2 APLP1 is correlated to Aβ42 and total tau in human CSF

Next, we wondered whether the levels of these BACE1 substrate NTFs were correlated with other AD-related proteins (Aβ42, total tau, and ptau-181) in the CSF. We explored these relationships in human CSF as simoa assays with mouse reactivity had not yet been developed for Aβ42 and ptau-181. Remarkably, analysis of 38 non-demented controls revealed that CSF levels of APLP1

NTFs are significantly correlated with Aβ42, total tau and ptau-181 (Figure 4.15; Aβ42: $p<0.01$; total tau: $p<0.0001$; ptau-181: $p<0.05$; n=38).

The correlation with Aβ42 is perhaps not entirely surprising as both Aβ42 and APLP1 NTFs are both downstream products of BACE1 cleavage. Yet, the correlations between APLP1 NTFs and both total tau and ptau-181 are unexplained by current knowledge, although recent in vitro work has shown that retromer deficiency promotes tau phosphorylation (Young, Fong et al. 2018). These associations in the CSF suggest that the pathways controlling secretion of BACE1-cleaved substrates and tau may be linked in the plaque-free mammalian brain.

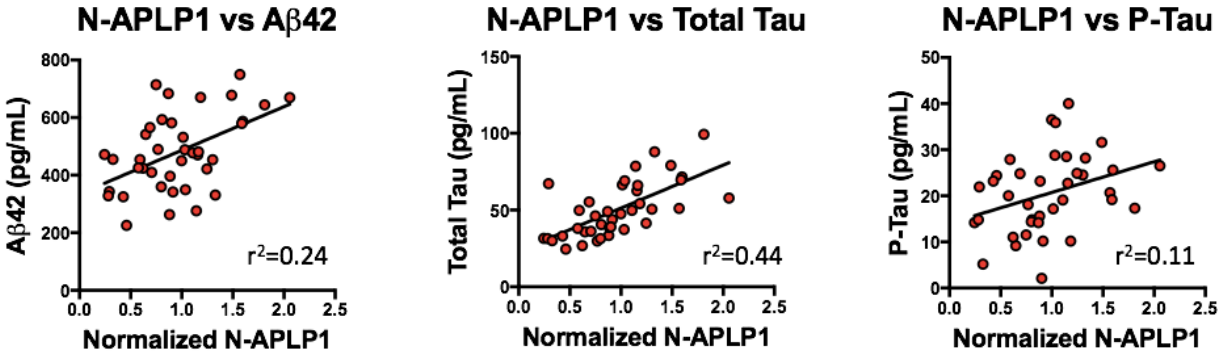

Figure 4.15 APLP1 NTFs are highly correlated with Aβ42 and total tau in human CSF.

A study of 38 non-demented healthy controls revealed significant correlations between CSF N-APLP1 and Aβ42 ($p<0.01$), total tau ($p<0.0001$), and ptau-181 ($p<0.05$).

4.2.4.3 APLP1 NTFs likely bind to amyloid plaques

The pathologic progression of AD generally involves the development of extensive extracellular plaques, which have been known to sop up secreted proteins, ultimately affecting their detection in the CSF (Fagan, Mintun et al. 2006). To date, the properties which render proteins likely to stick to plaques are not fully understood, though some have attempted to add clarity to this issue (Gozal, Cheng et al. 2006). The ultimate aim of our project is the translation of findings to human subjects in order to identify all individuals with endosomal dysfunction (both pre- and post-plaque development). As such, it is imperative that levels of our biomarker of endosomal dysfunction not be confounded by the presence of plaques.

A query of the literature turned up one report that in fact APP-related proteins such as APLP1 and APLP2 can accumulate in neuritic plaques in control and AD brains (McNamara, Ruff et al. 1998). We turned again to human CSF to see whether APLP1 NTFs might be sticking to plaques in human subjects. We obtained CSF from 5 patients with MCI who were biomarker-positive ($A\beta42>210$ and $Tau/A\beta42<0.39$) for AD (i.e. 'plaque-positive'). Using this limited set, we performed was a standard t-test of CSF APLP1 in plaque-positive AD patients vs age- and gender-matched controls. The underlying assumption for this query was that if APLP1 is not sticking to plaques, the levels would be either unchanged or elevated in plaque-positive patients versus controls. What we found instead was a marked decrease in the plaque-positive cohort (Figure 4.16), suggesting that like $A\beta42$, APLP1 NTFs might be binding plaques in the AD brain. We followed up with a correlation analysis of APLP1 and $A\beta42$ in CSF from the 5 AD patients with the assumption that if APLP1 is not accumulating in plaques as is $A\beta42$, this correlation should break. Despite the low statistical power of such a small dataset, the correlation between APLP1 and

Aβ42 remained quite strong (p=.003) in AD brains (data not shown). Taken together, these observations support prior findings and suggest that CSF levels of other BACE1 cleavage products such as APLP1 NTFs may be confounded by plaques in the AD brain, thus compromising their potential for biomarker utility.

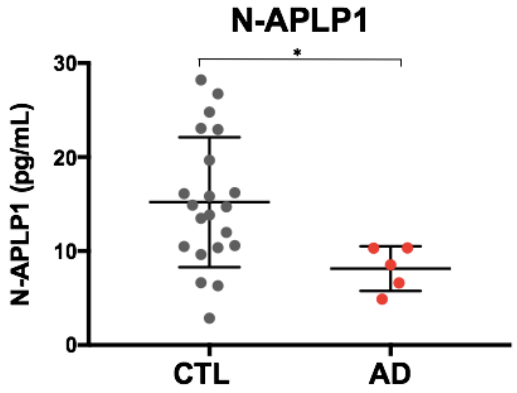

Figure 4.16 CSF Levels of APLP1 NTFs are lower in AD patients.

*N-APLP1 is lower in the CSF from plaque-positive AD patients than in age- and gender-matched controls (n=5, 22; *P<0.05).*

4.3 Discussion

CSF collection in mice is a highly technical procedure, often yielding no more than 5uL of fluid per mouse. Nonetheless, other groups have successfully characterized this fluid via LC-MS/MS (Smith, Angel et al. 2014, Dislich, Wohlrab et al. 2015), identifying over 700 proteins in as little as 2uL. As such, we sought out to uncover CSF protein biomarkers in two different models of retromer deficiency using a similar strategy.

4.3.1 VPS26a$^{+/-}$ CSF Proteomics

That we found no protein changes in the VPS26a-haploinsufficient CSF was surprising, particularly given the number of positively identified proteins (1215 in pooled replicates) available for discovery. There could be several explanations for this. First, it is entirely possible that a heterozygous model is insufficient to generate a clear protein-based profile in the CSF (or at least one strong enough to overcome the multiple comparison 'penalties' in such a large dataset). As we learned through our lipidomics studies of this model, perhaps using a later time point in these mice (e.g. six months instead of three—the age used for our VPS35 Camk2α model) would increase the likelihood of discovery through an exacerbation of cellular pathology.

A second explanation for is that the VPS26a-containing assembly is less critical to trafficking events which alter the cellular secretome. Yet, we know from in vitro studies that defects in VPS26a increase the secretion of proteins such as cathepsin D (Rojas, van Vlijmen et al. 2008); thus, we argue against such an explanation.

4.3.2 VPS35 Camk2α CSF Proteomics

Our unbiased CSF screen of neuronal-selective Vps35 knockout mice yielded a complement of proteins that most reliably accumulate in the CSF in a model of AD-associated endosomal dysfunction. After validating the most relevant proteins, we turned to human CSF to investigate whether the proposed relationship between these proteins occurs in the human brain. The main advantage of starting with a mouse model, besides greater experimental control, is that endosomal dysfunction can be restricted to cortical neurons, obviating any confusion of cell type

specificity. Although there is a significant overlap in endosomal machinery between mice and humans, cross-species differences might exist. Thus, while our positive findings are deemed reliable, we cannot exclude the importance of proteins that did not emerge from our primary mouse screen.

Our VPS35 Camk2α knockout CSF study demonstrates the deepest probe into the murine CSF proteome to date (by roughly 100% using a threshold of 1 unique peptide and 50% with a threshold of 2 unique peptides) with an unlabeled approach. This feat may be attributed to technical differences (e.g. equipment and handling), but it is likely at least in part a result of the pooling strategy we designed, allowing a larger volume per sample available for proteomic study than those used in prior studies.

4.3.2.1 BACE1 Substrate NTFs in Mice and Humans

The fact that APP fragments were among the hits from this screen provides additional unbiased evidence linking retromer to AD. More broadly, a number of previous studies, including a CSF proteomic screen in BACE1 KO mice, have established that APP, APLP2, APLP1, and CHL1 are substrates cleaved by BACE1 in the neuronal endosome, generating and secreting n-terminal fragments of each. Our screen identified fragments of all of these proteins, from which we conclude that retromer-dependent endosomal dysfunction promotes their accelerated cleavage and secretion. All four of these proteins, including BACE1 itself, are type I transmembrane proteins that traffic through the endosome. Retromer typically functions in trafficking these types of transmembrane proteins, and indeed, thus far, both APP and BACE1 have been found to

be trafficked by retromer, with retromer deficiency increasing their resident time in endosomal membranes. Thus, the observed accumulation of the four fragments may reflect a combination of mistrafficked substrate and their cleaving enzyme. We note that we did not detect Aβ in the CSF of WT or KO mice, even though retromer deficiency does cause an increase in Aβ in mouse brains, and in the media of cultured neurons. We consider it likely, therefore, that endogenous murine Aβ is below detection of the methods used. Our human studies support this interpretation, suggesting that in plaque-free individuals a marker of retromer-dependent endosomal dysfunction is positively associated with CSF Aβ.

Unfortunately, our studies corroborate other reports that BACE1 substrate NTFs may bind plaques in the brain (Bayer, Cappai et al. 1999), thus compromising their biomarker potential over the course of AD. It is possible, however, that they could provide utility in early (pre-plaque) AD patients or in plaque-free neurodegenerative disorders such as Parkinson's disease (PD).

4.3.2.2 Total Tau as a Biomarker of AD-Related Endosomal Dysfunction

Although tau is known to be secreted from the endolysosomal pathway, we consider the observation that retromer-dependent endosomal dysfunction causes an increase in CSF tau the more important and novel result from our studies. Prior patient studies provided some clues about this relationship. CSF studies in AD patients carrying deleterious genetic variants encoding the retromer receptor Sorl1 have shown that these variants are associated with relative increases in CSF tau. However, no studies, to our knowledge, have profiled the CSF in Sorl1 carriers who are plaque free. Since amyloid plaques are avid binders of APP fragments and many other

extracellular proteins, it would be interesting to probe the CSF of carriers of Sorl1 causative mutations, in pre-plaque stages of disease. Neimann-Pick type C1 (NPC1) is a disorder that is interesting in this regard, since it is a disorder whose abnormal cholesterol trafficking causes primary endosomal dysfunction, without causing plaque formation. Interestingly, these patients have been found to have CSF elevations in both tau and Aβ. While NPC1 patients do develop neurofibrillary tangles it is unlikely that their intraneuronal tau pathology accounts for the CSF tau findings, since FTD patients with aggressive tau pathology do not typically have increases in CSF tau.

Unlike fragments of APP and perhaps its homologues, tau does not bind amyloid plaques, which commonly exist in even normal aging individuals. Thus, among the proteins we investigated, elevation in CSF tau has the best potential of being a useful biomarker of AD-associated endosomal dysfunction. Our studies show that CSF tau can act as a sensitive marker of endosomal dysfunction, but says little about its specificity. As a biomarker of AD, chronic CSF elevation in total tau and ptau does not only have high sensitivity, but when observed chronically it appears to be specific. Other neurodegenerative diseases, with just as much neuronal death or NFT burden as AD, do not typically manifest elevations in CSF tau (Zetterberg 2017), and so AD's unique pathophysiology must drive this elevation and not cell death or tau pathology. While acute events, such as strokes or seizures, can cause an increase in CSF tau, this elevation is transient and not chronic.

What aspect, then, of AD's pathophysiology is the driver of chronic elevations in CSF tau? Since tau is secreted from the endolysosomal system we anticipate that any defect that increases tau accumulation in this compartment will play a role. Our studies permit us to conclude that retromer-dependent endosomal trafficking regulates CSF tau. It is likely that other defects in the endolysosomal system will have a similar effect. Additionally, defects in tau clearance, while still poorly understood, must also be considered. With the availability of new detection tools and reagents that measure mouse CSF tau, it is now possible to investigate multiple mouse models in order to map the full range of molecular defects that might regulate CSF tau. With the development of future reagents to measure not only total tau, but levels of its fragments and phosphorylation state, the unique molecular profile of CSF tau linked to different molecular defects will also be informative.

A series of recent studies illustrate how the current ability to detect total tau in mouse CSF can elegantly be used to begin clarifying these questions. These studies have shown that mice that express mutations in APP and PS1 develop elevations in CSF tau over time (Maia, Kaeser et al. 2013, Schelle, Hasler et al. 2017). Since these mice do not develop overt neurodegeneration or tangle pathology, they provide direct evidence that cell death or tau pathology per se is not required for CSF tau elevations. While these studies have shown that blocking APP cleavage with a BACE1 inhibitor reduces tau elevation (Schelle, Hasler et al. 2017), implicating APP fragments, how these fragments lead to increased tau secretion remains unknown. Interestingly, however, independent studies have shown that mice bearing these mutations develop retromer-dependent defects over time (Chu and Pratico 2017), and more broadly that the accumulation of

intraneuronal APP fragments cause endosomal dysfunction (Jiang, Mullaney et al. 2010, Xu, Weissmiller et al. 2016).

As recently reviewed, endosomal dysfunction represents a unified cell biological defect in AD (Small, Simoes-Spassov et al. 2017), which can be caused primarily by molecular defects that directly target the endosome, or secondarily via defects that elevate intraneuronal APP fragments. Moreover, evidence suggests that whether directly or indirectly, endosomal dysfunction can act a pathogenic hub, mediating common downstream abnormalities. Our results with retromer knockout mice show, for the first time, that molecules that directly target the endosome lead to established abnormalities in CSF tau. The prior studies with APP/PS1 mutant mice established that increasing APP fragments phenocopies the same abnormality. Whether in the latter case this occurs through the effect on APP fragments on endosomal dysfunction, remains to be tested. For the reasons listed above, this seems highly plausible. If so, then elevation in CSF tau would be considered a sensitive and specific biomarker of AD-associated endosomal dysfunction.

5. Chapter 5: Conclusions and future directions

5.1 Overview

A growing number of AD therapeutics have failed in clinical trials, prompting the quest for new drug targets. As a result, endosomal trafficking has emerged as a newly validated target for drug discovery. Currently lacking, however, are biomarkers of endosomal dysfunction, essential for addressing the epidemiology of this cellular deficit in AD and for tracking its course over disease progression and in clinical trials.

We sought to fulfill this urgent need using retromer deficiency as a model of AD-related endosomal dysfunction. Accordingly, we performed a battery of biochemical analyses on CSF and brain exosomes of mice with selective deletion of retromer's core proteins. Our studies include the first characterization of the mouse CSF lipidome and the deepest characterization of the mouse CSF proteome to date, and propose a CSF protein biomarker with clinical utility.

5.2 CSF lipidomics

VPS26a haploinsufficiency results in a mild CSF sphingolipid profile of non-neuronal origin, while complete knockout of VPS26a in forebrain neurons yields no lipidomic profile at all. Whether this indicates that the VPS26a-containing assembly is more critical to non-neuronal cells or that non-neuronal cells contribute more to the murine CSF lipidome cannot be concluded from this study. Yet, it warrants consideration that translation of this profile to human CSF is limited entirely to retromer dysfunction in non-neuronal cells (of a yet undetermined type). Further clarification of such a biomarker requires dissection of the extracellular lipidomic contribution by various glial

types. This could potentially be explored in vitro through lentiviral knockdown of retromer in cell type-specific cultures (e.g. astrocytes, microglia). Alternatively, in vivo studies of VPS26a-floxed mice using Cre-recombinase expression under other cell type-specific promoters (e.g. CX3CR1 for microglia) are warranted. As sphingomyelin studies in human CSF to date have yielded conflicting results and our CSF proteomic experiments unearthed more compelling leads, this lipidomic profile of non-neuronal retromer dysfunction was not pursued further.

Possible mechanisms for these changes might include mistrafficking of biosynthetic enzymes. Neutral sphingomyelinase, which converts sphingomyelin into ceramide, also regulates exosomal budding (Trajkovic, Hsu et al. 2008). As our brain-derived exosomal studies suggest retromer might impact exosomal biogenesis, enhanced endosomal retention of this sphingomyelinase is an intriguing hypothesis.

5.3 Brain exosome studies

Exploration of two retromer knockout models (full body knockout of VPS26b and forebrain-selective neuronal knockout of VPS35) revealed that the amyloidogenic effects of retromer knockout in neurons (via increased retention of both BACE1 and APP in the endosome) can be detected in brain exosomes. This enrichment of β-CTFs in exosomes, which take origin from the endosomal membrane, is perhaps unsurprising given the above-mentioned effects of retromer dysfunction on amyloidogenic processing pathways.

Follow-up studies in human serum exosomes of brain origin, however, failed to detect β-CTFs in these vesicles. Whether (a) these fragments do not end up in serum-circulating exosomes or (b) they simply cannot be detected using current technology is unknown. Studies to clarify this question are warranted in the pursuit of a brain exosome biomarker. The former would impose a different strategy, perhaps using serum exosomes in neuronal-selective retromer knockouts as a starting material for biomarker discovery to overcome the challenges associated with circulation entry. The latter would prompt development of more sensitive technologies (e.g. simoa) for detection of brain-derived proteins in serum exosomes.

An unexpected finding during the course of these studies was the potential impact of retromer deficiency on exosome biogenesis. This was suggested by reduction of exosomal markers alix and flotillin-1 and a possible (as yet descriptive) shift toward smaller vesicles. Interestingly, recent work by another group indicates that brain-derived exosomes from AD patients are smaller and bear fewer canonical exosomal markers than those of matched controls (Tran, Mustapic et al.). While these parallels are intriguing, further clarification of retromer's role in these exosomal biogenic pathways is required. Future studies would likely include electron microscopy and nanotracker analysis to precisely assess changes in morphology of both exosomes and the originating MVBs. In addition, proteomic studies could uncover changes in exosomal content and perhaps provide mechanistic clues. Though our biomarker studies became focused on the more compelling CSF proteomic findings, the impact of retromer deficiency on exosomal biogenesis is a continued interest of the lab, largely motivated by the results of this project.

5.4 CSF proteomics

It is interesting to note that haploinsufficiency of VPS26a yields no detectable protein changes in the CSF at three months. Perhaps, as in lipidomics, a later time point would intensify changes which may have been masked in this screen. Or perhaps a complete knockout is required to detect proteomic changes in the CSF of these mice. Considering these possibillities, we opted to make both of these adjustments through analysis of a complete knockout of VPS35 in forebrain neurons at six months of age, summarized below.

Knockout of VPS35 in forebrain neurons results in a significant change in numerous CSF proteins, including two categories particularly relevant to AD pathology: BACE1 substrate (APLP1, APLP2, CHL1, and APP) NTFs and Mapt (tau). Follow-up studies in vivo and in vitro confirmed the elevation of BACE1 substrate NTFs and total tau in retromer knockout CSF. Interestingly, Ingenuity Pathway Analysis positioned these two categories (APP and tau) as the top upstream 'regulators' of all CSF changes, suggesting their relevance in the downstream effects of retromer-dependent endosomal dysfunction. Follow-up studies in CSF from both mice and humans revealed striking correlations between levels of BACE1-cleaved fragments, implicating BACE1 modulation (e.g. by retromer dysfunction) as a primary driver of their extracellular release, which can be directly measured in CSF.

Perhaps most remarkable, however, was the correlation between the NTF of BACE1 substrate APLP1 and total tau in plaque-free human CSF, suggesting biological convergence (at the intracellular endosome) of these seemingly distinct categories of hits. Yet, follow-up studies in a

small cohort of plaque-positive AD patients support earlier reports that these APP-related BACE1 substrate NTFs may bind extracellular amyloid. And although these fragments might still carry biomarker potential in early (pre-plaque) patients or in other plaque-free neurodegenerative diseases such as PD, thier utility is therefore compromised in the progressive AD brain. Accordingly, CSF total tau emerges as the top validated hit as a biomarker of AD-related endosomal dysfunction with utility throughout the course of disease progression. Remarkably, studies from other groups have shown that APP mice, which undergo progressive retromer deficiency, also exhibit age-related elevations in CSF total tau (Maia, Kaeser et al. 2013).

Nonetheless, follow-up studies are required to confirm the specificity of CSF total tau as a biomarker of endosomal dysfunction and that agents which rescue this cellular deficit reduce CSF total tau. To address this question, investigations of other models of AD-relevant endosomal dysfunction are required. Various models might include neuronal-selective knockouts of Phosphatidylinositol 3-kinase VPS34 (Miranda, Lasiecka et al. 2018) and mice bearing the APOE4 allele (Nuriel, Peng et al. 2017). Additionally, treatment with retromer-stabilizing chaperones (Berman, Ringe et al. 2015) or viral delivery of retromer core proteins will aid this mission.

Post-translational modifications of tau are numerous and include various cleavage and phosphorylation events. Work in both mice and humans suggests that the majority of CSF tau is at least partially truncated at the C-terminal (and perhaps the N-terminal, as well) (Barten, Cadelina et al. 2011, Meredith, Sankaranarayanan et al. 2013). The tools we used in this study rely upon detection of a central epitope, as do standard assessments of CSF total tau in AD

patients. Future work to clarify the exact sequence may impart additional specificity to this marker while also informing on the underlying biology. Mass spectrometry of neuron culture media will greatly assist this inquiry (as murine CSF tau is nearly undetectable, even in retromer knockout mice).

While at least a portion of CSF tau is phosphorylated, the striking correlations between APLP1 NTFs and total tau we noted in human CSF were less significant in ptau. Therefore, we postulate that the pathways involved in the secretion of APLP1 NTFs and phosphorylated tau might be more distinct and we predict that the elevation in extracellular tau we see in our retromer knockout is not driven entirely by an increase in ptau181. Follow-up work in neuronal culture is required to confirm whether this is indeed true.

Although the general objective of this project was limited to biomarker identification, the identification of such an intriguing and AD-relevant biomarker motivates an increasing interest in the underlying biology. The endolysosomal system has been clearly linked to tau secretion (Saman, Kim et al. 2012, Rodriguez, Mohamed et al. 2017, Caballero, Wang et al. 2018). Yet, it remains unclear which of the various compartments contribute most to this process. Recent work has demonstrated that tau can accumulate in late endosomes (Caballero, Wang et al. 2018), compartments which can fuse with the plasma membrane, liberating their lumenal contents into the extracellular space. Other groups have demonstrated that tau can accumulate in exosomes (Wang, Balaji et al. 2017); yet, this vesicle-bound population comprises a very small percentage (2%) of extracellular tau (Wang, Balaji et al. 2017). Thus, we propose that the more than 5-fold

increase in extracellular tau in retromer knockout CSF is likely non-exosomal. Nonetheless, we hypothesize that it is these late endosomes/MVBs which give rise to the tau accumulation we see in both CSF and culture media. Further investigations to pinpoint this mechanism are warranted and include both immunocytochemistry and electron microscopy.

This comprehensive biomarker discovery project made use of an assortment of mouse models of AD-relevant endosomal dysfunction to uncover various biomarker candidates in brain exosomes and CSF. Translations to humans, however, is not always straight-forward, despite substantial genomic homology. The hurdle is further challenged here by the presence of extracellular plaques which are known to alter the CSF proteome of AD patients. Our translational explorations of various candidates suggest that CSF total tau—unaffected by the presence of AD plaques—is the most reliable biomarker of retromer-dependent endosomal dysfunction with clinical utility. Furthermore, if follow-up studies confirm sensitivity and specificity this molecular profile, then perhaps the most remarkable conclusion of this study is that endosomal dysfunction is a universal feature of AD pathology, presenting at the earliest of stages.

6. Materials and Methods

Antibodies and Reagents

The following antibodies were used for immunoblot: VPS35 (ab10099, mouse, 1:1000, Abcam), VPS26a (ab23892, rabbit, 1:1000, Abcam), VPS26b (NBP1-92575, rabbit, 1:500, Novus Biologicals), VPS29 (SAB2501105, goat, 1:500, Sigma Aldrich), Actin (NB600-535, mouse, 1:10000, Novus Biologicals), Albumin (NB600-41532, goat, 1:5000, Novus Biologicals), CHL1 (AF2147-SP, goat, 1:500, Novus Biologicals), CHL1 (25250-1-AP, rabbit, 1:1000, ProteinTech), APLP1 (AF3179-SP, rabbit, 1:500, R&D Systems), Tau (ab80579, mouse, 1:500, Abcam), beta-III tubulin (ab107216, chicken, 1:5000, Abcam), anti-mouse HRP (170-6516, Bio-Rad), anti-goat HRP (172-1034, rabbit, 1:3000, Bio-Rad), anti-rabbit HRP (1706515, goat, Bio-Rad), anti-chicken 800CW (925-32218, donkey, 1:20000, Licor), anti-mouse 680LT (925-68022, donkey, 1:20000, Licor), anti-rabbit (925-32211, goat, 1:20000, Licor)**,** Protein G-HRP (18-161, 1:10000, Sigma Aldrich), Protein A-HRP (101023, 1:10000, Thermo Fisher).

The following ELISA kits were used for mouse and human CSF experiments: Hemoglobin Mouse ELISA Kit (ab157715, Abcam), human APLP1 (LS-F8957-1, LS Bio). Roche lumi-light substrate (12015200001, Sigma Aldrich) was used for chemiluminescence.

Mouse models

All mice were housed in a barrier facility and used in accordance with National Institute of Health and Columbia University Institutional Animal Care and Use Committee regulations.

VPS35$^{fl/fl}$; Cam2α-Cre knockout mice

Mice expressing loxP-flanked VPS35 (VPS35$^{fl/fl}$) on a C57BL/6 background were crossed with mice expressing Cre-recombinase under the Camk2α promoter to knock-out VPS35 in forebrain neurons. VPS35$^{fl/fl}$ mice lacking Cre-recombinase served as the control condition. Mice ages 6-12 months were used for all experiments.

VPS26a$^{fl/fl}$; Cam2α-Cre knockout mice

Mice expressing loxP-flanked VPS26a (VPS26a$^{fl/fl}$) on a C57BL/6 background were crossed with mice expressing Cre-recombinase under the Camk2α promoter to knock-out VPS26a in forebrain neurons. VPS26a$^{fl/fl}$ mice lacking Cre-recombinase served as the control condition. Six-month-old mice were used for all lipidomics experiments.

VPS26b$^{-/-}$ Mice

VPS26b heterozygote were generated by a targeting vector containing a neomycin-resistant expression cassette flanked by genomic regions of VPS26b, negative selection, electroporation into embryonic stem cells, and injection into mouse blastocyst (as described previously)*(Kim, Lee et al. 2010)*. Chimeric males were mated with C57BL/6 female mice to generate a heterozygote colony(Kim, Lee et al. 2010). Heterozygotes were then mated to generate the complete knockout and the wildtype controls. Twelve-month-old mice were used for all exosome experiments.

VPS26a$^{+/-}$ Mice

Congenic VPS26a heterozygotes were crossed on a 120/SvEv agouti background

for 10 generations and maintained through sibling mating(Muhammad, Flores et al. 2008). Mice ages 3-6 months were used for all lipidomics and proteomics experiments.

Murine CSF collection

Murine CSF was collected in a post-mortem procedure following CO_2 overdose in accordance with IACUC guidelines. Briefly, euthanized mice were placed in a prone position and the skin covering the back of the neck was surgically excised. A cotton swab containing 70% ethanol was used to remove any hair or skin from the exposed tissue. Then, a 27-gauge needle (SV*27EL, Terumo Medical Products) attached to a 1-ml syringe (329650, BD Biosciences) was inserted into the cisterna magna allowing flow of CSF into the butterfly needle. After 10-15 seconds, the needle was removed and the CSF aspirated into microcentrifuge tubes (1605-0000, USA Scientific) which were immediately placed on dry ice and subsequently stored at -80C. Roughly 5-10uL of fluid was collected per mouse. CSF which was visibly contaminated with blood was discarded. All remaining samples underwent more stringent assessment for blood contamination via hemoglobin ELISA using 0.5uL in a 1:200 dilution. Samples below 0.01% blood contamination were retained for biochemical analyses. For each assay, both individual and pooled replicates between conditions were matched for hemoglobin content to reduce the likelihood of a blood contamination confound.

Lipidomic analyses

Lipids were extracted from equal volumes of murine CSF (30ul for pooled samples or 7uL for individual samples). Lipid extracts were prepared via chloroform-methanol extraction, spiked

with appropriate internal standards, and analyzed using a 6490 Triple Quadrupole LC/MS system (Agilent Technologies, Santa Clara, CA) as described previously(Chan, Oliveira et al. 2012). Glycerophospholipids and sphingolipids were separated with normal-phase HPLC using an Agilent Zorbax Rx-Sil column (inner diameter 2.1 x 100 mm) under the following conditions: mobile phase A (chloroform:methanol:1 M ammonium hydroxide, 89.9:10:0.1, v/v/v) and mobile phase B (chloroform:methanol:water:ammonium hydroxide, 55:39.9:5:0.1, v/v/v); 95% A for 2 min, linear gradient to 30% A over 18 min and held for 3 min, and linear gradient to 95% A over 2 min and held for 6 min. Quantification of lipid species was accomplished using multiple reaction monitoring (MRM) transitions that were developed in earlier studies(Chan, Oliveira et al. 2012) in conjunction with referencing of appropriate internal standards: ceramide d18:1/17:0 and sphingomyelin d18:1/12:0 (Avanti Polar Lipids, Alabaster, AL). Values are represented as mole fraction with respect to total lipid (% molarity). For this, lipid mass (in moles) of any specific lipid is normalized by the total mass (in moles) of all the lipids measured(Chan, Oliveira et al. 2012). In addition, all of our results were further normalized by protein content.

Proteomic analyses: Labeled LC-MS/MS of VPS26a$^{+/-}$ CSF

High quality CSF (<0.01% blood contamination) collected from VPS26$^{+/-}$ and wildtype littermates was pooled into four biological replicates per genotype of 30uL each. Each replicate was a composite of CSF from roughly 4-6 mice. Protein concentrations from each sample were determined by a fluorescent-based protein assay (Q33211, Life Technology). Concentrations ranged from 0.68-0.8μg/mL per sample. Equal amounts (20μg) from each sample were digested by trypsin and labeled with TMT isobaric mass tags. A reference sample (comprised of equal

amounts from each sample) was generated for quantification. After TMT labeling, all samples were mixed and peptides were fractionated by C18 reverse phase with a pH gradient (Life Technologies). Peptide mixtures were analyzed by Orbitrap Fusion Tribrid mass spectrometer (Thermo Fisher) and searched against the mouse Uniprot protein database using Proteome Discoverer 2.1 (Thermo Fisher). Overall intensity of each TMT channel was normalized to the reference sample. Minitab17 was used to perform statistical analyses and generate statistical plots. Qlucore Omic Exporer software was used to perform statistical analysis on phosphopeptides.

Proteomic analyses: Unlabeled LC-MS/MS of VPS35 Camk2α Knockout CSF

High quality CSF (<0.01% blood contamination) collected from VPS35 knockout and control littermates was pooled into biological replicates of 30uL each, which were roughly matched for hemoglobin content. Each replicate was a composite of CSF from 4-7 mice. The protein concentration of each sample was determined via Qubit Protein Quantification Assay (Q33211, Life Technology). Concentrations for each sample ranged from 0.10-0.16mg/ml. Each sample was loaded onto an S-trap column, digested with trypsin, eluted with trifluoroacetic acid, and dried. Each sample was divided into two technical replicates (each containing 1.5ug of digested protein). MS/MS was performed on each sample using a Thermo Orbitrap Fusion Tribrid Mass Sepctrometer (Thermo Fisher). Proteome Discoverer software (version 1.4) was used to search the acquited MS/MS data against a mouse protein database downloaded from UniProt. Positive identification was set at 1% protein FDR for those proteins having at least two quantifiable values detected. Any duplicated protein identifications from the database were removed. A total of

1505 mouse proteins were detected and included in the final data set. For each protein, quantification was determined by averaging the peak area of the three most abundant and distinct peptides. Total areas were used for normalization. Qlucore Omics Explorer and Minitab17 Software were used to perform correlation and statistical analyses. Spearman correlations of technical replicates were used to determine group outliers. One outlier per genotype was identified by the Proteomics Core and removed prior to downstream analyses.

Generation of GFP.Cre and GFP.Δ-Cre Virus for VPS35 Knockout in Cell Culture

HEK293T cells were grown to 70% confluence in media containing DMEM, 5% glutaMAx, 10% FBS, and pen/strep prior to lipofectamine (LTX) transfection with plasmids containing Δ8.2, VSVG, and either GFP.Cre or GFP.Δ-Cre. After 72 hours, media was collected and filtered (SE1M003M00, Millipore) before incubation with lenti-x concentrator (631231, Clontech) and centrifugation to collect the viral particles.

VPS35 Knockout in Primary Neuron Cultures

Hippocampi or cerebral cortices from $VPS35^{fl/fl}$ P0 pups were dissected in cold HBSS and digested in 0.5% Trypsin-EDTA (25200056, Invitrogen) for 20 minutes at 37C. The digested tissue was rinsed in HBSS and homogenized gently with a flame-polished glass pipette in NBA media containing Glutamax (35050-061, Life Technologies), B-27 (17504044, Thermo Fisher), and pen/strep (15140-122, Thermo Fisher). Neurons were plated in six-well plates (83.3921, Sarstedt) containing poly-D-lysine-coated 12mm glass coverslips (NC9702891, Thermo Fisher) for immunofluorescence or in poly-L-ornithine-coated 12-well plates (83.3921, Sarstedt) for

immunoblot and media collection experiments. Media was replaced at 24 hours and 1/3 media replacements were conducted every 5 days thereafter. On DIV5, lentivirus containing either GFP.Cre or GFP.Δ-Cre virus was added to each well. On DIV15, media was removed and neurons fixed in 4% paraformaldehyde (15710-S, Electron Microscopy Science) for downstream immunofluorescence or lysed in cold RIPA buffer (89901, Thermo Fisher) for immunoblot.

Immunoblotting

Samples were prepared in LDS sample buffer (NP0007, Thermo Fisher) and reducing agent (161-0792, Bio-Rad), boiled for 5 minutes at 90C and run via electrophoresis in 4-12% bis-tris gels (NP0336 or NP0335, Thermo Fisher) in MES buffer (NP0002-02, Thermo Fisher). For CSF and media experiments, equal volumes (5-15uL) were loaded in each lane; for lysate, equal masses were loaded in each lane. were loaded per lane. Proteins were then transferred to nitrocellulose membranes (IB3010-31, Invitrogen) via iBlot (P3; 7:40) and blocked for 1 hour in bovine serum albumin (A30075-100gm, Research Product International) or odyssey blocking buffer (927-40000, Licor) diluted 1:1 in PBS-T. Membranes were then probed with primary antibodies overnight at 4C, washed in PBS-T, probed with secondary antibodies (HRP-conjugated or IR-conjugated) for one hour at room temperature. Membranes were again washed in PBS-T and imaged in Roche substrate (12015196001, Sigma Aldrich) for ECL or alone with the Licor odyssey system.

Total Tau Quantification in Culture Media

Total tau was quantified from culture media using the MSD mouse total tau kit (K151DSD-1, MesoScale Discovery) according to the manufacturer's guidelines. Wells were first blocked for one hour and washed. Then, 25uL of culture media was added in duplicate wells along with the total tau standards prepared in NBA media (with glutamax, B-27, and pen-strep, as described above), and incubated for one hour. Wells were washed and incubated with detection antibody for an additional hour before washing and analyzing in read buffer T solution on the MSD instrument. Cell death was assessed via LDH levels in the cultured media using CytoTox-ONE™ Homogeneous Membrane Integrity Assay (G7890, Promega). Values for total tau and LDH were normalized to total protein, which was measured using BCA (23227, Pierce).

Total Tau Quantification in Murine CSF

CSF total tau was quantified by SIMOA using the mouse total tau assay (102209, Quanterix). Individual CSF samples (5uL) were diluted 1:80 in sample buffer and then split into technical duplicates. Standards and samples were run according to the manufacturer's instructions and read on the HD-1 analyzer (Quanterix).

Human CSF Studies

CSF from patients with Alzheimer's disease or Mild Cognitive Impairment, and Normal Controls, was requested from the Columbia University Alzheimer's Disease Research Center (ADRC) CSF bank. This CSF bank includes CSF obtained by lumbar puncture and banked for research according to protocols approved by the Columbia University IRB. CSF was stored frozen in 400 uL aliquots, in polypropylene tubes, at -80C. Frozen CSF aliquots were later thawed, and analyzed

for Aβ42, total tau, and phospho-tau, by the ADRC Clinical Core, using a multiplex fluorimetric microsphere xMAP bead-based sandwich immunoassay using monoclonal antibodies covalently coupled to spectrally specific fluorescent beads. This assay (Inno-BIA AlzBio3, Fujirebio US Inc, Alpharetta, GA) was performed using a Luminex 100 machine. Identical frozen CSF aliquots were thawed and used for the experiments described here**.** N-APLP1 and N-CHL1 were measured via immunoblot as described above. N-APLP1 were also measured via ELISA (LS-F8957-1, LS Bio) in duplicate according to the manufacturer's instructions following a 1:20 dilution as informed by early optimizations in control CSF. Total protein was calculated via BCA (23227, Pierce). Thresholds implemented to confirm plaque positivity in AD patients includes Aβ42<210pg/mL and total tau/Aβ42≥0.39.

Statistical methods

Student's t-test was used for all biochemical experiments and immunohistochemical analysis using two-tailed distribution with equal variance ($P < 0.05$). Limma software was used for analysis of CSF proteomics, and FDR-corrected q-values are reported. Significance is indicated as *P < 0.05, **P < 0.01 and ***P < 0.001; ****P < 0.0001).

7. References

Abner, E. L., G. A. Jicha, L. M. Shaw, J. Q. Trojanowski and E. J. Goetzl (2016). "Plasma neuronal exosomal levels of Alzheimer's disease biomarkers in normal aging." Ann Clin Transl Neurol **3**(5): 399-403.

Alonso, A., T. Zaidi, M. Novak, I. Grundke-Iqbal and K. Iqbal (2001). "Hyperphosphorylation induces self-assembly of tau into tangles of paired helical filaments/straight filaments." Proc Natl Acad Sci U S A **98**(12): 6923-6928.

Altmann, A., B. Ng, S. M. Landau, W. J. Jagust, M. D. Greicius and I. Alzheimer's Disease Neuroimaging (2015). "Regional brain hypometabolism is unrelated to regional amyloid plaque burden." Brain **138**(Pt 12): 3734-3746.

Altmann, A., L. Tian, V. W. Henderson, M. D. Greicius and I. Alzheimer's Disease Neuroimaging Initiative (2014). "Sex modifies the APOE-related risk of developing Alzheimer disease." Ann Neurol **75**(4): 563-573.

Alvarez-Erviti, L., Y. Seow, A. H. Schapira, C. Gardiner, I. L. Sargent, M. J. Wood and J. M. Cooper (2011). "Lysosomal dysfunction increases exosome-mediated alpha-synuclein release and transmission." Neurobiol Dis **42**(3): 360-367.

Andreasen, N., L. Minthon, P. Davidsson, E. Vanmechelen, H. Vanderstichele, B. Winblad and K. Blennow (2001). "Evaluation of CSF-tau and CSF-Abeta42 as diagnostic markers for Alzheimer disease in clinical practice." Arch Neurol **58**(3): 373-379.

APA. (2017). "What is Alzheimer's Disease?", from https://www.psychiatry.org/patients-families/alzheimers/what-is-alzheimers-disease.

Archer, H. A., P. Edison, D. J. Brooks, J. Barnes, C. Frost, T. Yeatman, N. C. Fox and M. N. Rossor (2006). "Amyloid load and cerebral atrophy in Alzheimer's disease: an 11C-PIB positron emission tomography study." Ann Neurol **60**(1): 145-147.

Arighi, C. N., L. M. Hartnell, R. C. Aguilar, C. R. Haft and J. S. Bonifacino (2004). "Role of the mammalian retromer in sorting of the cation-independent mannose 6-phosphate receptor." J Cell Biol **165**(1): 123-133.

Armstrong, A., N. Mattsson, H. Appelqvist, C. Janefjord, L. Sandin, L. Agholme, B. Olsson, S. Svensson, K. Blennow, H. Zetterberg and K. Kagedal (2014). "Lysosomal network proteins as potential novel CSF biomarkers for Alzheimer's disease." Neuromolecular Med **16**(1): 150-160.

Asai, H., S. Ikezu, S. Tsunoda, M. Medalla, J. Luebke, T. Haydar, B. Wolozin, O. Butovsky, S. Kugler and T. Ikezu (2015). "Depletion of microglia and inhibition of exosome synthesis halt tau propagation." Nat Neurosci **18**(11): 1584-1593.

Ashford, J. W. (2004). "APOE genotype effects on Alzheimer's disease onset and epidemiology." J Mol Neurosci **23**(3): 157-165.

Askanas, V., W. K. Engel, M. Bilak, R. B. Alvarez and D. J. Selkoe (1994). "Twisted tubulofilaments of inclusion body myositis muscle resemble paired helical filaments of Alzheimer brain and contain hyperphosphorylated tau." Am J Pathol **144**(1): 177-187.

Attar, N. and P. J. Cullen (2010). "The retromer complex." Adv Enzyme Regul **50**(1): 216-236.

Bales, K. R., T. Verina, D. J. Cummins, Y. Du, R. C. Dodel, J. Saura, C. E. Fishman, C. A. DeLong, P. Piccardo, V. Petegnief, B. Ghetti and S. M. Paul (1999). "Apolipoprotein E is essential for amyloid deposition in the APP(V717F) transgenic mouse model of Alzheimer's disease." Proc Natl Acad Sci U S A **96**(26): 15233-15238.

Barten, D. M., G. W. Cadelina, N. Hoque, L. B. DeCarr, V. L. Guss, L. Yang, S. Sankaranarayanan, P. D. Wes, M. E. Flynn, J. E. Meredith, M. K. Ahlijanian and C. F. Albright (2011). "Tau transgenic mice as models for cerebrospinal fluid tau biomarkers." J Alzheimers Dis **24 Suppl 2**: 127-141.

Bayer, T. A., R. Cappai, C. L. Masters, K. Beyreuther and G. Multhaup (1999). "It all sticks together--the APP-related family of proteins and Alzheimer's disease." Mol Psychiatry **4**(6): 524-528.

Bechler, M. E., A. M. Doody, K. D. Ha, B. L. Judson, I. Chen and W. J. Brown (2011). "The phospholipase A(2) enzyme complex PAFAH Ib mediates endosomal membrane tubule formation and trafficking." Mol Biol Cell **22**(13): 2348-2359.

Bejanin, A., D. R. Schonhaut, R. La Joie, J. H. Kramer, S. L. Baker, N. Sosa, N. Ayakta, A. Cantwell, M. Janabi, M. Lauriola, J. P. O'Neil, M. L. Gorno-Tempini, Z. A. Miller, H. J. Rosen, B. L. Miller, W. J. Jagust and G. D. Rabinovici (2017). "Tau pathology and neurodegeneration contribute to cognitive impairment in Alzheimer's disease." Brain **140**(12): 3286-3300.

Berman, D. E., D. Ringe, G. A. Petsko and S. A. Small (2015). "The use of pharmacological retromer chaperones in Alzheimer's disease and other endosomal-related disorders." Neurotherapeutics **12**(1): 12-18.

Bhalla, A., C. P. Vetanovetz, E. Morel, Z. Chamoun, G. Di Paolo and S. A. Small (2012). "The location and trafficking routes of the neuronal retromer and its role in amyloid precursor protein transport." Neurobiol Dis **47**(1): 126-134.

Bird, T. D. (1993). Early-Onset Familial Alzheimer Disease. GeneReviews((R)). M. P. Adam, H. H. Ardinger, R. A. Pagon et al. Seattle (WA).

Bitan, G., M. D. Kirkitadze, A. Lomakin, S. S. Vollers, G. B. Benedek and D. B. Teplow (2003). "Amyloid beta -protein (Abeta) assembly: Abeta 40 and Abeta 42 oligomerize through distinct pathways." Proc Natl Acad Sci U S A **100**(1): 330-335.

Bloom, G. S. (2014). "Amyloid-beta and tau: the trigger and bullet in Alzheimer disease pathogenesis." JAMA Neurol **71**(4): 505-508.

Braak, H. and E. Braak (1991). "Neuropathological stageing of Alzheimer-related changes." Acta Neuropathol **82**(4): 239-259.

Bugarcic, A., I. Vetter, S. Chalmers, G. Kinna, B. M. Collins and R. D. Teasdale (2015). "Vps26B-retromer negatively regulates plasma membrane resensitization of PAR-2." Cell Biol Int **39**(11): 1299-1306.

Caballero, B., Y. Wang, A. Diaz, I. Tasset, Y. R. Juste, B. Stiller, E. M. Mandelkow, E. Mandelkow and A. M. Cuervo (2018). "Interplay of pathogenic forms of human tau with different autophagic pathways." Aging Cell **17**(1).

Capodivento, G., D. Visigalli, M. Garnero, R. Fancellu, M. D. Ferrara, A. Basit, Z. Hamid, V. P. Pastore, S. Garibaldi, A. Armirotti, G. Mancardi, C. Serrati, E. Capello, A. Schenone and L. Nobbio (2017). "Sphingomyelin as a myelin biomarker in CSF of acquired demyelinating neuropathies." Sci Rep **7**(1): 7831.

Carter, C. L., E. M. Resnick, M. Mallampalli and A. Kalbarczyk (2012). "Sex and gender differences in Alzheimer's disease: recommendations for future research." J Womens Health (Larchmt) **21**(10): 1018-1023.

Cataldo, A. M., J. L. Barnett, C. Pieroni and R. A. Nixon (1997). "Increased neuronal endocytosis and protease delivery to early endosomes in sporadic Alzheimer's disease: neuropathologic evidence for a mechanism of increased beta-amyloidogenesis." J Neurosci **17**(16): 6142-6151.

Cataldo, A. M., C. M. Peterhoff, J. C. Troncoso, T. Gomez-Isla, B. T. Hyman and R. A. Nixon (2000). "Endocytic pathway abnormalities precede amyloid beta deposition in sporadic Alzheimer's disease and Down syndrome: differential effects of APOE genotype and presenilin mutations." Am J Pathol **157**(1): 277-286.

Chan, R. B., T. G. Oliveira, E. P. Cortes, L. S. Honig, K. E. Duff, S. A. Small, M. R. Wenk, G. Shui and G. Di Paolo (2012). "Comparative lipidomic analysis of mouse and human brain with Alzheimer disease." J Biol Chem **287**(4): 2678-2688.

Chartier-Harlin, M. C., F. Crawford, H. Houlden, A. Warren, D. Hughes, L. Fidani, A. Goate, M. Rossor, P. Roques, J. Hardy and et al. (1991). "Early-onset Alzheimer's disease caused by mutations at codon 717 of the beta-amyloid precursor protein gene." Nature **353**(6347): 844-846.

Chen, F. W., R. E. Gordon and Y. A. Ioannou (2005). "NPC1 late endosomes contain elevated levels of non-esterified ('free') fatty acids and an abnormally glycosylated form of the NPC2 protein." Biochem J **390**(Pt 2): 549-561.

Childs-Disney, J. L., M. Wu, A. Pushechnikov, O. Aminova and M. D. Disney (2007). "A small molecule microarray platform to select RNA internal loop-ligand interactions." ACS Chem Biol **2**(11): 745-754.

Choy, R. W., Z. Cheng and R. Schekman (2012). "Amyloid precursor protein (APP) traffics from the cell surface via endosomes for amyloid beta (Abeta) production in the trans-Golgi network." Proc Natl Acad Sci U S A **109**(30): E2077-2082.

Choy, R. W., M. Park, P. Temkin, B. E. Herring, A. Marley, R. A. Nicoll and M. von Zastrow (2014). "Retromer mediates a discrete route of local membrane delivery to dendrites." Neuron **82**(1): 55-62.

Chu, J. and D. Pratico (2017). "The retromer complex system in a transgenic mouse model of AD: influence of age." Neurobiol Aging **52**: 32-38.

Collino, F., M. Pomatto, S. Bruno, R. S. Lindoso, M. Tapparo, W. Sicheng, P. Quesenberry and G. Camussi (2017). "Exosome and Microvesicle-Enriched Fractions Isolated from Mesenchymal Stem Cells by Gradient Separation Showed Different Molecular Signatures and Functions on Renal Tubular Epithelial Cells." Stem Cell Rev **13**(2): 226-243.

Costa-Silva, B., N. M. Aiello, A. J. Ocean, S. Singh, H. Zhang, B. K. Thakur, A. Becker, A. Hoshino, M. T. Mark, H. Molina, J. Xiang, T. Zhang, T. M. Theilen, G. Garcia-Santos, C. Williams, Y. Ararso, Y. Huang, G. Rodrigues, T. L. Shen, K. J. Labori, I. M. Lothe, E. H. Kure, J. Hernandez, A. Doussot, S. H. Ebbesen, P. M. Grandgenett, M. A. Hollingsworth, M. Jain, K. Mallya, S. K. Batra, W. R. Jarnagin, R. E. Schwartz, I. Matei, H. Peinado, B. Z. Stanger, J. Bromberg and D. Lyden (2015). "Pancreatic cancer exosomes initiate pre-metastatic niche formation in the liver." Nat Cell Biol **17**(6): 816-826.

Cozier, G. E., J. Carlton, A. H. McGregor, P. A. Gleeson, R. D. Teasdale, H. Mellor and P. J. Cullen (2002). "The phox homology (PX) domain-dependent, 3-phosphoinositide-mediated association of sorting nexin-1 with an early sorting endosomal compartment is required for its ability to regulate epidermal growth factor receptor degradation." J Biol Chem **277**(50): 48730-48736.

Cutler, R. G., J. Kelly, K. Storie, W. A. Pedersen, A. Tammara, K. Hatanpaa, J. C. Troncoso and M. P. Mattson (2004). "Involvement of oxidative stress-induced abnormalities in ceramide and cholesterol metabolism in brain aging and Alzheimer's disease." Proc Natl Acad Sci U S A **101**(7): 2070-2075.

Demory Beckler, M., J. N. Higginbotham, J. L. Franklin, A. J. Ham, P. J. Halvey, I. E. Imasuen, C. Whitwell, M. Li, D. C. Liebler and R. J. Coffey (2013). "Proteomic analysis of exosomes from mutant KRAS colon cancer cells identifies intercellular transfer of mutant KRAS." Mol Cell Proteomics **12**(2): 343-355.

Derivery, E. and A. Gautreau (2010). "Evolutionary conservation of the WASH complex, an actin polymerization machine involved in endosomal fission." Commun Integr Biol **3**(3): 227-230.

Di Paolo, G. and T. W. Kim (2011). "Linking lipids to Alzheimer's disease: cholesterol and beyond." Nat Rev Neurosci **12**(5): 284-296.

Dislich, B., F. Wohlrab, T. Bachhuber, S. A. Muller, P. H. Kuhn, S. Hogl, M. Meyer-Luehmann and S. F. Lichtenthaler (2015). "Label-free Quantitative Proteomics of Mouse Cerebrospinal Fluid Detects beta-Site APP Cleaving Enzyme (BACE1) Protease Substrates In Vivo." Mol Cell Proteomics **14**(10): 2550-2563.

Duncan, H. D., J. Nikelski, R. Pilon, J. Steffener, H. Chertkow and N. A. Phillips (2017). "Structural brain differences between monolingual and multilingual patients with mild cognitive impairment and Alzheimer disease: Evidence for cognitive reserve." Neuropsychologia **109**: 270-282.

Edgar, A. J. and J. M. Polak (2000). "Human homologues of yeast vacuolar protein sorting 29 and 35." Biochem Biophys Res Commun **277**(3): 622-630.

Fagan, A. M., M. A. Mintun, R. H. Mach, S. Y. Lee, C. S. Dence, A. R. Shah, G. N. LaRossa, M. L. Spinner, W. E. Klunk, C. A. Mathis, S. T. DeKosky, J. C. Morris and D. M. Holtzman (2006). "Inverse relation between in vivo amyloid imaging load and cerebrospinal fluid Abeta42 in humans." Ann Neurol **59**(3): 512-519.

Fjorback, A. W., M. Seaman, C. Gustafsen, A. Mehmedbasic, S. Gokool, C. Wu, D. Militz, V. Schmidt, P. Madsen, J. R. Nyengaard, T. E. Willnow, E. I. Christensen, W. B. Mobley, A. Nykjaer and O. M. Andersen (2012). "Retromer binds the FANSHY sorting motif in SorLA to regulate amyloid precursor protein sorting and processing." J Neurosci **32**(4): 1467-1480.

Foley, P. (2010). "Lipids in Alzheimer's disease: A century-old story." Biochim Biophys Acta **1801**(8): 750-753.

Fonteh, A. N., C. Ormseth, J. Chiang, M. Cipolla, X. Arakaki and M. G. Harrington (2015). "Sphingolipid metabolism correlates with cerebrospinal fluid Beta amyloid levels in Alzheimer's disease." PLoS One **10**(5): e0125597.

Ghossoub, R., F. Lembo, A. Rubio, C. B. Gaillard, J. Bouchet, N. Vitale, J. Slavik, M. Machala and P. Zimmermann (2014). "Syntenin-ALIX exosome biogenesis and budding into multivesicular bodies are controlled by ARF6 and PLD2." Nat Commun **5**: 3477.

Glabe, C. G. (2006). "Common mechanisms of amyloid oligomer pathogenesis in degenerative disease." Neurobiol Aging **27**(4): 570-575.

Glerup, S., M. Lume, D. Olsen, J. R. Nyengaard, C. B. Vaegter, C. Gustafsen, E. I. Christensen, M. Kjolby, A. Hay-Schmidt, D. Bender, P. Madsen, M. Saarma, A. Nykjaer and C. M. Petersen (2013). "SorLA controls neurotrophic activity by sorting of GDNF and its receptors GFRalpha1 and RET." Cell Rep **3**(1): 186-199.

Goetzl, E. J., A. Boxer, J. B. Schwartz, E. L. Abner, R. C. Petersen, B. L. Miller, O. D. Carlson, M. Mustapic and D. Kapogiannis (2015). "Low neural exosomal levels of cellular survival factors in Alzheimer's disease." Ann Clin Transl Neurol **2**(7): 769-773.

Goetzl, E. J., A. Boxer, J. B. Schwartz, E. L. Abner, R. C. Petersen, B. L. Miller and D. Kapogiannis (2015). "Altered lysosomal proteins in neural-derived plasma exosomes in preclinical Alzheimer disease." Neurology **85**(1): 40-47.

Goetzl, E. J., M. Mustapic, D. Kapogiannis, E. Eitan, I. V. Lobach, L. Goetzl, J. B. Schwartz and B. L. Miller (2016). "Cargo proteins of plasma astrocyte-derived exosomes in Alzheimer's disease." FASEB J **30**(11): 3853-3859.

Gomez, T. S. and D. D. Billadeau (2009). "A FAM21-containing WASH complex regulates retromer-dependent sorting." Dev Cell **17**(5): 699-711.

Gong, C. X. and K. Iqbal (2008). "Hyperphosphorylation of microtubule-associated protein tau: a promising therapeutic target for Alzheimer disease." Curr Med Chem **15**(23): 2321-2328.

Gonzales, P. A., T. Pisitkun, J. D. Hoffert, D. Tchapyjnikov, R. A. Star, R. Kleta, N. S. Wang and M. A. Knepper (2009). "Large-scale proteomics and phosphoproteomics of urinary exosomes." J Am Soc Nephrol **20**(2): 363-379.

Gozal, Y. M., D. Cheng, D. M. Duong, J. J. Lah, A. I. Levey and J. Peng (2006). "Merger of laser capture microdissection and mass spectrometry: a window into the amyloid plaque proteome." Methods Enzymol **412**: 77-93.

Grundke-Iqbal, I., K. Iqbal, M. Quinlan, Y. C. Tung, M. S. Zaidi and H. M. Wisniewski (1986). "Microtubule-associated protein tau. A component of Alzheimer paired helical filaments." J Biol Chem **261**(13): 6084-6089.

Grundke-Iqbal, I., K. Iqbal, Y. C. Tung, M. Quinlan, H. M. Wisniewski and L. I. Binder (1986). "Abnormal phosphorylation of the microtubule-associated protein tau (tau) in Alzheimer cytoskeletal pathology." Proc Natl Acad Sci U S A **83**(13): 4913-4917.

Guerreiro, R., J. Bras and J. Hardy (2013). "SnapShot: genetics of Alzheimer's disease." Cell **155**(4): 968-968 e961.

Haft, C. R., M. de la Luz Sierra, R. Bafford, M. A. Lesniak, V. A. Barr and S. I. Taylor (2000). "Human orthologs of yeast vacuolar protein sorting proteins Vps26, 29, and 35: assembly into multimeric complexes." Mol Biol Cell **11**(12): 4105-4116.

Harbour, M. E., S. Y. Breusegem, R. Antrobus, C. Freeman, E. Reid and M. N. Seaman (2010). "The cargo-selective retromer complex is a recruiting hub for protein complexes that regulate endosomal tubule dynamics." J Cell Sci **123**(Pt 21): 3703-3717.

Hardy, J. and D. Allsop (1991). "Amyloid deposition as the central event in the aetiology of Alzheimer's disease." Trends Pharmacol Sci **12**(10): 383-388.

Harrison, M. S., C. S. Hung, T. T. Liu, R. Christiano, T. C. Walther and C. G. Burd (2014). "A mechanism for retromer endosomal coat complex assembly with cargo." Proc Natl Acad Sci U S A **111**(1): 267-272.

Harterink, M., F. Port, M. J. Lorenowicz, I. J. McGough, M. Silhankova, M. C. Betist, J. R. T. van Weering, R. van Heesbeen, T. C. Middelkoop, K. Basler, P. J. Cullen and H. C. Korswagen (2011). "A SNX3-dependent retromer pathway mediates retrograde transport of the Wnt sorting receptor Wntless and is required for Wnt secretion." Nat Cell Biol **13**(8): 914-923.

Hebert, L. E., J. Weuve, P. A. Scherr and D. A. Evans (2013). "Alzheimer disease in the United States (2010-2050) estimated using the 2010 census." Neurology **80**(19): 1778-1783.

Holtzman, D. M. (2001). "Role of apoe/Abeta interactions in the pathogenesis of Alzheimer's disease and cerebral amyloid angiopathy." J Mol Neurosci **17**(2): 147-155.

Holtzman, D. M., K. R. Bales, T. Tenkova, A. M. Fagan, M. Parsadanian, L. J. Sartorius, B. Mackey, J. Olney, D. McKeel, D. Wozniak and S. M. Paul (2000). "Apolipoprotein E isoform-dependent amyloid deposition and neuritic degeneration in a mouse model of Alzheimer's disease." Proc Natl Acad Sci U S A **97**(6): 2892-2897.

Hoshino, A., B. Costa-Silva, T. L. Shen, G. Rodrigues, A. Hashimoto, M. Tesic Mark, H. Molina, S. Kohsaka, A. Di Giannatale, S. Ceder, S. Singh, C. Williams, N. Soplop, K. Uryu, L. Pharmer, T. King, L. Bojmar, A. E. Davies, Y. Ararso, T. Zhang, H. Zhang, J. Hernandez, J. M. Weiss, V. D. Dumont-Cole, K. Kramer, L. H. Wexler, A. Narendran, G. K. Schwartz, J. H. Healey, P. Sandstrom, K. J. Labori, E. H. Kure, P. M. Grandgenett, M. A. Hollingsworth, M. de Sousa, S. Kaur, M. Jain, K. Mallya, S. K. Batra, W. R. Jarnagin, M. S. Brady, O. Fodstad, V. Muller, K. Pantel, A. J. Minn, M. J. Bissell, B. A. Garcia, Y. Kang, V. K. Rajasekhar, C. M. Ghajar, I. Matei, H. Peinado, J. Bromberg and D. Lyden (2015). "Tumour exosome integrins determine organotropic metastasis." Nature **527**(7578): 329-335.

Hu, W., X. Zhang, Y. C. Tung, S. Xie, F. Liu and K. Iqbal (2016). "Hyperphosphorylation determines both the spread and the morphology of tau pathology." Alzheimers Dement **12**(10): 1066-1077.

Huhmer, A. F., R. G. Biringer, H. Amato, A. N. Fonteh and M. G. Harrington (2006). "Protein analysis in human cerebrospinal fluid: Physiological aspects, current progress and future challenges." Dis Markers **22**(1-2): 3-26.

Israel, M. A., S. H. Yuan, C. Bardy, S. M. Reyna, Y. Mu, C. Herrera, M. P. Hefferan, S. Van Gorp, K. L. Nazor, F. S. Boscolo, C. T. Carson, L. C. Laurent, M. Marsala, F. H. Gage, A. M. Remes, E. H. Koo and L. S. Goldstein (2012). "Probing sporadic and familial Alzheimer's disease using induced pluripotent stem cells." Nature **482**(7384): 216-220.

Jiang, Y., K. A. Mullaney, C. M. Peterhoff, S. Che, S. D. Schmidt, A. Boyer-Boiteau, S. D. Ginsberg, A. M. Cataldo, P. M. Mathews and R. A. Nixon (2010). "Alzheimer's-related endosome dysfunction in Down syndrome is Abeta-independent but requires APP and is reversed by BACE-1 inhibition." Proc Natl Acad Sci U S A **107**(4): 1630-1635.

Karch, C. M. and A. M. Goate (2015). "Alzheimer's disease risk genes and mechanisms of disease pathogenesis." Biol Psychiatry **77**(1): 43-51.

Karran, E., M. Mercken and B. De Strooper (2011). "The amyloid cascade hypothesis for Alzheimer's disease: an appraisal for the development of therapeutics." Nat Rev Drug Discov **10**(9): 698-712.

Kerr, M. C., J. S. Bennetts, F. Simpson, E. C. Thomas, C. Flegg, P. A. Gleeson, C. Wicking and R. D. Teasdale (2005). "A novel mammalian retromer component, Vps26B." Traffic **6**(11): 991-1001.

Khalyfa, A., D. Gozal and L. Kheirandish-Gozal (2017). "Plasma Exosomes Disrupt Blood Brain Barrier in Children with OSA and Neurocognitive Deficits." Am J Respir Crit Care Med.

Khan, U. A., L. Liu, F. A. Provenzano, D. E. Berman, C. P. Profaci, R. Sloan, R. Mayeux, K. E. Duff and S. A. Small (2014). "Molecular drivers and cortical spread of lateral entorhinal cortex dysfunction in preclinical Alzheimer's disease." Nat Neurosci **17**(2): 304-311.

Kim, E., Y. Lee, H. J. Lee, J. S. Kim, B. S. Song, J. W. Huh, S. R. Lee, S. U. Kim, S. H. Kim, Y. Hong, I. Shim and K. T. Chang (2010). "Implication of mouse Vps26b-Vps29-Vps35 retromer complex in sortilin trafficking." Biochem Biophys Res Commun **403**(2): 167-171.

Kirschner, D. A., H. Inouye, L. K. Duffy, A. Sinclair, M. Lind and D. J. Selkoe (1987). "Synthetic peptide homologous to beta protein from Alzheimer disease forms amyloid-like fibrils in vitro." Proc Natl Acad Sci U S A **84**(19): 6953-6957.

Klingeborn, M., W. M. Dismuke, N. P. Skiba, U. Kelly, W. D. Stamer and C. Bowes Rickman (2017). "Directional Exosome Proteomes Reflect Polarity-Specific Functions in Retinal Pigmented Epithelium Monolayers." Sci Rep **7**(1): 4901.

Kochanek KD, M. S., Xu JQ, Tejada-Vera B. (2016). Deaths: Final Data for 2014. National Vital Statistics Reports. Hyattsville, Md., National Center for Health Statistics. **65**.

Kosicek, M., H. Zetterberg, N. Andreasen, J. Peter-Katalinic and S. Hecimovic (2012). "Elevated cerebrospinal fluid sphingomyelin levels in prodromal Alzheimer's disease." Neurosci Lett **516**(2): 302-305.

Kosik, K. S., C. L. Joachim and D. J. Selkoe (1986). "Microtubule-associated protein tau (tau) is a major antigenic component of paired helical filaments in Alzheimer disease." Proc Natl Acad Sci U S A **83**(11): 4044-4048.

Kramer, A., J. Green, J. Pollard, Jr. and S. Tugendreich (2014). "Causal analysis approaches in Ingenuity Pathway Analysis." Bioinformatics **30**(4): 523-530.

LaFerla, F. M., K. N. Green and S. Oddo (2007). "Intracellular amyloid-beta in Alzheimer's disease." Nat Rev Neurosci **8**(7): 499-509.

Lambert, J. C., C. A. Ibrahim-Verbaas, D. Harold, A. C. Naj, R. Sims, C. Bellenguez, A. L. DeStafano, J. C. Bis, G. W. Beecham, B. Grenier-Boley, G. Russo, T. A. Thorton-Wells, N. Jones, A. V. Smith, V. Chouraki, C. Thomas, M. A. Ikram, D. Zelenika, B. N. Vardarajan, Y. Kamatani, C. F. Lin, A. Gerrish, H. Schmidt, B. Kunkle, M. L. Dunstan, A. Ruiz, M. T. Bihoreau, S. H. Choi, C. Reitz, F. Pasquier, C. Cruchaga, D. Craig, N. Amin, C. Berr, O. L. Lopez, P. L. De Jager, V. Deramecourt, J. A. Johnston, D. Evans, S. Lovestone, L. Letenneur, F. J. Moron, D. C. Rubinsztein, G. Eiriksdottir, K. Sleegers, A. M. Goate, N. Fievet, M. W. Huentelman, M. Gill, K. Brown, M. I. Kamboh, L. Keller, P. Barberger-Gateau, B. McGuiness, E. B. Larson, R. Green, A. J. Myers, C. Dufouil, S. Todd, D. Wallon, S. Love, E. Rogaeva, J. Gallacher, P. St George-Hyslop, J. Clarimon, A. Lleo, A. Bayer, D. W. Tsuang, L. Yu, M. Tsolaki, P. Bossu, G. Spalletta, P. Proitsi, J. Collinge, S. Sorbi, F. Sanchez-Garcia, N. C. Fox, J. Hardy, M. C. Deniz Naranjo, P. Bosco, R. Clarke, C. Brayne, D. Galimberti, M. Mancuso, F. Matthews, I. European Alzheimer's Disease, Genetic, D. Environmental Risk in Alzheimer's, C. Alzheimer's Disease Genetic, H. Cohorts for, E. Aging Research in Genomic, S. Moebus, P. Mecocci, M. Del Zompo, W. Maier, H. Hampel, A. Pilotto, M. Bullido, F. Panza, P. Caffarra, B. Nacmias, J. R. Gilbert, M. Mayhaus, L. Lannefelt, H. Hakonarson, S. Pichler, M. M. Carrasquillo, M. Ingelsson, D. Beekly, V. Alvarez, F. Zou, O. Valladares, S. G. Younkin, E. Coto, K. L. Hamilton-Nelson, W. Gu, C. Razquin, P. Pastor, I. Mateo, M. J. Owen, K. M. Faber, P. V. Jonsson, O. Combarros, M. C. O'Donovan, L. B. Cantwell, H. Soininen, D. Blacker, S. Mead, T. H. Mosley, Jr., D. A. Bennett, T. B. Harris, L. Fratiglioni, C. Holmes, R. F. de Bruijn, P. Passmore, T. J. Montine, K. Bettens, J. I. Rotter, A. Brice, K. Morgan, T. M. Foroud, W. A. Kukull, D. Hannequin, J. F. Powell, M. A. Nalls, K. Ritchie, K. L. Lunetta, J. S. Kauwe, E. Boerwinkle, M. Riemenschneider, M. Boada, M. Hiltuenen, E. R. Martin, R. Schmidt, D. Rujescu, L. S. Wang, J. F. Dartigues, R. Mayeux, C. Tzourio, A. Hofman, M. M. Nothen, C. Graff, B. M. Psaty, L. Jones, J. L. Haines, P. A. Holmans, M. Lathrop, M. A. Pericak-Vance, L. J. Launer, L. A. Farrer, C. M. van Duijn, C. Van Broeckhoven, V. Moskvina, S. Seshadri, J. Williams, G. D. Schellenberg and P. Amouyel (2013). "Meta-analysis of 74,046 individuals identifies 11 new susceptibility loci for Alzheimer's disease." Nat Genet **45**(12): 1452-1458.

Lane, R. F., S. M. Raines, J. W. Steele, M. E. Ehrlich, J. A. Lah, S. A. Small, R. E. Tanzi, A. D. Attie and S. Gandy (2010). "Diabetes-associated SorCS1 regulates Alzheimer's amyloid-beta metabolism: evidence for involvement of SorL1 and the retromer complex." J Neurosci **30**(39): 13110-13115.

Lane, R. F., P. St George-Hyslop, B. L. Hempstead, S. A. Small, S. M. Strittmatter and S. Gandy (2012). "Vps10 family proteins and the retromer complex in aging-related neurodegeneration and diabetes." J Neurosci **32**(41): 14080-14086.

Levy-Lahad, E., W. Wasco, P. Poorkaj, D. M. Romano, J. Oshima, W. H. Pettingell, C. E. Yu, P. D. Jondro, S. D. Schmidt, K. Wang and et al. (1995). "Candidate gene for the chromosome 1 familial Alzheimer's disease locus." Science **269**(5226): 973-977.

Luchsinger, J. A. (2008). "Adiposity, hyperinsulinemia, diabetes and Alzheimer's disease: an epidemiological perspective." Eur J Pharmacol **585**(1): 119-129.

Luchsinger, J. A., M. X. Tang, Y. Stern, S. Shea and R. Mayeux (2001). "Diabetes mellitus and risk of Alzheimer's disease and dementia with stroke in a multiethnic cohort." Am J Epidemiol **154**(7): 635-641.

Lucin, K. M., C. E. O'Brien, G. Bieri, E. Czirr, K. I. Mosher, R. J. Abbey, D. F. Mastroeni, J. Rogers, B. Spencer, E. Masliah and T. Wyss-Coray (2013). "Microglial beclin 1 regulates retromer trafficking and phagocytosis and is impaired in Alzheimer's disease." Neuron **79**(5): 873-886.

Maia, L. F., S. A. Kaeser, J. Reichwald, M. Hruscha, P. Martus, M. Staufenbiel and M. Jucker (2013). "Changes in amyloid-beta and Tau in the cerebrospinal fluid of transgenic mice overexpressing amyloid precursor protein." Sci Transl Med **5**(194): 194re192.

Manczak, M. and P. H. Reddy (2013). "Abnormal interaction of oligomeric amyloid-beta with phosphorylated tau: implications to synaptic dysfunction and neuronal damage." J Alzheimers Dis **36**(2): 285-295.

Marquer, C., H. Tian, J. Yi, J. Bastien, C. Dall'Armi, Y. Yang-Klingler, B. Zhou, R. B. Chan and G. Di Paolo (2016). "Arf6 controls retromer traffic and intracellular cholesterol distribution via a phosphoinositide-based mechanism." Nat Commun **7**: 11919.

McNamara, M. J., C. T. Ruff, W. Wasco, R. E. Tanzi, G. Thinakaran and B. T. Hyman (1998). "Immunohistochemical and in situ analysis of amyloid precursor-like protein-1 and amyloid precursor-like protein-2 expression in Alzheimer disease and aged control brains." Brain Res **804**(1): 45-51.

Meredith, J. E., Jr., S. Sankaranarayanan, V. Guss, A. J. Lanzetti, F. Berisha, R. J. Neely, J. R. Slemmon, E. Portelius, H. Zetterberg, K. Blennow, H. Soares, M. Ahlijanian and C. F. Albright (2013). "Characterization of novel CSF Tau and ptau biomarkers for Alzheimer's disease." PLoS One **8**(10): e76523.

Michaelson, D. M. (2014). "APOE epsilon4: the most prevalent yet understudied risk factor for Alzheimer's disease." Alzheimers Dement **10**(6): 861-868.

Mim, C. and V. M. Unger (2012). "Membrane curvature and its generation by BAR proteins." Trends Biochem Sci **37**(12): 526-533.

Miranda, A. M., Z. M. Lasiecka, Y. Xu, J. Neufeld, S. Shahriar, S. Simoes, R. B. Chan, T. G. Oliveira, S. A. Small and G. Di Paolo (2018). "Neuronal lysosomal dysfunction releases exosomes harboring APP C-terminal fragments and unique lipid signatures." Nat Commun **9**(1): 291.

Morabito, M. V., D. E. Berman, R. T. Schneider, Y. Zhang, R. L. Leibel and S. A. Small (2014). "Hyperleucinemia causes hippocampal retromer deficiency linking diabetes to Alzheimer's disease." Neurobiol Dis **65**: 188-192.

Morel, E., Z. Chamoun, Z. M. Lasiecka, R. B. Chan, R. L. Williamson, C. Vetanovetz, C. Dall'Armi, S. Simoes, K. S. Point Du Jour, B. D. McCabe, S. A. Small and G. Di Paolo (2013). "Phosphatidylinositol-3-phosphate regulates sorting and processing of amyloid precursor protein through the endosomal system." Nat Commun **4**: 2250.

Muhammad, A., I. Flores, H. Zhang, R. Yu, A. Staniszewski, E. Planel, M. Herman, L. Ho, R. Kreber, L. S. Honig, B. Ganetzky, K. Duff, O. Arancio and S. A. Small (2008). "Retromer deficiency observed in Alzheimer's disease causes hippocampal dysfunction, neurodegeneration, and Abeta accumulation." Proc Natl Acad Sci U S A **105**(20): 7327-7332.

Nixon, R. A. (2017). "Amyloid precursor protein and endosomal-lysosomal dysfunction in Alzheimer's disease: inseparable partners in a multifactorial disease." FASEB J **31**(7): 2729-2743.

Novak, M. (1994). "Truncated tau protein as a new marker for Alzheimer's disease." Acta Virol **38**(3): 173-189.

Nuriel, T., K. Y. Peng, A. Ashok, A. A. Dillman, H. Y. Figueroa, J. Apuzzo, J. Ambat, E. Levy, M. R. Cookson, P. M. Mathews and K. E. Duff (2017). "The Endosomal-Lysosomal Pathway Is Dysregulated by APOE4 Expression in Vivo." Front Neurosci **11**: 702.

Offe, K., S. E. Dodson, J. T. Shoemaker, J. J. Fritz, M. Gearing, A. I. Levey and J. J. Lah (2006). "The lipoprotein receptor LR11 regulates amyloid beta production and amyloid precursor protein traffic in endosomal compartments." J Neurosci **26**(5): 1596-1603.

Perez-Gonzalez, R., S. A. Gauthier, A. Kumar and E. Levy (2012). "The exosome secretory pathway transports amyloid precursor protein carboxyl-terminal fragments from the cell into the brain extracellular space." J Biol Chem **287**(51): 43108-43115.

Pickford, F., E. Masliah, M. Britschgi, K. Lucin, R. Narasimhan, P. A. Jaeger, S. Small, B. Spencer, E. Rockenstein, B. Levine and T. Wyss-Coray (2008). "The autophagy-related protein beclin 1 shows reduced expression in early Alzheimer disease and regulates amyloid beta accumulation in mice." J Clin Invest **118**(6): 2190-2199.

Pottier, C., D. Hannequin, S. Coutant, A. Rovelet-Lecrux, D. Wallon, S. Rousseau, S. Legallic, C. Paquet, S. Bombois, J. Pariente, C. Thomas-Anterion, A. Michon, B. Croisile, F. Etcharry-Bouyx, C. Berr, J. F. Dartigues, P. Amouyel, H. Dauchel, C. Boutoleau-Bretonniere, C. Thauvin, T. Frebourg, J. C. Lambert, D. Campion and P. G. Collaborators (2012). "High frequency of potentially pathogenic SORL1 mutations in autosomal dominant early-onset Alzheimer disease." Mol Psychiatry **17**(9): 875-879.

Priller, C., T. Bauer, G. Mitteregger, B. Krebs, H. A. Kretzschmar and J. Herms (2006). "Synapse formation and function is modulated by the amyloid precursor protein." J Neurosci **26**(27): 7212-7221.

Raja, W. K., A. E. Mungenast, Y. T. Lin, T. Ko, F. Abdurrob, J. Seo and L. H. Tsai (2016). "Self-Organizing 3D Human Neural Tissue Derived from Induced Pluripotent Stem Cells Recapitulate Alzheimer's Disease Phenotypes." PLoS One **11**(9): e0161969.

Reinhardt, T. A., R. E. Sacco, B. J. Nonnecke and J. D. Lippolis (2013). "Bovine milk proteome: quantitative changes in normal milk exosomes, milk fat globule membranes and whey proteomes resulting from Staphylococcus aureus mastitis." J Proteomics **82**: 141-154.

Rentz, D. M., J. J. Locascio, J. A. Becker, E. K. Moran, E. Eng, R. L. Buckner, R. A. Sperling and K. A. Johnson (2010). "Cognition, reserve, and amyloid deposition in normal aging." Ann Neurol **67**(3): 353-364.

Rodriguez, L., N. V. Mohamed, A. Desjardins, R. Lippe, E. A. Fon and N. Leclerc (2017). "Rab7A regulates tau secretion." J Neurochem **141**(4): 592-605.

Rogaeva, E., Y. Meng, J. H. Lee, Y. Gu, T. Kawarai, F. Zou, T. Katayama, C. T. Baldwin, R. Cheng, H. Hasegawa, F. Chen, N. Shibata, K. L. Lunetta, R. Pardossi-Piquard, C. Bohm, Y. Wakutani, L. A. Cupples, K. T. Cuenco, R. C. Green, L. Pinessi, I. Rainero, S. Sorbi, A. Bruni, R. Duara, R. P. Friedland, R. Inzelberg, W. Hampe, H. Bujo, Y. Q. Song, O. M. Andersen, T. E. Willnow, N. Graff-Radford, R. C. Petersen, D. Dickson, S. D. Der, P. E. Fraser, G. Schmitt-Ulms, S. Younkin, R. Mayeux, L. A. Farrer and P. St George-Hyslop (2007). "The neuronal sortilin-related receptor SORL1 is genetically associated with Alzheimer disease." Nat Genet **39**(2): 168-177.

Rojas, R., S. Kametaka, C. R. Haft and J. S. Bonifacino (2007). "Interchangeable but essential functions of SNX1 and SNX2 in the association of retromer with endosomes and the trafficking of mannose 6-phosphate receptors." Mol Cell Biol **27**(3): 1112-1124.

Rojas, R., T. van Vlijmen, G. A. Mardones, Y. Prabhu, A. L. Rojas, S. Mohammed, A. J. Heck, G. Raposo, P. van der Sluijs and J. S. Bonifacino (2008). "Regulation of retromer recruitment to endosomes by sequential action of Rab5 and Rab7." J Cell Biol **183**(3): 513-526.

Romeo, G. R., K. S. Moulton and A. Kazlauskas (2007). "Attenuated expression of profilin-1 confers protection from atherosclerosis in the LDL receptor null mouse." Circ Res **101**(4): 357-367.

Rozek, W., M. Ricardo-Dukelow, S. Holloway, H. E. Gendelman, V. Wojna, L. M. Melendez and P. Ciborowski (2007). "Cerebrospinal fluid proteomic profiling of HIV-1-infected patients with cognitive impairment." J Proteome Res **6**(11): 4189-4199.

Saman, S., W. Kim, M. Raya, Y. Visnick, S. Miro, S. Saman, B. Jackson, A. C. McKee, V. E. Alvarez, N. C. Lee and G. F. Hall (2012). "Exosome-associated tau is secreted in tauopathy models and is

selectively phosphorylated in cerebrospinal fluid in early Alzheimer disease." J Biol Chem **287**(6): 3842-3849.

Scarmeas, N., J. A. Luchsinger, N. Schupf, A. M. Brickman, S. Cosentino, M. X. Tang and Y. Stern (2009). "Physical activity, diet, and risk of Alzheimer disease." JAMA **302**(6): 627-637.

Scarmeas, N., Y. Stern, M. X. Tang, R. Mayeux and J. A. Luchsinger (2006). "Mediterranean diet and risk for Alzheimer's disease." Ann Neurol **59**(6): 912-921.

Scarmeas, N., E. Zarahn, K. E. Anderson, C. G. Habeck, J. Hilton, J. Flynn, K. S. Marder, K. L. Bell, H. A. Sackeim, R. L. Van Heertum, J. R. Moeller and Y. Stern (2003). "Association of life activities with cerebral blood flow in Alzheimer disease: implications for the cognitive reserve hypothesis." Arch Neurol **60**(3): 359-365.

Scarmeas, N., E. Zarahn, K. E. Anderson, L. S. Honig, A. Park, J. Hilton, J. Flynn, H. A. Sackeim and Y. Stern (2004). "Cognitive reserve-mediated modulation of positron emission tomographic activations during memory tasks in Alzheimer disease." Arch Neurol **61**(1): 73-78.

Schelle, J., L. M. Hasler, J. C. Gopfert, T. O. Joos, H. Vanderstichele, E. Stoops, E. M. Mandelkow, U. Neumann, D. R. Shimshek, M. Staufenbiel, M. Jucker and S. A. Kaeser (2017). "Prevention of tau increase in cerebrospinal fluid of APP transgenic mice suggests downstream effect of BACE1 inhibition." Alzheimers Dement **13**(6): 701-709.

Schutzer, S. E., T. Liu, B. H. Natelson, T. E. Angel, A. A. Schepmoes, S. O. Purvine, K. K. Hixson, M. S. Lipton, D. G. Camp, P. K. Coyle, R. D. Smith and J. Bergquist (2010). "Establishing the proteome of normal human cerebrospinal fluid." PLoS One **5**(6): e10980.

Schwagerl, A. L., P. S. Mohan, A. M. Cataldo, J. P. Vonsattel, N. W. Kowall and R. A. Nixon (1995). "Elevated levels of the endosomal-lysosomal proteinase cathepsin D in cerebrospinal fluid in Alzheimer disease." J Neurochem **64**(1): 443-446.

Seaman, M. N. (2004). "Cargo-selective endosomal sorting for retrieval to the Golgi requires retromer." J Cell Biol **165**(1): 111-122.

Seaman, M. N., M. E. Harbour, D. Tattersall, E. Read and N. Bright (2009). "Membrane recruitment of the cargo-selective retromer subcomplex is catalysed by the small GTPase Rab7 and inhibited by the Rab-GAP TBC1D5." J Cell Sci **122**(Pt 14): 2371-2382.

Seaman, M. N., E. G. Marcusson, J. L. Cereghino and S. D. Emr (1997). "Endosome to Golgi retrieval of the vacuolar protein sorting receptor, Vps10p, requires the function of the VPS29, VPS30, and VPS35 gene products." J Cell Biol **137**(1): 79-92.

Seaman, M. N., J. M. McCaffery and S. D. Emr (1998). "A membrane coat complex essential for endosome-to-Golgi retrograde transport in yeast." J Cell Biol **142**(3): 665-681.

Serrano-Pozo, A., M. P. Frosch, E. Masliah and B. T. Hyman (2011). "Neuropathological alterations in Alzheimer disease." Cold Spring Harb Perspect Med **1**(1): a006189.

Seyer, A., S. Boudah, S. Broudin, C. Junot and B. Colsch (2016). "Annotation of the human cerebrospinal fluid lipidome using high resolution mass spectrometry and a dedicated data processing workflow." Metabolomics **12**: 91.

Sherrington, R., E. I. Rogaev, Y. Liang, E. A. Rogaeva, G. Levesque, M. Ikeda, H. Chi, C. Lin, G. Li, K. Holman, T. Tsuda, L. Mar, J. F. Foncin, A. C. Bruni, M. P. Montesi, S. Sorbi, I. Rainero, L. Pinessi, L. Nee, I. Chumakov, D. Pollen, A. Brookes, P. Sanseau, R. J. Polinsky, W. Wasco, H. A. Da Silva, J. L. Haines, M. A. Perkicak-Vance, R. E. Tanzi, A. D. Roses, P. E. Fraser, J. M. Rommens and P. H. St George-Hyslop (1995). "Cloning of a gene bearing missense mutations in early-onset familial Alzheimer's disease." Nature **375**(6534): 754-760.

Shibata, M., S. Yamada, S. R. Kumar, M. Calero, J. Bading, B. Frangione, D. M. Holtzman, C. A. Miller, D. K. Strickland, J. Ghiso and B. V. Zlokovic (2000). "Clearance of Alzheimer's amyloid-ss(1-40) peptide from brain by LDL receptor-related protein-1 at the blood-brain barrier." J Clin Invest **106**(12): 1489-1499.

Shores, K. S. and D. R. Knapp (2007). "Assessment approach for evaluating high abundance protein depletion methods for cerebrospinal fluid (CSF) proteomic analysis." J Proteome Res **6**(9): 3739-3751.

Skogberg, G., J. Gudmundsdottir, S. van der Post, K. Sandstrom, S. Bruhn, M. Benson, L. Mincheva-Nilsson, V. Baranov, E. Telemo and O. Ekwall (2013). "Characterization of human thymic exosomes." PLoS One **8**(7): e67554.

Small, S. A. and K. Duff (2008). "Linking Abeta and tau in late-onset Alzheimer's disease: a dual pathway hypothesis." Neuron **60**(4): 534-542.

Small, S. A. and S. Gandy (2006). "Sorting through the cell biology of Alzheimer's disease: intracellular pathways to pathogenesis." Neuron **52**(1): 15-31.

Small, S. A., K. Kent, A. Pierce, C. Leung, M. S. Kang, H. Okada, L. Honig, J. P. Vonsattel and T. W. Kim (2005). "Model-guided microarray implicates the retromer complex in Alzheimer's disease." Ann Neurol **58**(6): 909-919.

Small, S. A. and G. A. Petsko (2015). "Retromer in Alzheimer disease, Parkinson disease and other neurological disorders." Nat Rev Neurosci **16**(3): 126-132.

Small, S. A., S. Simoes-Spassov, R. Mayeux and G. A. Petsko (2017). "Endosomal Traffic Jams Represent a Pathogenic Hub and Therapeutic Target in Alzheimer's Disease." Trends Neurosci **40**(10): 592-602.

Smith, J. S., T. E. Angel, C. Chavkin, D. J. Orton, R. J. Moore and R. D. Smith (2014). "Characterization of individual mouse cerebrospinal fluid proteomes." Proteomics **14**(9): 1102-1106.

Steinberg, S., H. Stefansson, T. Jonsson, H. Johannsdottir, A. Ingason, H. Helgason, P. Sulem, O. T. Magnusson, S. A. Gudjonsson, U. Unnsteinsdottir, A. Kong, S. Helisalmi, H. Soininen, J. J. Lah, DemGene, D. Aarsland, T. Fladby, I. D. Ulstein, S. Djurovic, S. B. Sando, L. R. White, G. P. Knudsen, L. T. Westlye, G. Selbaek, I. Giegling, H. Hampel, M. Hiltunen, A. I. Levey, O. A. Andreassen, D. Rujescu, P. V. Jonsson, S. Bjornsson, J. Snaedal and K. Stefansson (2015). "Loss-of-function variants in ABCA7 confer risk of Alzheimer's disease." Nat Genet **47**(5): 445-447.

Stern, Y. (2006). "Cognitive reserve and Alzheimer disease." Alzheimer Dis Assoc Disord **20**(2): 112-117.

Strauss, K., C. Goebel, H. Runz, W. Mobius, S. Weiss, I. Feussner, M. Simons and A. Schneider (2010). "Exosome secretion ameliorates lysosomal storage of cholesterol in Niemann-Pick type C disease." J Biol Chem **285**(34): 26279-26288.

Strittmatter, W. J., K. H. Weisgraber, D. Y. Huang, L. M. Dong, G. S. Salvesen, M. Pericak-Vance, D. Schmechel, A. M. Saunders, D. Goldgaber and A. D. Roses (1993). "Binding of human apolipoprotein E to synthetic amyloid beta peptide: isoform-specific effects and implications for late-onset Alzheimer disease." Proc Natl Acad Sci U S A **90**(17): 8098-8102.

Sullivan, C. P., A. G. Jay, E. C. Stack, M. Pakaluk, E. Wadlinger, R. E. Fine, J. M. Wells and P. J. Morin (2011). "Retromer disruption promotes amyloidogenic APP processing." Neurobiol Dis **43**(2): 338-345.

Tanzi, R. E., R. D. Moir and S. L. Wagner (2004). "Clearance of Alzheimer's Abeta peptide: the many roads to perdition." Neuron **43**(5): 605-608.

Teller, J. K., C. Russo, L. M. DeBusk, G. Angelini, D. Zaccheo, F. Dagna-Bricarelli, P. Scartezzini, S. Bertolini, D. M. Mann, M. Tabaton and P. Gambetti (1996). "Presence of soluble amyloid beta-peptide precedes amyloid plaque formation in Down's syndrome." Nat Med **2**(1): 93-95.

Temkin, P., W. Morishita, D. Goswami, K. Arendt, L. Chen and R. Malenka (2017). "The Retromer Supports AMPA Receptor Trafficking During LTP." Neuron **94**(1): 74-82 e75.

Tholen, S., M. L. Biniossek, M. Gansz, T. D. Ahrens, M. Schlimpert, J. N. Kizhakkedathu, T. Reinheckel and O. Schilling (2014). "Double deficiency of cathepsins B and L results in massive secretome alterations and suggests a degradative cathepsin-MMP axis." Cell Mol Life Sci **71**(5): 899-916.

Tholen, S., M. L. Biniossek, A. L. Gessler, S. Muller, J. Weisser, J. N. Kizhakkedathu, T. Reinheckel and O. Schilling (2011). "Contribution of cathepsin L to secretome composition and cleavage pattern of mouse embryonic fibroblasts." Biol Chem **392**(11): 961-971.

Trajkovic, K., C. Hsu, S. Chiantia, L. Rajendran, D. Wenzel, F. Wieland, P. Schwille, B. Brugger and M. Simons (2008). "Ceramide triggers budding of exosome vesicles into multivesicular endosomes." Science **319**(5867): 1244-1247.

Tran, J., M. Mustapic, N. Voigt, B. Bendlin and D. Kapogiannis 2017 Neuroscience Meeting Planner. Washingto, D.C. Society for Neuroscience, 2017. Online.

.

Tran, J. M., M.; Voigt, N.; Bendlin, B.; Kapogiannis, D. (2017). Extracellular Vesicle Biomarkers in Alzheimer's Disease, Mild Cognitive Impairment, and Non-Cognitively Impaired Older Adults. 2017 Neuroscience Meeting Planner, Washingto, D.C. , Society for Neuroscience, 2017.

Tyan, S. H., A. Y. Shih, J. J. Walsh, H. Maruyama, F. Sarsoza, L. Ku, S. Eggert, P. R. Hof, E. H. Koo and D. L. Dickstein (2012). "Amyloid precursor protein (APP) regulates synaptic structure and function." Mol Cell Neurosci **51**(1-2): 43-52.

Vardarajan, B. N., S. Y. Bruesegem, M. E. Harbour, R. Inzelberg, R. Friedland, P. St George-Hyslop, M. N. Seaman and L. A. Farrer (2012). "Identification of Alzheimer disease-associated variants in genes that regulate retromer function." Neurobiol Aging **33**(9): 2231 e2215-2231 e2230.

Vardarajan, B. N., Y. Zhang, J. H. Lee, R. Cheng, C. Bohm, M. Ghani, C. Reitz, D. Reyes-Dumeyer, Y. Shen, E. Rogaeva, P. St George-Hyslop and R. Mayeux (2015). "Coding mutations in SORL1 and Alzheimer disease." Ann Neurol **77**(2): 215-227.

Verheijen, J., T. Van den Bossche, J. van der Zee, S. Engelborghs, R. Sanchez-Valle, A. Llado, C. Graff, H. Thonberg, P. Pastor, S. Ortega-Cubero, M. A. Pastor, L. Benussi, R. Ghidoni, G. Binetti, J. Clarimon, A. Lleo, J. Fortea, A. de Mendonca, M. Martins, O. Grau-Rivera, E. Gelpi, K. Bettens, L. Mateiu, L. Dillen, P. Cras, P. P. De Deyn, C. Van Broeckhoven and K. Sleegers (2016). "A comprehensive study of the genetic impact of rare variants in SORL1 in European early-onset Alzheimer's disease." Acta Neuropathol **132**(2): 213-224.

Walsh, D. M., I. Klyubin, J. V. Fadeeva, W. K. Cullen, R. Anwyl, M. S. Wolfe, M. J. Rowan and D. J. Selkoe (2002). "Naturally secreted oligomers of amyloid beta protein potently inhibit hippocampal long-term potentiation in vivo." Nature **416**(6880): 535-539.

Wang, J. Z., Y. Y. Xia, I. Grundke-Iqbal and K. Iqbal (2013). "Abnormal hyperphosphorylation of tau: sites, regulation, and molecular mechanism of neurofibrillary degeneration." J Alzheimers Dis **33 Suppl 1**: S123-139.

Wang, Y., V. Balaji, S. Kaniyappan, L. Kruger, S. Irsen, K. Tepper, R. Chandupatla, W. Maetzler, A. Schneider, E. Mandelkow and E. M. Mandelkow (2017). "The release and trans-synaptic transmission of Tau via exosomes." Mol Neurodegener **12**(1): 5.

Wassmer, T., N. Attar, M. V. Bujny, J. Oakley, C. J. Traer and P. J. Cullen (2007). "A loss-of-function screen reveals SNX5 and SNX6 as potential components of the mammalian retromer." J Cell Sci **120**(Pt 1): 45-54.

Wen, L., F. L. Tang, Y. Hong, S. W. Luo, C. L. Wang, W. He, C. Shen, J. U. Jung, F. Xiong, D. H. Lee, Q. G. Zhang, D. Brann, T. W. Kim, R. Yan, L. Mei and W. C. Xiong (2011). "VPS35 haploinsufficiency increases Alzheimer's disease neuropathology." J Cell Biol **195**(5): 765-779.

Wibowo, A. S., M. Singh, K. M. Reeder, J. J. Carter, A. R. Kovach, W. Meng, M. Ratnam, F. Zhang and C. E. Dann, 3rd (2013). "Structures of human folate receptors reveal biological trafficking states and diversity in folate and antifolate recognition." Proc Natl Acad Sci U S A **110**(38): 15180-15188.

Wu, D., M. D. Milutinovic and D. R. Walt (2015). "Single molecule array (Simoa) assay with optimal antibody pairs for cytokine detection in human serum samples." Analyst **140**(18): 6277-6282.

Wu, L. and L. Zhao (2016). "ApoE2 and Alzheimer's disease: time to take a closer look." Neural Regen Res **11**(3): 412-413.

Xiao, T., W. Zhang, B. Jiao, C. Z. Pan, X. Liu and L. Shen (2017). "The role of exosomes in the pathogenesis of Alzheimer' disease." Transl Neurodegener **6**: 3.

Xiong, H., D. Callaghan, A. Jones, D. G. Walker, L. F. Lue, T. G. Beach, L. I. Sue, J. Woulfe, H. Xu, D. B. Stanimirovic and W. Zhang (2008). "Cholesterol retention in Alzheimer's brain is responsible for high beta- and gamma-secretase activities and Abeta production." Neurobiol Dis **29**(3): 422-437.

Xu, W., A. M. Weissmiller, J. A. White, 2nd, F. Fang, X. Wang, Y. Wu, M. L. Pearn, X. Zhao, M. Sawa, S. Chen, S. Gunawardena, J. Ding, W. C. Mobley and C. Wu (2016). "Amyloid precursor protein-mediated endocytic pathway disruption induces axonal dysfunction and neurodegeneration." J Clin Invest **126**(5): 1815-1833.

Yang, T., P. Martin, B. Fogarty, A. Brown, K. Schurman, R. Phipps, V. P. Yin, P. Lockman and S. Bai (2015). "Exosome delivered anticancer drugs across the blood-brain barrier for brain cancer therapy in Danio rerio." Pharm Res **32**(6): 2003-2014.

Young, J., L. Fong, H. Frankowski, G. Petsko, S. A. Small and L. Goldstein (2018). "Stabilizing the retromer complex in a human stem cell model of Alzheimer's disease reduces Tau phosphorylation independent of Amyloid Precursor Protein." Stem Cell Reports **In Press**.

Yuan, X. and D. M. Desiderio (2005). "Proteomics analysis of prefractionated human lumbar cerebrospinal fluid." Proteomics **5**(2): 541-550.

Yuyama, K., N. Yamamoto and K. Yanagisawa (2008). "Accelerated release of exosome-associated GM1 ganglioside (GM1) by endocytic pathway abnormality: another putative pathway for GM1-induced amyloid fibril formation." J Neurochem **105**(1): 217-224.

Zarrouk, A., M. Debbabi, M. Bezine, E. M. Karym, A. Badreddine, O. Rouaud, T. Moreau, M. Cherkaoui-Malki, M. El Ayeb, B. Nasser, M. Hammami and G. Lizard (2017). "Lipid Biomarkers in Alzheimer's Disease." Curr Alzheimer Res.

Zetterberg, H. (2017). "Review: Tau in biofluids - relation to pathology, imaging and clinical features." Neuropathol Appl Neurobiol **43**(3): 194-199.

Zhang, L., S. Zhang, J. Yao, F. J. Lowery, Q. Zhang, W. C. Huang, P. Li, M. Li, X. Wang, C. Zhang, H. Wang, K. Ellis, M. Cheerathodi, J. H. McCarty, D. Palmieri, J. Saunus, S. Lakhani, S. Huang, A. A. Sahin, K. D. Aldape, P. S. Steeg and D. Yu (2015). "Microenvironment-induced PTEN loss by exosomal microRNA primes brain metastasis outgrowth." Nature **527**(7576): 100-104.

Zhang, Y., K. Chen, S. A. Sloan, M. L. Bennett, A. R. Scholze, S. O'Keeffe, H. P. Phatnani, P. Guarnieri, C. Caneda, N. Ruderisch, S. Deng, S. A. Liddelow, C. Zhang, R. Daneman, T. Maniatis, B. A. Barres and J. Q. Wu (2014). "An RNA-sequencing transcriptome and splicing database of glia, neurons, and vascular cells of the cerebral cortex." J Neurosci **34**(36): 11929-11947.

Zhao, X., S. Nothwehr, R. Lara-Lemus, B. Y. Zhang, H. Peter and P. Arvan (2007). "Dominant-negative behavior of mammalian Vps35 in yeast requires a conserved PRLYL motif involved in retromer assembly." Traffic **8**(12): 1829-1840.

Zheng, W. H., S. Bastianetto, F. Mennicken, W. Ma and S. Kar (2002). "Amyloid beta peptide induces tau phosphorylation and loss of cholinergic neurons in rat primary septal cultures." Neuroscience **115**(1): 201-211.

Zlokovic, B. V., C. L. Martel, E. Matsubara, J. G. McComb, G. Zheng, R. T. McCluskey, B. Frangione and J. Ghiso (1996). "Glycoprotein 330/megalin: probable role in receptor-mediated transport of apolipoprotein J alone and in a complex with Alzheimer disease amyloid beta at the blood-brain and blood-cerebrospinal fluid barriers." Proc Natl Acad Sci U S A **93**(9): 4229-4234.